NAVAL POSTGRADUATE SCHOOL
Monterey, California

THESIS

SEA LEVELS AND METERED CURRENTS
OFF CENTRAL CALIFORNIA

by

Donald A. Dreves

September 1980

Thesis Advisors: J. B. Wickham
                                     S. P. Tucker

Approved for public release; distribution unlimited.

T196257

REPORT DOCUMENTATION PAGE		READ INSTRUCTIONS BEFORE COMPLETING FORM
1. REPORT NUMBER	2. GOVT ACCESSION NO.	3. RECIPIENT'S CATALOG NUMBER
4. TITLE (and Subtitle) Sea Levels and Metered Currents Off Central California		5. TYPE OF REPORT & PERIOD COVERED Master's Thesis; September 1980
		6. PERFORMING ORG. REPORT NUMBER
7. AUTHOR(s) Donald A. Dreves		8. CONTRACT OR GRANT NUMBER(s)
9. PERFORMING ORGANIZATION NAME AND ADDRESS Naval Postgraduate School Monterey, California 93940		10. PROGRAM ELEMENT, PROJECT, TASK AREA & WORK UNIT NUMBERS
11. CONTROLLING OFFICE NAME AND ADDRESS Naval Postgraduate School Monterey, California 93940		12. REPORT DATE September 1980
		13. NUMBER OF PAGES 94
14. MONITORING AGENCY NAME & ADDRESS(If different from Controlling Office)		15. SECURITY CLASS. (of this report) Unclassified
		15a. DECLASSIFICATION/DOWNGRADING SCHEDULE

16. DISTRIBUTION STATEMENT (of this Report)

Approved for public release; distribution unlimited.

17. DISTRIBUTION STATEMENT (of the abstract entered in Block 20, if different from Report)

18. SUPPLEMENTARY NOTES

19. KEY WORDS (Continue on reverse side if necessary and identify by block number)

Sea levels, Eastern boundary currents, central California coastal currents, metered currents, alongshore slopes.

20. ABSTRACT (Continue on reverse side if necessary and identify by block number)

Sea levels from two locations, the alongshore sea level gradient and direct measurement of currents by moored current meters are examined and discussed. The observations were made off the central California coast during the Davidson Current period 1978-9.

Analysis for spectral variance of hourly and low pass filtered sea levels, alongshore sea level gradient and

DD FORM 1473 EDITION OF 1 NOV 65 IS OBSOLETE
1 JAN 73
(Page 1)   S/N 0102-014-6601 :

#20 - ABSTRACT - CONTINUED

alongshore and cross shelf currents was performed. Comparison
of spectral estimates of low pass filtered data indicate
that current and sea level gradient energy distributions are
in close agreement. This is interpreted to suggest that a
relationship may exist between the observed currents and the
longshore sea level gradient. In contrast, the low pass
filtered sea level spectrum indicates energy concentrated
at lower frequencies than was observed for currents.

Sea Levels and Metered Currents
Off Central California

by

Donald A. Dreves
Lieutenant, NOAA
B.S., State University of New York, Maritime College, 1969

Submitted in partial fulfillment of the
requirements for the degree of

MASTER OF SCIENCE IN OCEANOGRAPHY (HYDROGRAPHY)

from the

NAVAL POSTGRADUATE SCHOOL
September 1980

ABSTRACT

Sea levels from two locations, the alongshore sea
level gradient and direct measurement of currents by
moored current meters are examined and discussed. The
observations were made off the central California coast
during the Davidson Current period 1978-9.

Analysis for spectral variance of hourly and low pass
filtered sea levels, alongshore sea level gradient and
alongshore and cross shelf currents was performed.
Comparison of spectral estimates of low pass filtered
data indicate that current and sea level gradient
energy distributions are in close agreement. This is
interpreted to suggest that a relationship may exist
between the observed currents and the longshore sea
level gradient. In contrast, the low pass filtered sea
level spectrum indicates energy concentrated at lower
frequencies than was observed for currents.

TABLE OF CONTENTS

LIST OF FIGURES

ACKNOWLEDGEMENTS

I. INTRODUCTION

Eastern boundary current systems, like that of the California Current, are increasingly the subject of investigation. In particular, upwelling conditions associated with the southward flowing surface water(s) are of economic importance, due to the connection between upwelling and local fisheries. During periods of upwelling, cold, nutrient rich water from mid-depths flows shoreward and rises to the surface, stimulating concentrations of food fish in relatively accessible locations.

The occurrence of upwelling, however, varies through the year. On the California coast the upwelling period - in spring and summer seasons - is preceeded by a period during which warm, saline surface water flows in a northerly direction inshore of the southward flowing California Current. This is the Davidson Current, possibly a surface manifestation of the California Undercurrent, a year-round poleward flow, whose core is at a depth of some few hundreds of meters.

The main objective of this study is to examine connections between coastal sea levels and currents by identifying similarities between their variance spectra. The assumption is made that where similarities

in the spectra exist, the two observed phenomena may be
considered to be interrelated, or responding to a common
driving mechanism.

There is precedent for this type of study. Many
authors (including Hickey, 1978, Huyer et al., 1978)
recognize that low frequency fluctuations in ocean
currents are coherent with fluctuations in wind stress.
Smith (1974) finds that the cross spectra between winds
and sea levels have significant coherence in the vicinity
of 0.25 and 0.4 cpd. Huyer et al., (1979) report that
there is good correlation between alongshore currents
and sea levels on the Oregon coast, and in particular
observe that low frequency near surface alongshore flow
is approximately in balance with the offshore sea surface
slope. Huyer et al., (1978) indicate that current
fluctuations are well correlated with sea level observations
at a tide station 50 to 75 km distant from their current
meter arrays. Bretschneider and McLain (1979) observe
that since 1940 anomalously high sea levels, in a long
term sense, have coincided with the occurrence of
El Nino in the South Pacific Ocean.

Smith (1974 and 1978) reports significant coherence
at low frequencies (< 0.25 cpd) between currents and sea
levels. He further reports that low frequency fluctuations
in current are independent of local winds, but that

coherence between sea level and currents is significant in this frequency band.

Osmer and Huyer (1978) conclude that sea level fluctuations along the Pacific Northwest coast of the United States propogate northward, although wind stress fluctuations tend to propogate southward. They suggest that a significant portion of the sea level fluctuation is probably associated with coastally trapped waves. This is supported by Smith (1978) who observed that poleward propagating current fluctuations along the coast of Peru were internally coherent over distances of hundreds of kilometers, and that the speed of propagation was consistent with that of trapped waves. Chelton (1980) concurs that there is a connection between coastally trapped waves and sea levels at low frequencies.

II. OCEAN PROCESSES IN THE STUDY AREA

The large scale sub-tropical oceanic circulation in
the North Pacific ocean is dominated by a clockwise
ocean-wide gyre driven by the anticyclonic atmospheric
flow of the North Pacific High. When the eastward
flowing North Pacific Current impacts the North American
continent and continental shelf in the vicinity of
southern Canada, it bifurcates, one limb heading north
to the Gulf of Alaska to form the counterclockwise
flowing Alaskan Current, and the other becoming the
southward flowing California Current, a diffuse, slow
moving eastern boundary current. This current is the
dominant large scale oceanographic feature in the Monterey
Bay area.

The ocean regime in Monterey Bay exhibits a three-
season variability (Skogsberg, 1936); Skogsberg refers
to the "Upwelling Period," the "Oceanic Period," and
the "Davidson Current Period." The calendar period
of these seasons varies from year to year, but on the
average is as follows: During the Upwelling period,
generally March through August, anti-cyclonic atmospheric
circulation is especially strong. As the atmosphere
warms during spring, the large wintertime low pressure
cell centered over the Aleutian Islands weakens, and
the North Pacific high strengthens and drifts northward.

This anticyclonic flow of the North Pacific high causes persistent north and northwesterly winds over the waters west of the United States reinforcing the southward flowing California current. Near the coast there may be a submerged poleward flow, the California undercurrent. Ekman transport assoicated with the northerly winds causes a westward surface flow, water pile-up offshore, and a general lowering of sea level along the coast. The offshore/onshore sea level gradient stimulates a subsurface onshore flow beneath the offshore surface flow. The onshore flow extends to a depth of several hundred meters.

When this onshore flow enters relatively shallow water, some of it is driven down and returns to deeper water. The remainder is driven upward and manifests itself as coastal upwelling of cold, nutrient laden water. Upwelling generally reaches a maximum in May or June (Bakun, 1975).

The Oceanic period begins in late summer and early fall. The North Pacific high weakens and drifts southward, and the Aleutial Low reforms. During this period the persistent northerly winds associated with the summertime North Pacific high decrease, becoming weak and variable, reducing surface offshore water mass transport and allowing the sea level to equalize.

With this change, subsurface onshore flow and upwelling cease.

Closing out the seasonal year, the Davidson Current period, generally from November into March, is characterized by continued weak and variable northerly winds. During this season the California Current moves offshore and becomes more diffuse. Inshore of the California Current, a warm, salty northward flow appears in the surface layers, the Davidson Current. Periodically, strong southerly winds interrupt the anticyclonic atmospheric circulatory pattern of the weakened North Pacific high, stimulating and reinforcing the northward flowing Davidson Current. The southerly winds also generate onshore Ekman transport, resulting in a general rise in sea level due to water pile-up at the coastal boundary. The elevated sea level, in turn, causes downwelling and offshore cross shelf flow below the Ekman layer.

III. <u>FLUCTUATIONS IN SEA LEVEL - AN OVERVIEW</u>

The observed elevation of the ocean's surface at any location or time is influenced by a combination of factors, including the large scale atmospheric circulation described in the preceeding section. Generally, the 12.5- and 24- hr tide-raising forces of the earth-moon-sun system generate the most conspicuous and easily recognized of all ocean tides with periodicities of minutes or longer. The observed sea level however, is modified by combinations of other less predictable and quantifiable factors, operating individually or in concert. These include atmospherically driven on- and offshore Ekman mass transport, direct set-up or set-down of water due to winds, spatial and temporal variations in atmospheric pressure, wind generated waves and swell, density variations in the water column, crustal subsidence or uplift, eustatic sea level variations resulting from changes in the mass of the polar ice packs, surge from distant storms or tsunamis, and low frequency astronomical tide-raising forces.

IV. SEA LEVEL DATA

Sea level data from two NOS tide observation stations were used in the study. Observations from the stations were compared to determine if a sea level difference - an indication of an alongshore sea surface slope - could be detected. The calculated sea level differences, and the station data were low pass filtered to eliminate powerful diurnal and semidiurnal tidal signals, and variance spectra for the filtered records were determined using a fast fourier transform technique.

Hourly heights of tide from Port San Luis and Monterey, California, were provided by the National Ocean Survey (NOS), National Oceanic and Atmospheric Administration (NOAA). These stations were selected for their proximity to and because they bracket current meter deployment locations to be discussed later (see Figure 1). The stations are approximately 100 nmi (185 km) apart and are nearly equidistant from the current meter sites.

The height-of-tide records for both stations were continuous for the period 1 January 1978 - 31 July 1979, except for occasional short gaps. The longest break in either record occurred at Port San Luis on 25-26 June 1978, when 24 hours of data were missed. This number of missed records falls well within the NOS 72-hr limit for
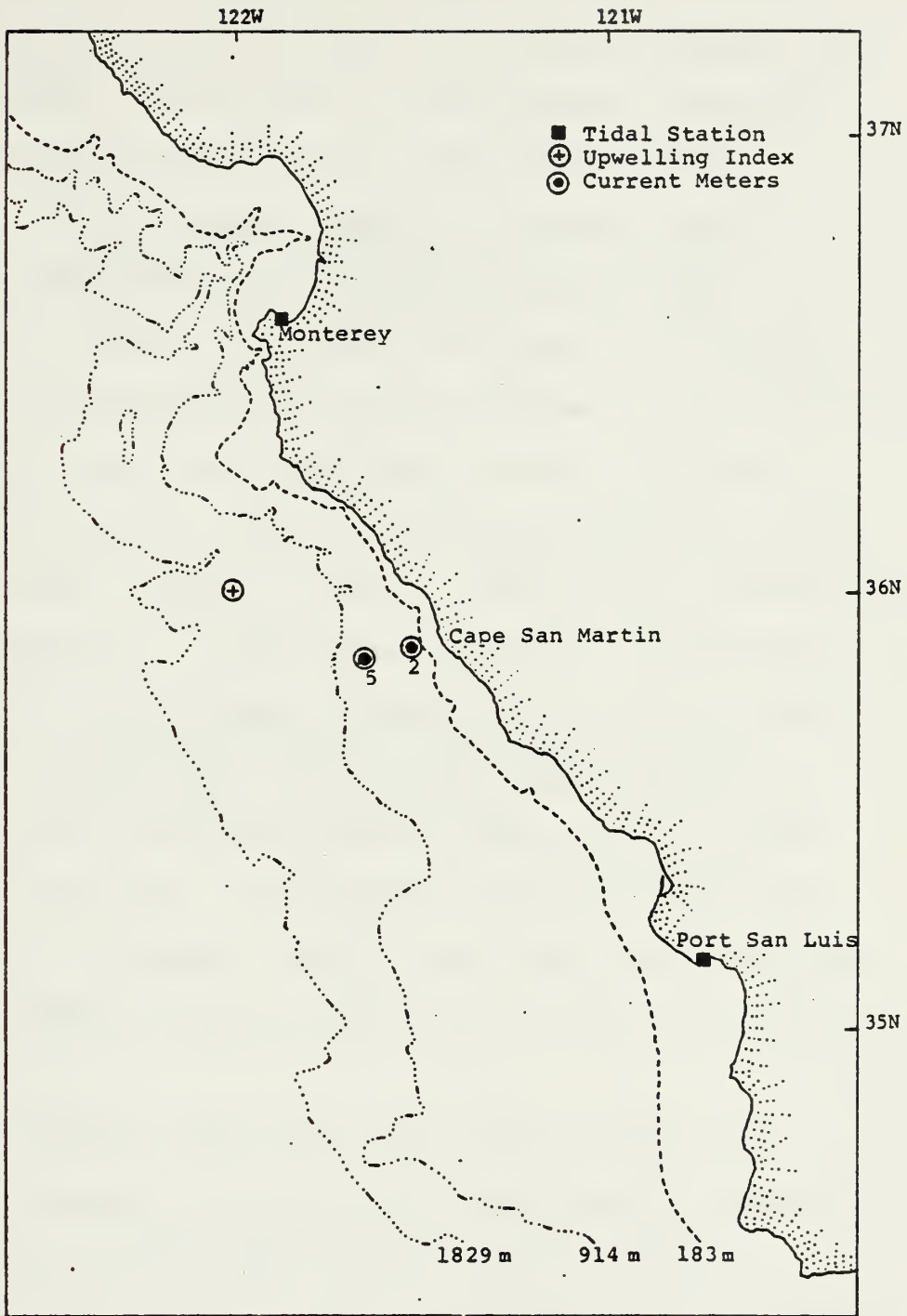
Figure 1.   The study area.

17

interpolation of missed tidal observations. Appendix A
is a list of missing records. The missing records were
interpolated for according to NOS standard practice
(Manual of Tide Observations, Coast and Geodetic
Survey). This involves analysis of several days'
records both preceeding and succeeding the break in
the data. The gap is filled with records conforming
with the adjacent preceeding and succeeding observations.

Hourly values for both stations were low pass
filtered in order to remove the large diurnal and semi-
diurnal tidal signals. Godin's (1966) filter accomplished
this effectively. The filter performs an unweighted
arithmetic running mean of the data set, passing over
the data three times. It averages sequences of 24
values on the first and second passes, and 25 values
on the third pass. The hourly and filtered data are
presented in Figures 2 and 3. The three presentations
in each figure contain seven months of data to allow
overlap.

The filtered data from both tide stations show
greater variability during the winter months (November
through March) than for the remainder of the year.
Analysis for spectral variance was performed on two-month
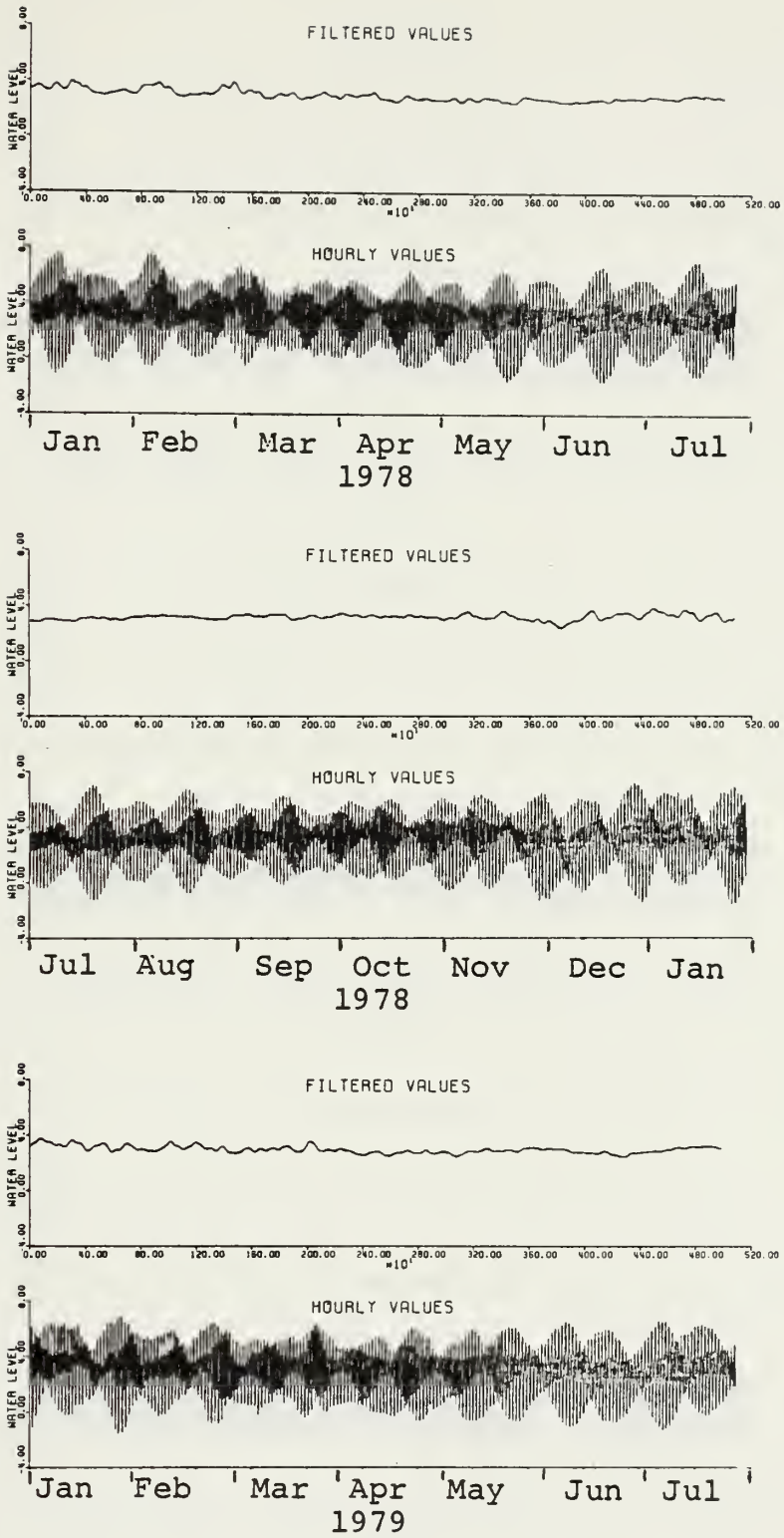blocks of filtered data for eighteen of the nineteen data
months. (January-February, March-April, etc.). Variance
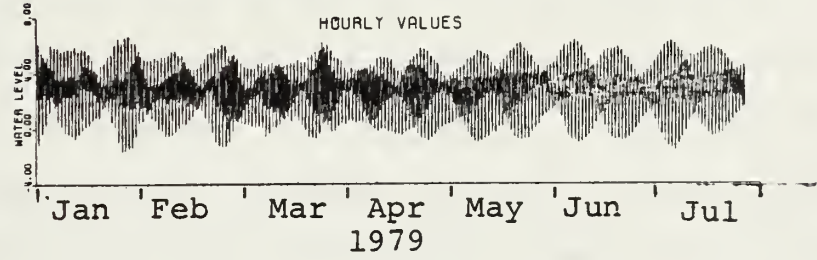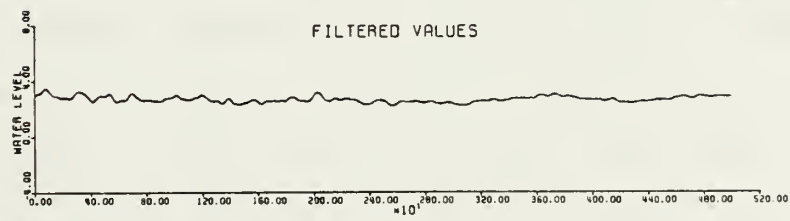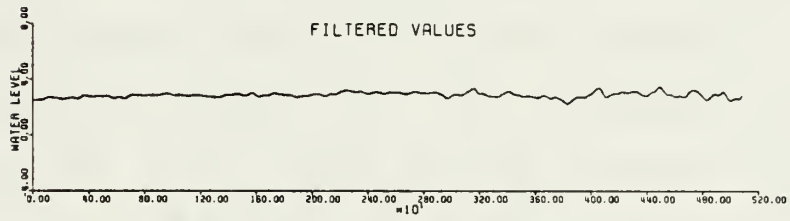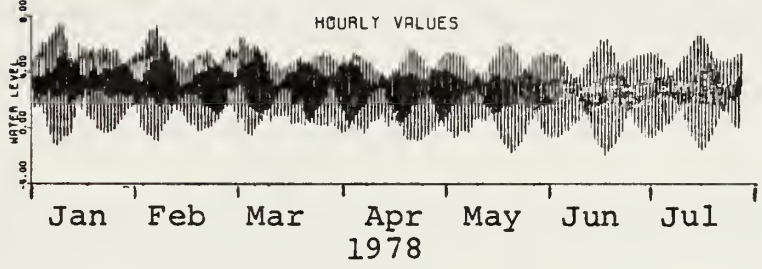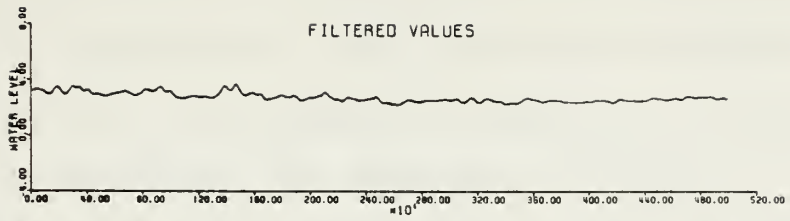
18

Figure 2. Monterey sea level data.

19

Figure 3. Port San Luis sea level data.

20

spectra of these two-month analyses are graphically
presented in Appendix B. The results were ensemble
averaged in order to increase the stability of the
spectral estimates and are presented in Figure 4
($\Delta f = 1/512$ hr^{-1} is the resolution). The ensemble
average is

$$\bar{S}(k) = \frac{1}{N}\sum_{i=1}^{N}\left[S(k)\right]_i$$

where S(k) is the estimated variance spectrum for each
(i^{th}) data set (low pass filtered sea level, in this
case, N the number of data sets in the ensemble,
$\bar{S}(k)$ the ensemble average, and k is a frequency index.
In summary, the S(k) (throughout this thesis) have
resolution $\Delta f = 1/512$ hr^{-1} and four degrees of freedom,
and the ensemble averages $\bar{S}(k)$ have the same resolution
and 4N degrees of freedom.

Since, for the eighteen month ensemble average, the
ensemble consisted of nine two-month variance spectra
for each station, Monterey and Port San Luis. (All
references to "two-month" spectra in this thesis
actually refer to the first 1024 hourly (43 days)
values occurring during the two-month time block.)
After ensemble averaging these spectral values have
36 degrees of freedom. The energy in frequencies above
.014 cycles per hour (periods less than 73 hrs) quickly
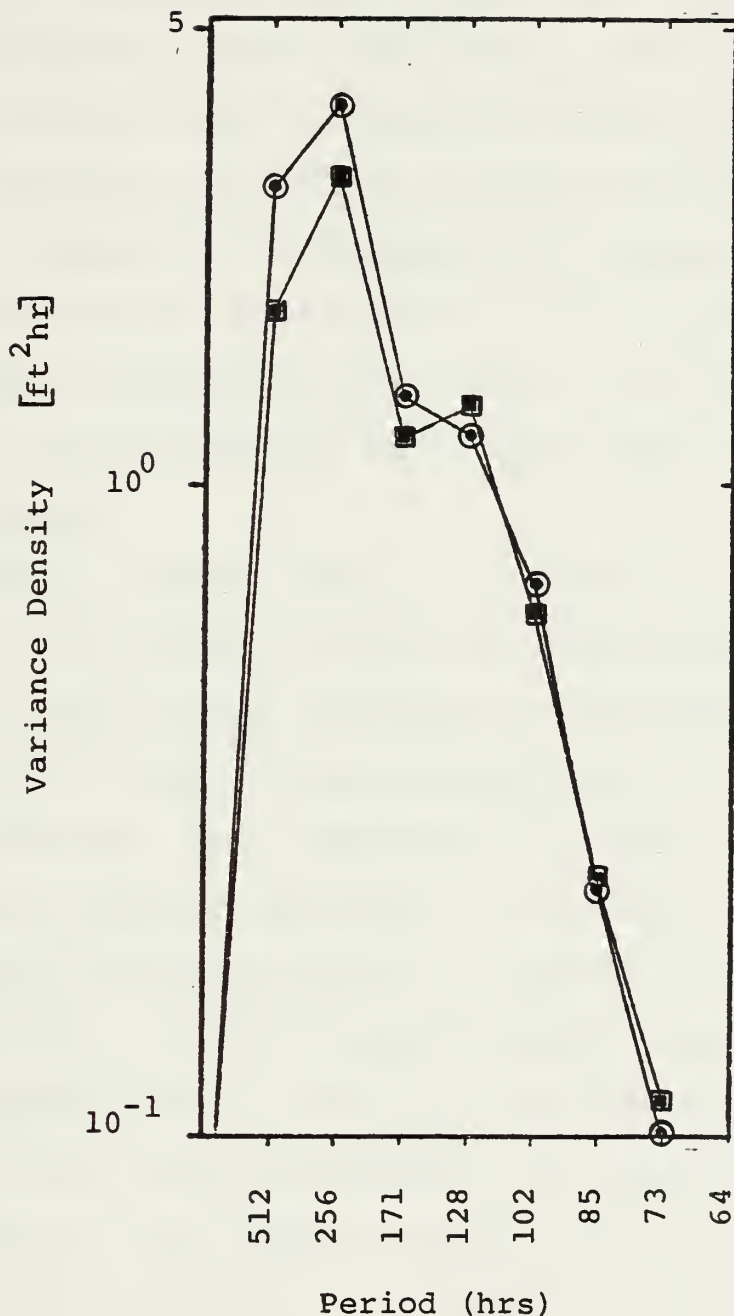tends toward zero, and consequently these frequencies

21

Figure 4. Eighteen month ensemble (nine two-month intervals) averaged low pass filtered sea level variance density. (36 degrees of freedom in each spectral estimate.) ⊙ Monterey; ■ Port San Luis.

22

are omitted. This sharp cut-off held true for both hourly and filtered data, with the exception of the extremely strong energy peaks at the 12.5- and 24-hr lunar-solar tidal periods in the hourly data.

The variance spectra of filtered data are similar for both stations, as might be expected due to their geographic proximity. Both spectra show energy concentrated at periods of 256 hr and at 128 hr. This suggests that the non-tidal components of sea level at both stations respond to the same driving mechanisms, such as passing weather systems.

In order to examine seasonal differences, filtered data from each station were then ensemble averaged as referenced earlier using Skogsberg's three-season annual cycle to define three corresponding ensembles. As before, sea levels were analyzed for spectral variance in two-month segments, and the nine two-month blocks were ensemble averaged by season: Davidson Current period (winter), Upwelling period (spring-summer), and Oceanic period (fall). Due to the constraints imposed by the two-month analysis process, the seasonal periods each contain an even number of months, with "transition months" - March and August - included in the Upwelling period. Winter, the Davidson Current period, is defined as the four-month period November through February,

23

spring-summer, the Upwelling period, is the six-month
period March through August, and September and October
comprise fall, the Oceanic period. These spectra are
presented in Figure 5.

The variance spectra from both stations are similar
on a seasonal basis, and each resembles the 18-month
ensemble averaged spectrum. During winter, both stations
exhibit maximum energy at 256 hr with secondary maxima
at the 128-hr period. Winter spectra from both staions
show much more energy at 64-hr period than appears in the
other seasons.

The summer and fall spectra are similar to the winter
spectra at both stations, except that neither exhibits the
high frequency energy observed in the two winter spectra.
Both show high energy concentrations at the low
frequency end of the spectrum, although this may be
slightly misleading. Included in the lowest frequency
of the spectra is energy whose periods are unresolveable
with the existing record length and confidence interval.
Both also show energy concentrations with a period of
102 hr. At higher frequencies, variance density quickly
falls off.

Some work has been done to evaluate the influence
of alongshore pressure gradients on longshore oceanic
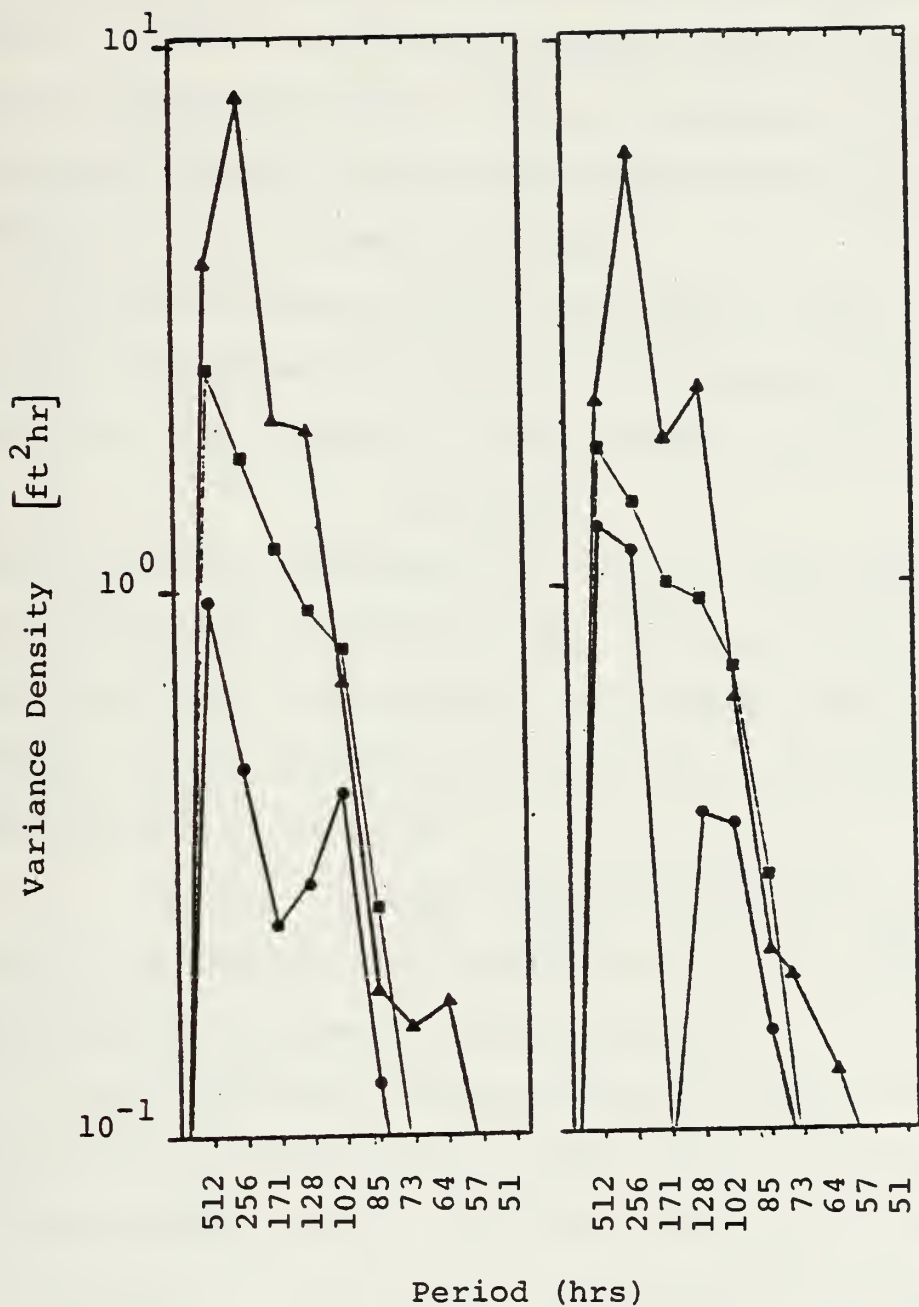flow. Mittelstaedt (1978) suggests that large scale

24

Figure 5. Ensemble averaged low pass filtered sea
level spectra according to season. ▲ Davidson
Current period (winter), eight degrees of freedom;
■ Upwelling period (spring/summer), twelve degrees
of freedom; ● Oceanic period (fall), four degrees
of freedom.

25

atmospheric pressure gradients contribute to the longshore oceanic pressure variation. Preller and O'Brien (1979) consider the relationship between alongshore atmospheric pressure gradient forcing and alongshore flow using Hurlburt's (1974) numerical model.

It can be assumed that at some depth in the ocean a level surface exists common to both Monterey and Port San Luis. The pressure at this surface is given by

$$P = P_a + \bar{\rho} g h$$

where P_a is the atmospheric pressure, h the height of the water column above the level surface, and $\bar{\rho}$ is the mean density of that column. The pressure difference between Monterey and Port San Luis observed at this level surface is given by

$$P_M - P_{PSL} = \left[(P_a)_M - (P_a)_{PSL} \right] + \bar{\rho} g \left[\eta_M - \eta_{PSL} \right]$$

where η is the sea surface elevation, and $\bar{\rho}$ and g are considered to be equal at both locations.

If the atmospheric pressure contribution to this equation is considered to be small[1] due to the proximity of Monterey and Port San Luis tide stations to each other, the equation for the pressure differential (gradient) can be simplified to

$$\Delta P \sim \eta_M - \eta_{PSL}$$

_____

[1]Ideally $(P_a)_M - (P_a)_{PSL}$ should be obtained from meteorological records and steric influences evaluated at each station, but time did not permit the inclusion of such analysis in this thesis.

26

In order to evaluate $\eta_M - \eta_{PSL}$, the hourly data for
the entire 19-month period for each station were summed
and an average value determined. This value, an average
"height of tide," is then defined as the "mean sea level"
for the time interval of the data used in this thesis
and is assumed to be constant and equal at both stations,
and therefore, parallel to the level surface previously
discussed. This terminology should not be confused
with the standard NOS definition of mean sea level,
which is derived from evaluation of sea level heights
for an entire 18.61 year lunar nodal cycle. Since the
19-month observational period is less than 10% of the
lunar nodal cycle, the variations caused by this long
term periodicity are neglected. The mean sea level
values for the two stations were compared, and a correction
of +0.84 ft was applied to the Monterey data in order
to make its mean value consistent with the Port San Luis
mean sea level value. The "correction" permits the
differences in level $\eta_M - \eta_{PSL}$ to be interpreted as
(approximately) absolute differences. To examine the
alongshore sea level gradient $\eta_M - \eta_{PSL}$ was formed from
hourly values of the sea levels. The height differences
were then low pass filtered in the same manner as
previously mentioned, and the results presented in
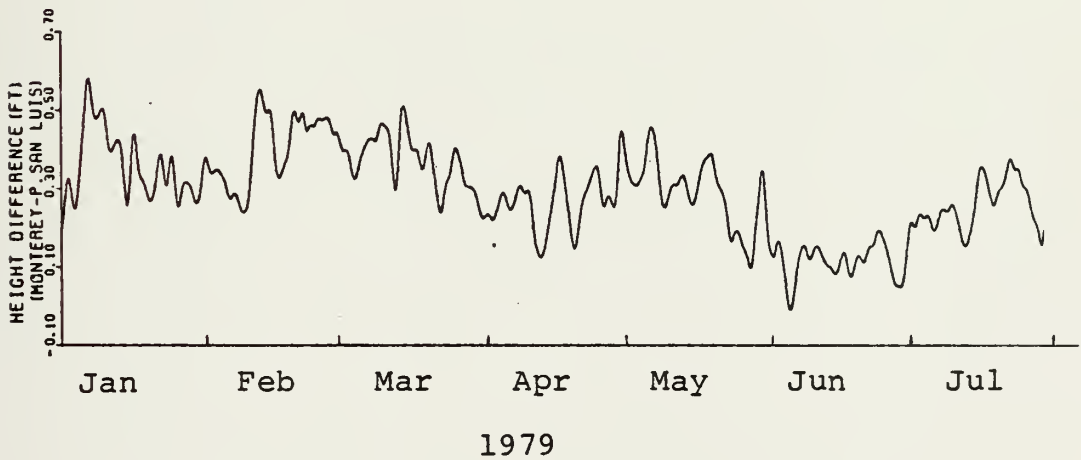Figure 6. Again, the seven-month format has been used

27
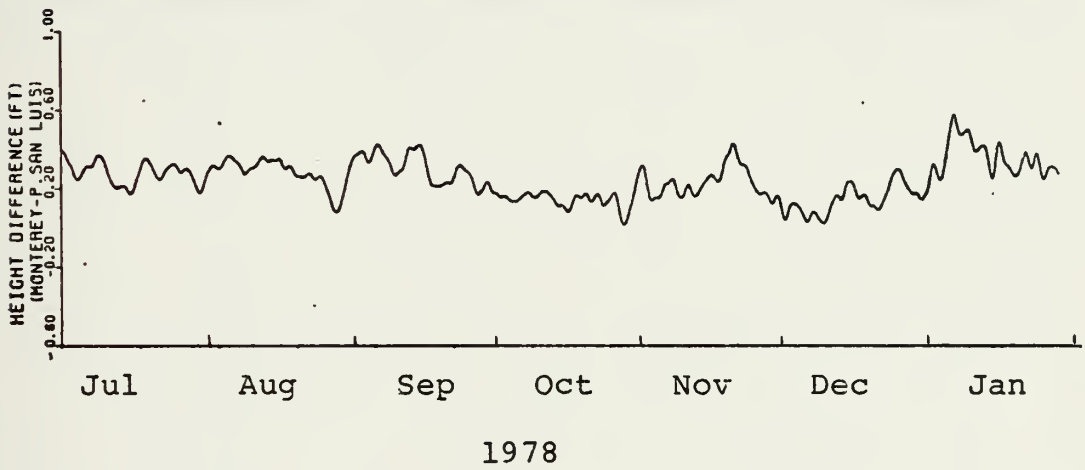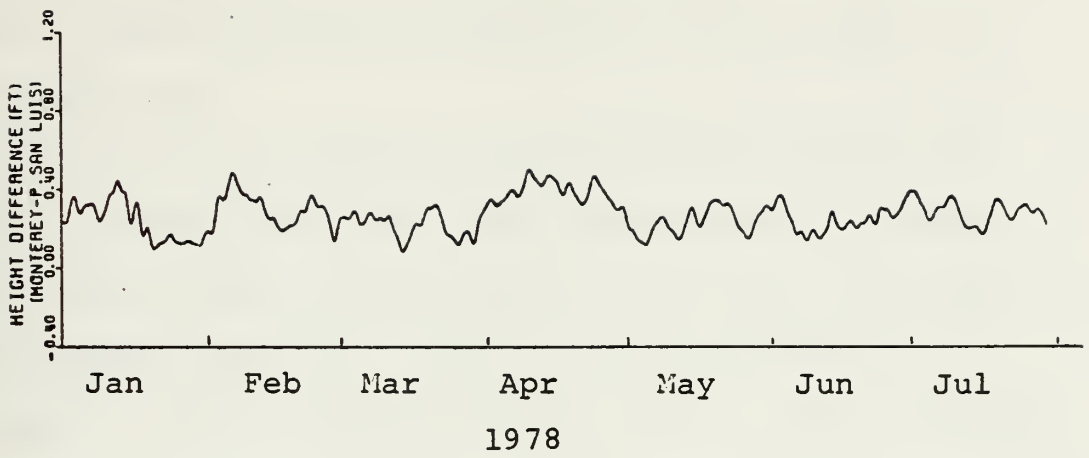
Figure 6.   Low Pass filtered sea level
differences (Monterey - Port San Luis)

28

for presentation of these data. (Note that the vertical
scale on the bottom presentation is twice as great as
the upper two.)

The variance spectra of the low pass filtered sea
level difference data for the winter periods November-
December 1978 and January-February 1979 were calculated
and ensemble averaged. The results are presented in
Figure 7. At periods shorter than 39 hr, the calculated
variance approached zero, and is therefore, not presented.

Figure 7. Ensemble averaged sea level difference (Monterey - Port San Luis) energy spectra for two-month observational periods November-December 1978, and January-February 1979. (Eight degrees of freedom).

30

V.   CURRENT OBSERVATIONS

A.   DESCRIPTION OF METERING AND NATURE OF DATA
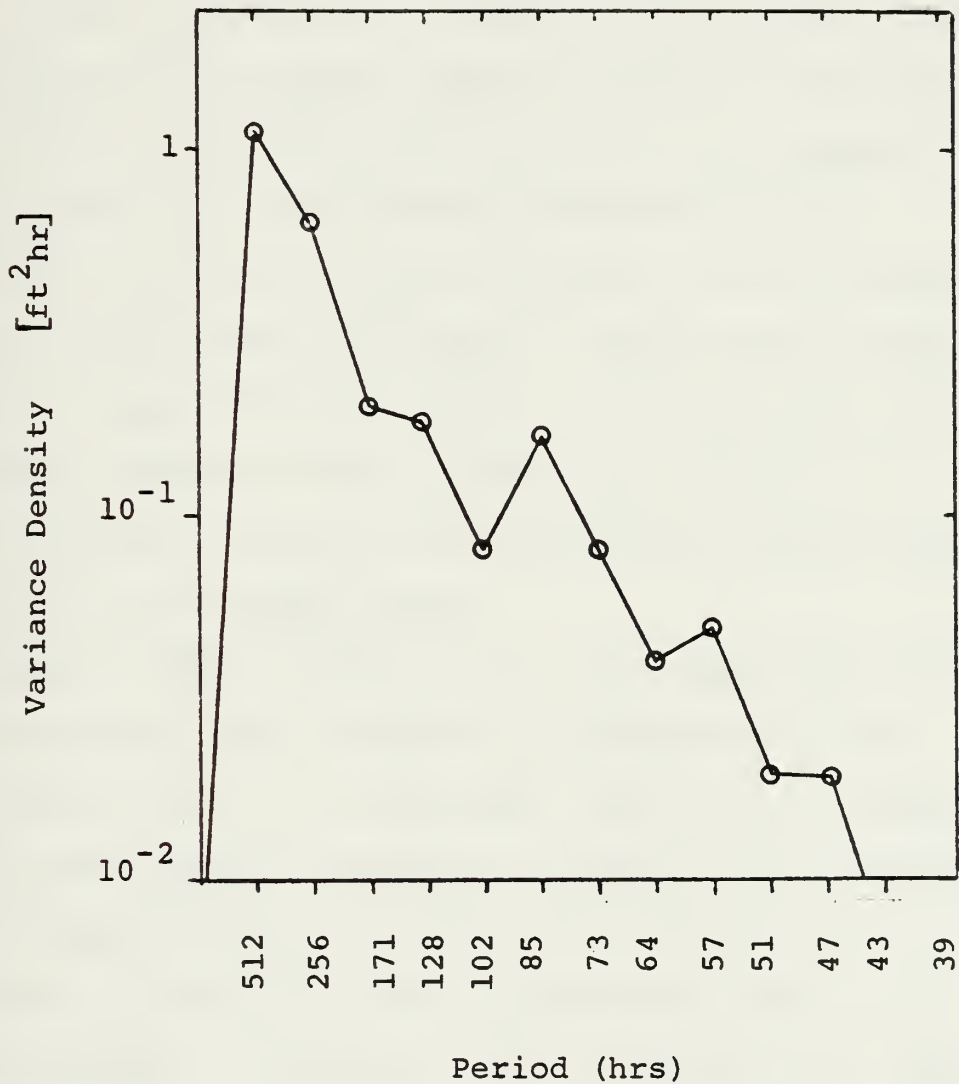
Current data from two of the mooring sites to the west of Cape San Martin were used in this study. The mooring sites are roughly midway between the Monterey and Port San Luis tide stations (Figure 1). Station 2 lies 3.8 nmi (7.0 km) offshore (Latitude 35°52'N, Longitude 121°33'W) in 350 m of water, a short distance seaward of the narrow and steeply sloping shelf break. Station 5 lies seaward of station 2, 10.2 nmi (18.9 km) offshore (Latitude 35°52'N, Longitude 121°41'W) in 780 m of water. Figure 8 illustrates the relative meter locations in the water column.

Aanderra RCM-4 current meters were deployed on both moorings which were anchored by railroad wheels and connected by 5/32", 7x7 stainless stell wire. Buoyancy for the mooring was provided by strings of 17-in Benthos glass spheres housed in plastic "hard hats," and connected in pairs with 3/8-in galvanized chain. No surface markers or surface floatation were used. This, combined with a 100-m nominal depth for the uppermost meter, minimized noise in the current record caused by surface pumping of the mooring. Figure 9 schematically portrays the arrays, except that three meters were deployed on each mooring, instead of the two illustrated.
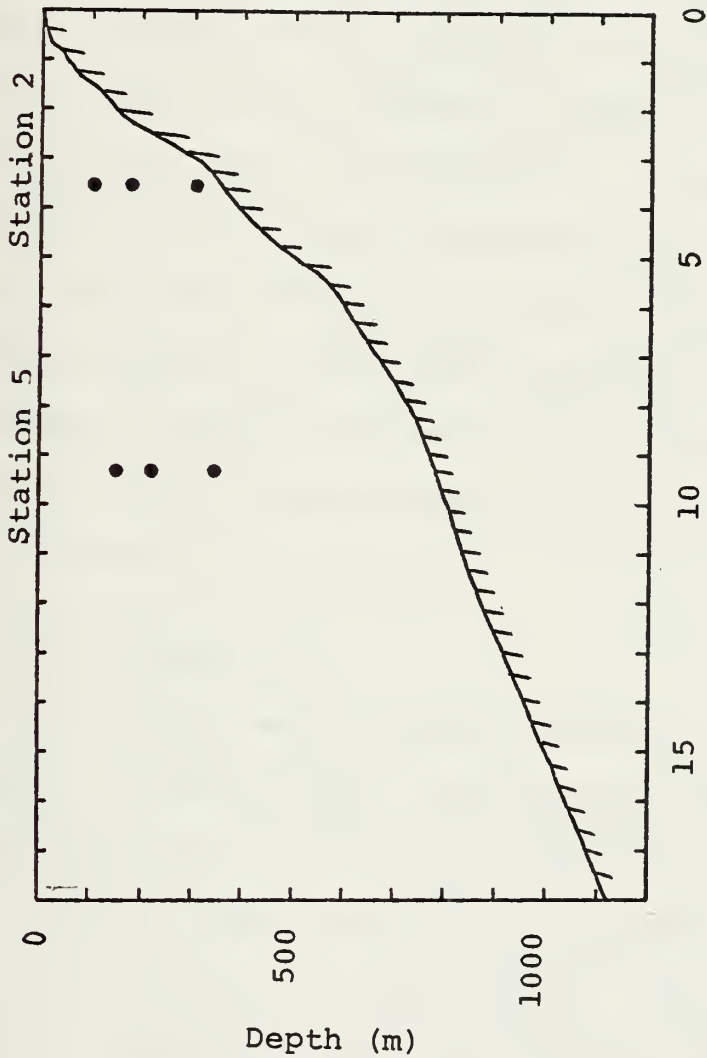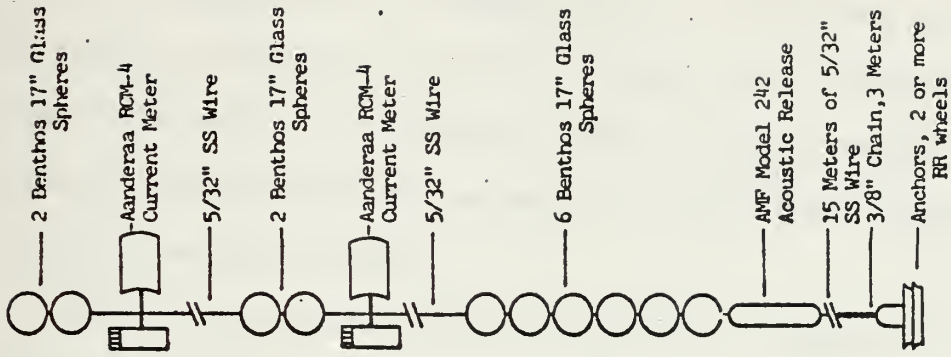
Figure 8. Current meter (●) locations.

Figure 9. Current meter array.

32

Both moorings were deployed on 27 November 1978 and were recovered on 22 January 1979. All three meters deployed at Station 2 operated well. The upper meter was deployed at 100-m depth, the mid-depth meter at 175-m, and the deepest meter at 300-m, approximately 50-m above the bottom.

Two of the three meters deployed at Station 5 operated well. The upper meter was deployed at 140-m depth, and the mid-depth meter at 215-m. The third meter, which did not produce a speed record due to an inoperative rotor, was deployed at a depth of 340-m, 440-m above the bottom. Consequently, data from this meter were not available for use in subsequent variance density analysis. Since the direction records were good, a constant speed of 20 cm/sec was introduced into the record to permit observation of the direction record on stickplots (Appendix C).

B. DATA PROCESSING

All current meters used a ten minute sampling interval. Occasionally, the recorded meter reference number did not match that specified by the manufacturer, and this was taken as an indication that the digitizer had malfunctioned for that record. During the initial stage of processing these records were zero filled. Before stickplots were made of the current records, and

33

before the record was subjected to spectral analysis, speed and direction records associated with incorrect reference numbers were replaced by interpolated values. This was done to avoid biasing later results by including records which were completely out of line with the remainder of the data.

Interpolated speed values were obtained by arithmetic-ally averaging four adjacent speed values, two preceeding and two following the erroneous data point. A direction was assigned to this speed value by averaging the directions immediately preceeding and following the erroneous data point. Since two solutions are possible when averaging two angles (directions), the solution used was always that which produced the smallest angular difference in bisecting the "parent" angles (directions). This technique worked well when a single record was missed - which was the usual case - but was increasingly less effective as the number of successive erroneous records increased. In the few cases where numerous - on the order of 10-12 - successive records were missing, the interpolation technique tapered the record from good data to none, where zeros occurred.

Following the insertion of interpolated values for missed records, 10 min records were filtered via a nine-point binominal filtering process (Hickey and

34

Hamilton, 1979) to produce hourly speed values. The observed (recorded) direction coincident with the time of the calculated hourly speed observation was assigned to the hourly speed for later analysis. The effect of this procedure on the data is discussed in Data and Reliability of Spectral Estimates (page 46).

The hourly current vectors for each meter - including the meter with the blocked rotor - are shown as stickplots with true north "up" (Appendix C). Progressive vector diagrams for the five operating meters are presented in Appendix D (from Coddington, 1979).

Subsequently, current records were converted into "alongshore" and "cross shelf" components for further study. An alongshore direction was defined for each station. The direction chosen was the average direction of the bottom contour between the mooring site and a point 15-nmi to the south, estimated by eye from National Ocean Survey Bathymetric Map NOS 1306N-20, 1975. The directions selected for the stations were Station 2, 340° (true); Station 5, 350° (true). Although this procedure may seem arbitrary, calculated alongshore vs. cross shelf variances tend to confirm the choice (Figure 10 shows that alongshore variance density is nearly ten times the cross shelf variance density.)

C. ANALYSIS

Spectral analysis was performed on current obser-
vations to permit a more detailed comparison of current
to sea level data than would otherwise be possible.
This analysis showed that the semi-diurnal signal was
large in both the alongshore and cross shelf records
for all meters. The diurnal signal also appeared in
both records, but with less energy than the semidiurnal
signal.

Both components were low pass filtered with the
Godin (1966) filter, again using 24-, 24-, and 25-hr
running means. These data were spectrally analyzed.
Their spectra along with spectral analysis of the
hourly data, are presented in Appendix E and show that
little energy is contained in frequencies above .04
cycles per hour (25-hr period). These spectra were
then ensemble averaged and are presented in Figure 10.
The resolution in that spectrum is $1/512$ hr^{-1}, and
each spectral estimate has four degrees of freedom.

In the cross shelf component, energy is concentrated
above background in minor peaks at 256-, 102- and 51-hr
periods. The alongshore spectrum shows energy concentrated
in prominent peaks at 256-, 73-, 51-, and 43-hr periods,
and generally large high frequency energy. The 256-hr
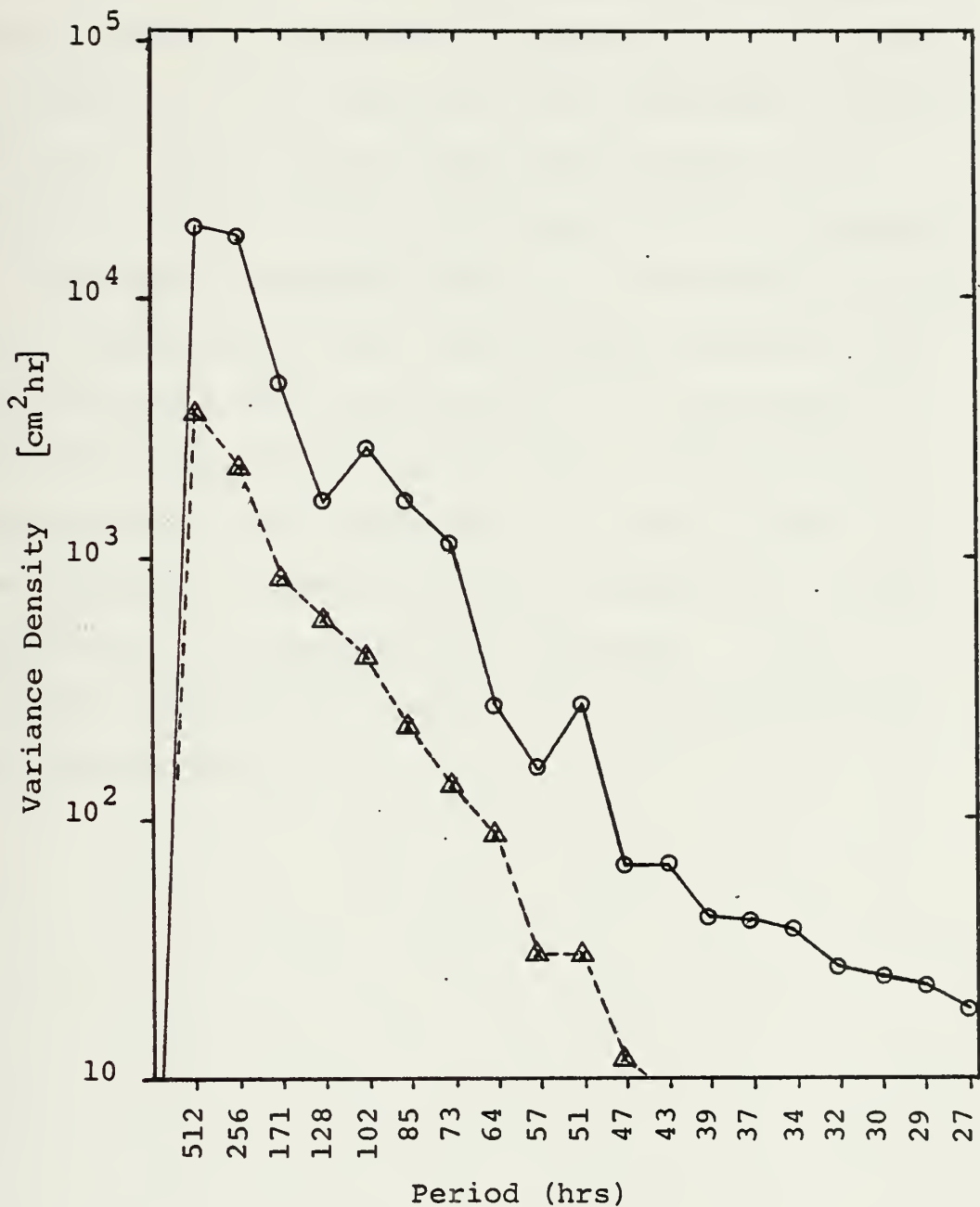peaks agree with both the spectra of the 18-month sea

36

Figure 10. Ensemble averaged (over all five fully operating meters) low pass filtered alongshore (o) and cross shelf (▲) variance spectra. Twenty degrees of freedom for each spectrum

level record (Figure 4), and the winter sea level
record (Figure 5). The 102-hr signal in each component
current spectrum (especially alongshore) has a corres-
ponding peak in the winter sea level spectrum (Figure 5),
and may be associated with the 128-hr peak in the
18-month ensemble averaged sea level spectrum (Figure 4).

The higher frequency signals in the alongshore flow
do not match up with any high frequency peaks in the
sea level data from either station, but do coincide
with peaks observed in the sea level difference data,
suggesting that the alongshore sea level gradient and
the alongshore poleward flow are interrelated, or are
responding to the same driving mechanism. Cross-
spectral analysis is a logical next step in defining
this relationship.

VI. CONSIDERATION OF POSSIBLE LOCAL FORCING

The relation between wind stress and ocean currents, and wind stress and sea levels has been examined by other authors. To examine these relationships, coastal upwelling indices (Figure 11a and 11b) for Latitude 36°N, Longitude 122°W were obtained, derived by Bakun (personal communication, 1980). Index units are metric tons per second per 100-m of coastline, and are an indication of relative fluctuations in onshore/offshore Ekman transport, estimated from wind stress, not an absolute measure. Coastline distance is measured along a straight line following the dominant trend of the coast (Bakun, 1975).

During 1978 the largest average week-long index value occurred during the week beginning 30 April, but the sustained maximum (in weekly averages) occurred during June and July, slightly later than "average." From this sustained maximum period, the index declined steadily in a general sense, approaching the zero, or no upwelling level, during the week beginning 12 November. The weekly average remained at a relatively low value for two weeks, when a sudden positive pulse occurred during the week of 26 November. This pulse was sustained for a period of about a week, from 29 November through 6 December.

NOAA/NMFS PACIFIC ENVIRONMENTAL GROUP - MONTEREY, CALIFORNIA
COASTAL UPWELLING INDICES, DAILY AND WEEKLY MEANS

DURING 1978   AT 36N, 122W

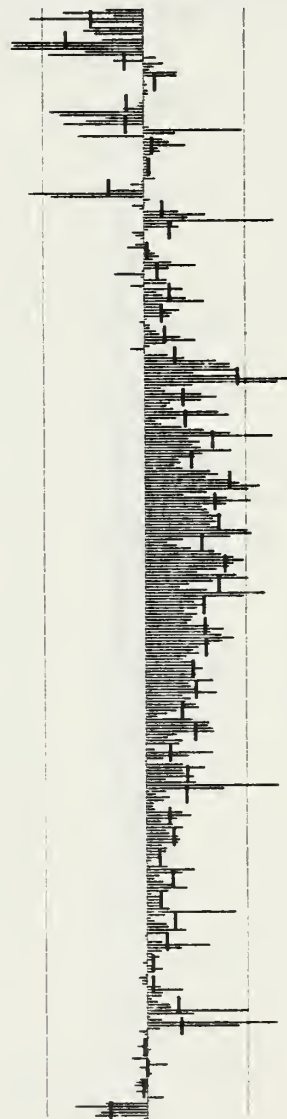| WEEK BEGINNING	SUN	MON	TUE	WED	THU	FRI	SAT	WEEKLY MEAN	CUBIC METERS PER SECOND PER 100 METERS OF COASTLINE −400 −200 0 200 400
1 JAN	-75	-150	-58	-224	-103	-8	-108	-105	
8 JAN	-117	-96	-2	-82	-260	-255	-262	-154	
15 JAN	-118	-188	25	-58	38	18	13	-38	
22 JAN	68	87	1	3	7	-8	8	22	
29 JAN	7	2	2	-7	-12	-48	-186	-33	
5 FEB	-167	-78	-114	-159	18	194	62	-36	
12 FEB	-129	35	49	61	28	31	12	15	
19 FEB	5	11	12	8	11	15	5	10	
26 FEB	22	-5	-28	-6	-64	-228	-185	-70	
5 MAR	12	1	-23	-7	67	121	85	37	
12 MAR	257	58	68	9	-22	-16	-8	49	
19 MAR	1	-18	-93	12	23	31	18	5	
26 MAR	55	182	48	-4	-58	-8	44	26	
2 APR	44	-26	78	24	38	81	118	50	
9 APR	36	32	68	55	58	4	-9	34	
16 APR	18	18	22	38	71	188	42	41	
23 APR	18	-28	-8	48	78	148	167	59	
30 APR	168	188	95	166	287	262	94	183	
7 MAY	32	41	113	142	112	58	43	76	
14 MAY	55	146	168	82	28	32	73	79	
21 MAY	118	189	252	87	188	94	118	134	
28 MAY	178	114	97	87	68	57	75	93	
4 JUN	128	143	128	167	167	228	283	168	
11 JUN	123	76	163	288	161	113	123	138	
18 JUN	125	158	133	138	128	142	283	146	
25 JUN	288	167	73	43	61	98	135	111	
2 JUL	146	173	183	174	168	142	182	157	
9 JUL	188	288	194	68	67	121	235	147	
16 JUL	193	118	95	119	182	76	182	115	
23 JUL	91	88	61	125	154	128	149	117	
30 JUL	174	151	128	185	94	188	79	119	
6 AUG	73	84	97	113	93	97	92	94	
13 AUG	131	83	87	182	148	72	88	101	
20 AUG	79	87	185	59	42	23	188	72	
27 AUG	125	122	132	134	61	42	71	98	
3 SEP	65	-1	17	132	84	35	-2	47	
10 SEP	73	118	72	76	95	39	99	81	
17 SEP	262	159	98	18	46	35	14	81	
24 SEP	12	18	71	88	61	28	53	47	
1 OCT	72	36	48	63	65	62	31	54	
8 OCT	41	39	28	29	6	1	41	27	
15 OCT	93	78	23	15	32	58	68	52	
22 OCT	42	8	24	23	24	28	44	28	
29 OCT	176	36	5	14	38	42	75	55	
5 NOV	42	-5	-1	38	123	87	27	41	
12 NOV	18	23	12	-8	11	38	18	13	
19 NOV	-4	-15	-18	-18	25	89	31	12	
26 NOV	28	8	28	45	48	197	93	62	
3 DEC	4	28	257	182	24	-15	-5	68	
10 DEC	1	-8	-9	-18	5	9	-9	-5	
17 DEC	-29	4	37	-18	-4	7	-3	-1	
24 DEC	-16	-22	-25	-7	-22	8	31	-9	
31 DEC	2	-84	-144	-82	-92	-184	-8	-73	

Figure 11a.   Coastal upwelling indices
(from Bakun).

NOAA/NMFS PACIFIC ENVIRONMENTAL GROUP - MONTEREY, CALIFORNIA
COASTAL UPWELLING INDICES, DAILY AND WEEKLY MEANS
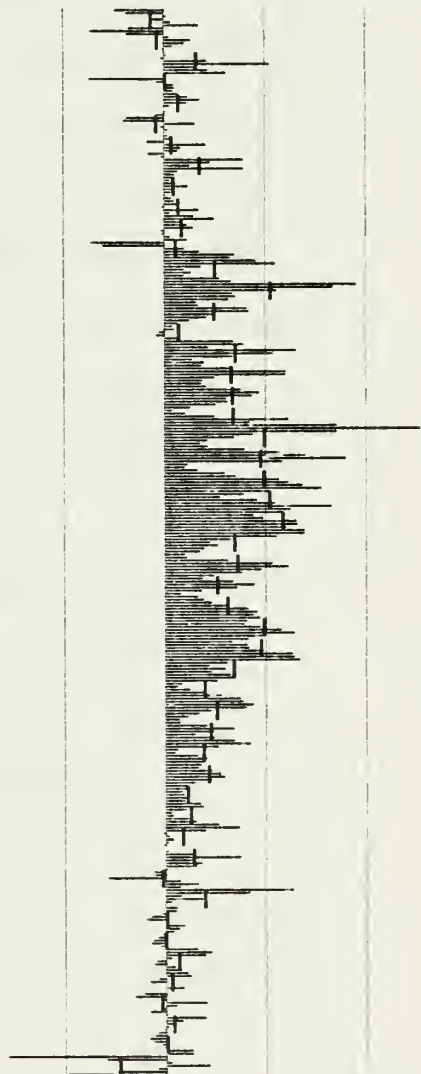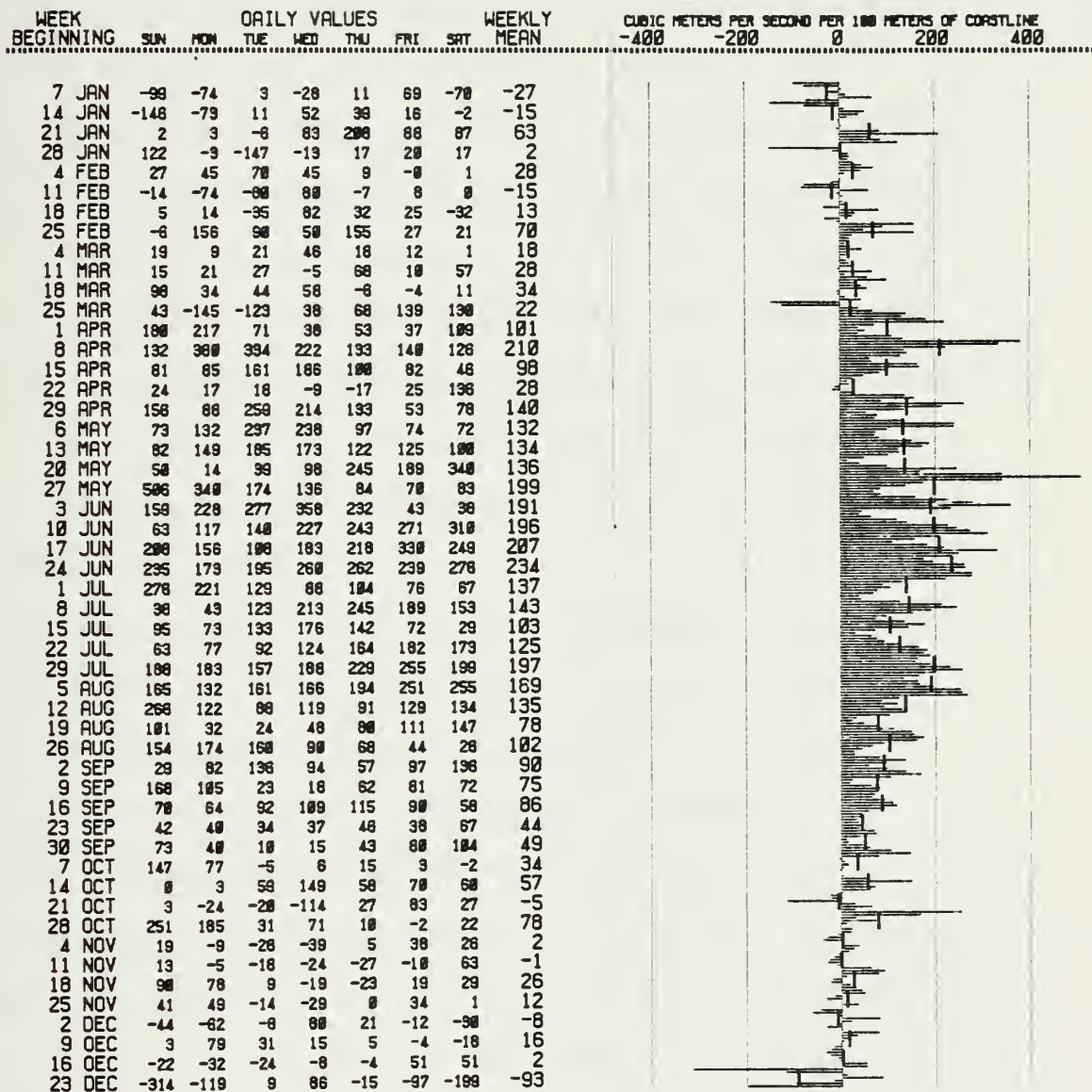
DURING 1979   AT   36N, 122W

WEEK BEGINNING	SUN	MON	TUE	WED	THU	FRI	SAT	WEEKLY MEAN	CUBIC METERS PER SECOND PER 100 METERS OF COASTLINE (-400 -200 0 200 400)
7 JAN	-99	-74	3	-28	11	69	-70	-27	
14 JAN	-148	-79	11	52	39	16	-2	-15	
21 JAN	2	3	-8	83	208	88	87	63	
28 JAN	122	-9	-147	-13	17	20	17	2	
4 FEB	27	45	70	45	9	-0	1	28	
11 FEB	-14	-74	-80	80	-7	8	0	-15	
18 FEB	5	14	-95	82	32	25	-32	13	
25 FEB	-8	156	98	50	155	27	21	70	
4 MAR	19	9	21	46	18	12	1	18	
11 MAR	15	21	27	-5	68	10	57	28	
18 MAR	98	34	44	58	-8	-4	11	34	
25 MAR	43	-145	-123	38	68	139	130	22	
1 APR	180	217	71	36	53	37	109	101	
8 APR	132	380	394	222	133	140	128	210	
15 APR	81	85	161	166	100	82	48	98	
22 APR	24	17	18	-9	-17	25	136	28	
29 APR	158	86	259	214	133	53	78	140	
6 MAY	73	132	297	238	97	74	72	132	
13 MAY	82	149	185	173	122	125	100	134	
20 MAY	58	14	99	98	245	189	340	136	
27 MAY	506	340	174	136	84	70	83	199	
3 JUN	159	228	277	358	232	43	38	191	
10 JUN	63	117	140	227	243	271	310	196	
17 JUN	200	156	100	183	218	330	249	207	
24 JUN	235	179	195	260	262	239	278	234	
1 JUL	278	221	129	88	104	76	67	137	
8 JUL	38	43	123	213	245	189	153	143	
15 JUL	95	73	133	176	142	72	29	103	
22 JUL	63	77	92	124	164	182	173	125	
29 JUL	180	183	157	188	229	255	199	197	
5 AUG	165	132	161	166	194	251	255	169	
12 AUG	268	122	80	119	91	129	134	135	
19 AUG	101	32	24	48	80	111	147	78	
26 AUG	154	174	160	90	68	44	28	102	
2 SEP	29	82	136	94	57	97	198	90	
9 SEP	168	105	23	18	62	81	72	75	
16 SEP	70	64	92	109	115	90	58	86	
23 SEP	42	40	34	37	48	38	67	44	
30 SEP	73	40	10	15	43	80	104	49	
7 OCT	147	77	-5	6	15	3	-2	34	
14 OCT	0	3	58	149	58	70	68	57	
21 OCT	3	-24	-20	-114	27	83	27	-5	
28 OCT	251	185	31	71	10	-2	22	78	
4 NOV	19	-9	-28	-39	5	38	26	2	
11 NOV	13	-5	-18	-24	-27	-18	63	-1	
18 NOV	90	78	9	-19	-23	19	29	26	
25 NOV	41	49	-14	-29	0	34	1	12	
2 DEC	-44	-62	-8	80	21	-12	-90	-8	
9 DEC	3	79	31	15	5	-4	-18	16	
16 DEC	-22	-32	-24	-8	-4	51	51	2	
23 DEC	-314	-119	9	86	-15	-97	-199	-93	

Figure 11b. Coastal upwelling indices
(from Bakun).

41

The impact of this impulse may be observed in the current record of five of the six meters (see stickplots, Appendix C). The upper two meters at Station 2, and all three meters at Station 5 showed predominantly northward flow at the time of deployment on 27 November 1978. Following the upwelling pulse on 29 November, the flow at all five meters changed. The middle meter at both stations (175-m at Station 2, 215-m at Station 5) and the deepest meter at Station 5 responded most quickly, with flow rapidly changing in a clockwise direction to become eastward, then more southward. The upper meter (100-m) at Station 2 recorded a similar direction change, but about a day later. The upper meter at Station 5, also recorded a similar change, but about two days after the upwelling pulse.

After the pulse subsided on 7 December, the current reocrds from the five meters again show a clockwise rotation of current, passing through westward flow. The stickplots show that the upper two meters at Station 2 changed most rapidly, indicating northward flow within a day of the decrease in positive upwelling index. The three meters at Station 5 responded almost in unison, but about a day later than the response at Station 2.

42

The deepest meter at Station 2 (300-m depth) apparently did not show a clear response to the upwelling index changes. Its record appears to be dominated by strong and periodic reversals of flow which suggest a coastal or bottom trapped wave.

Following the upwelling pulse, the index becomes weakly negative during the week of 10 December 1978. A negative index indicates downwelling at the coast and offshore cross shelf flow at depth, which is deflected poleward by the Coriolis force. The current record confirms this activity (Appendix C).

The variance density spectrum of six-hourly upwelling indices was also obtained from Bakun (personal communication, 1980) and is presented (Figure 12). It presents the mean spectrum for eight consecutive (1968-1975) three-month periods (December-February) for Latitude 33°N.

The spectrum shows a spike at the diurnal period, which was also observed in the spectra of unfiltered sea level and current meter data discussed earlier. In addition to this spike, some variance above background is also observed at 120-hr, and 80- and 60-hr periods. The remainder of the record is largely "red noise," a general decrease in energy with increasing frequency, but with a relatively high level remaining at high

43
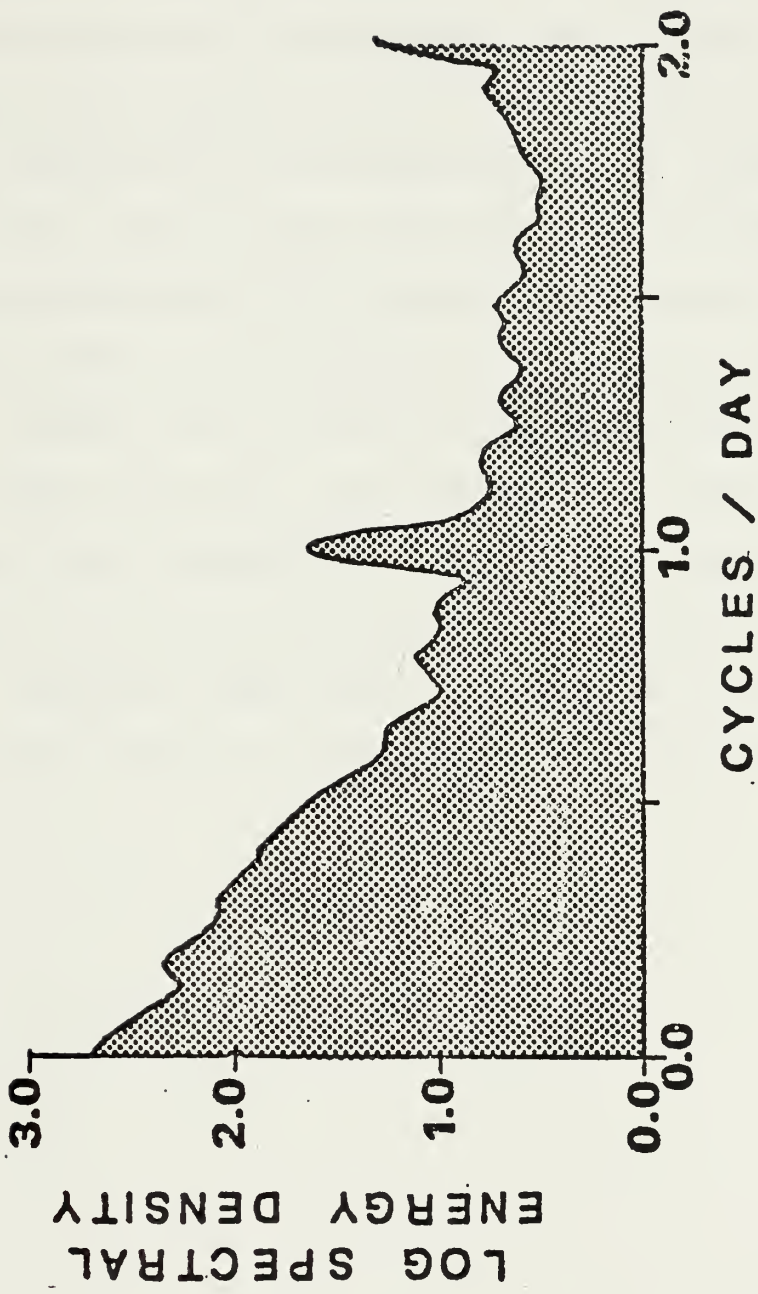
Figure 12. Energy spectrum for Coastal Upwelling
index for latitude 33°N. (After Bakun)

44

frequencies. Sea level and current data discussed
earlier were low pass filtered, and this noise in the
high frequency end of the spectra was not observed.

These observations demonstrate that at least large
scale amplitude fluctuations in the upwelling indices
manifest themselves in corresponding local current
fluctuations. This is not surprising, since wind
stress is recognized to be a major driving force in
the establishment and maintenance of nearshore current
system. Further, the periods at which there are peaks
in the winter upwelling index spectrum correspond to those
observed in the longshore and cross shelf spectra of
the current records obtained during the Davidson Current
period. Together, they tend to confirm the interrelated-
ness of wind stress, up- and downwelling, and nearshore
flow.

VII. DATA AND RELIABILITY OF SPECTRAL ESTIMATES

An inherent problem in dealing in spectral estimates
is balancing loss of resolution with increased confidence.
Since a fast fourier technique was used in determining
the spectral estimates, the number of records analyzed
had to be a power of two. The largest record length in
a two month data set of hourly values which meets this
requirement is 1024. To achieve even four degrees of
freedom in the spectral estimates, frequency resolution
was reduced to $1/512$ hr^{-1}. Attempting to reduce further
the confidence interval of a two month record would have
caused unacceptable loss in resolution. The solution,
therefore, was to ensemble average the spectra in order
to achieve more stable estimates. The shortcoming in
this approach is recognized, since the ensemble
averaging process smooths strong activity occurring in
some data sets but not in others, e.g., summer vs. winter
spectra. When the members of the ensemble are carefully
chosen, however, the averages are both stable and
meaningful. In summary, then, the data sets were handled
in a way which was a compromise among resolution,
confidence, and meaning in the spectral estimates.

This study addressed events with subtidal frequencies.
Since the accuracy of spectral estimates is influenced
by leakage, it was decided to filter higher frequencies,

which were not of interest, in order to minimize potential inaccuracies from this source. The spectral estimates, (aside from the red noise background) therefore, are believed to be fairly accurate, within the confidence interval limitations which accompany the number of degrees of freedom inherent to each estimate.

The spectral estimates developed for the alongshore and cross shelf components of created hourly currents still display considerable high frequency energy. Since the Nyquist frequency for hourly observations is 1/2-hr, potential aliasing of high frequency energy into lower frequencies presents a threat to the accuracy of spectral estimates. Consequently, current records were low pass filtered in the same manner as the sea level records in order to minimize the influence of frequencies higher than tidal frequency. With these considerations in mind, the analyses will be discussed, considering sea levels first.

Hourly sea level data were separated into two month blocks, each containing between 1416 and 1488 hourly values. The spectra calculated for the two month data sets via a fast fourier technique are derived from only the first hourly 1024 values, a power of two as required by that analysis method. Those 1024 values were further divided into two data "windows," each containing

512 records. The fundamental record length is thus 512 hours and the corresponding resolution for all spectra shown is 1/512 hours. This is sufficient to resolve frequencies as low as 1/20 cycles per day.

Since each data window provides two degrees of freedom, each two month sea level energy spectral estimate has a statistical variation of a Chi-squared distribution with only four degrees of freedom. Whenever data sets seemed to belong to a common family, as for sea levels or current records in the same season, they were ensemble averaged to increase the number of degrees of freedon, thus increasing stability (narrowing the confidence interval). The 18-month ensemble averaged sea level energy spectrum (Figure 4) contains 36 degrees of freedom, and consequently has the narrowest confidence interval. However, since 18 months does not contain an integral number of annual cycles, this spectrum is not truly representative of the yearly distribution of variance in sea level, being weighted toward the winter regime.

The weakest record is the fall sea level energy spectrum (Figure 5), derived from only a single two-month data period (September-October 1978). Consequently, this spectrum has only four degrees of freedom, and a correspondingly large confidence interval. Because of

this, relatively little reliance should be put on details of the information contained in this record, and it is presented principally as a reference, for want of a larger data set. There is, however, a strong similarity between the spectra at Monterey and Port San Luis during this "interval," lending some credence to the spectral form for this period.

Similarly, the spectrum of the sea level difference data has rather wide confidence limits. Since only three two-month blocks of "winter" hourly heights of tide were obtained from NOS, the ensemble averaged sea level difference energy spectrum could contain 12 degrees of freedom (four from each two-month block, as before). However, by including sea level data from the January-February 1978 data block (ten months before the experiment) in an attempt to narrow the confidence interval, the sea level energy spectrum could easily be distorted into one not physically related to the experimental setting. This is a problem when dealing with small data sets: zeal in trying to stabilize the spectral estimates by appending data must be balanced by careful consideration of the negative impacts of including data not properly a part of the process being studied. With this in mind, only the data for the 1978-9 winter were used in evaluating the sea level difference variance

spectrum. Because of this decision, the spectrum has only eight degrees of freedom and a large confidence interval.

The current meter data sets are of two months duration, recorded at ten minute intervals. The ten minute sampling interval was favored over a longer sampling interval - which would have permitted a longer record - to avoid aliasing of high frequency signals into lower frequencies, which were of interest to this study. It is felt that the alongshore and cross shelf variance spectra (found from ensemble averaging spectra of all five meters) each containing 20 degrees of freedom, are fairly representative of winter (Davidson Current period) flow, since averaging the spectra of all meters tends to smooth out the positional-dependent variations, such as coastal or bottom trapped motions.

The derived hourly current values suffer potential error from another source. The speed values were obtained via a nine-point binomial filtering technique (Hickey and Hamilton, 1980). The direction assigned to this speed was the direction which was recorded at the regular ten minute observation coinciding with the hourly speed value. It is recognized that Aanderra meters record the direction of meter orientation at the time of the observation, and that no vector averaging is

performed by the instrument. These instantaneous
direction values, thus, differ randomly from the mean
for the interval. However, the stickplots - especially
for strong currents - demonstrate that the hourly records
for all meters are internally consistent, except for
only a few "wild" directions. This suggests that the
process used in establishing directions for hourly
values did not create significant distortion in either
the stickplots, or in the spectral estimates. Errors
in the hourly direction value tend to increase the
variance by aliasing high frequency events into low,
but the general shape of the variance spectra should
not be affected, as the aliased high frequency energy
was likely distributed evenly to all frequencies. No
quantitative estimates were made of this effect.

VIII. CONCLUSIONS

The spectra for low pass filtered hourly sea levels at two stations were ensemble averaged over each season and compared. Winter records contained energy peaks at periods of 256- and 128-hr at both Monterey and Port San Luis.

Sea level differences between the two stations were calculated for the study period and the spectrum of this difference was examined to consider the relationship of alongshore sea level gradients between Monterey and Port San Luis to nearby ocean flow. This spectrum showed energy peaks at 128-, 85-, and 57-hr periods. These are considered to indicate response in the longshore sea surface gradient to two energy periods: the first of two to three days, and the second of about five days.

Spectral analysis was also performed on current meter data. The analyses showed energy concentrations above background in the 102- and 51-hr periods for both the alongshore and cross shelf components of current, with the alongshore component almost an order of magnitude greater in these peak bands than the cross shelf component. This is interpreted to be in close agreement with the energy bands found in the alongshore sea level gradient previously discussed. Since resolution between adjacent frequency bands is not perfect, it is believed that peaks

in adjacent bands of the sea level difference and current spectra may indicate response to the same driving mechanism, or that one is responding to the other. In either case, the longshore sea surface gradient and the alongshore flow are interpreted to be interrelated, as suggested by Preller and O'Brien (1979).

In the cross shelf component, energy is concentrated above background in minor peaks at 256-, 102- and 51-hr periods. The alongshore spectrum shows energy concentrated in prominent peaks at 256-, 73-, 51-, and 43-hr periods, and generally large high frequency energy. The 256-hr peaks agree with both the spectra of the 18-month sea level record (Figure 4), and the winter sea level record (Figure 5). The 102-hr signal in each component current spectrum (especially alongshore) has a corresponding peak in the winter sea level spectrum (Figure 5), and may be assoicated with the 128-hr peak in the 18-month ensemble averaged sea level spectrum (Figure 4).

The variance spectra from both stations are similar on a seasonal basis, and each resembles the 18-month ensemble averaged spectrum. During winter, both stations exhibit maximum energy at 256 hr with secondary maxima at the 128-hr period. Winter spectra from both stations show much more energy at 64-hr period than appears in the other seasons.

The summer and fall spectra are similar to the winter spectra at both stations, except that neither exhibits the high frequency energy observed in the two winter spectra. Both show energy high concentrations at the low frequency end of the spectrum, although this may be slightly misleading. Included in the lowest frequency of the spectra is energy whose periods are unresolveable with the existing record length and confidence interval. Both also show energy concentrations with a period of 102 hr. At higher frequencies, variance density quickly falls off.

The winter season sea level spectral estimates indicated energy concentrations in the 256-, 128-, and 64-hr periods. In comparison, the mean winter season spectrum of Bakun's upwelling indices does not indicate energy concentrated in the 256-hr period, but does indicate concentrations at 120-, 80-, and 60-hr periods, which are interpreted to agree with the referenced sea level spectra.

APPENDIX A

List of missing records from hourly heights of tide.

Monterey

| 0300-0800 | 15 June 1978 | (5 hours) |
| 0900 1 April 1979 - 0800 2 April 1979 | (23 hours) |

Port San Luis

1100-1200	1 April 1978	(2 hours)
1000-1500	20 April 1978	(5 hours)
0100-0500	5 June 1978	(4 hours)
1400 25 June 1978 - 1400 26 June 1978	(24 hours)
1400-1500	29 June 1978	(2 hours)
1200 - 23 March 1979	(1 hour)
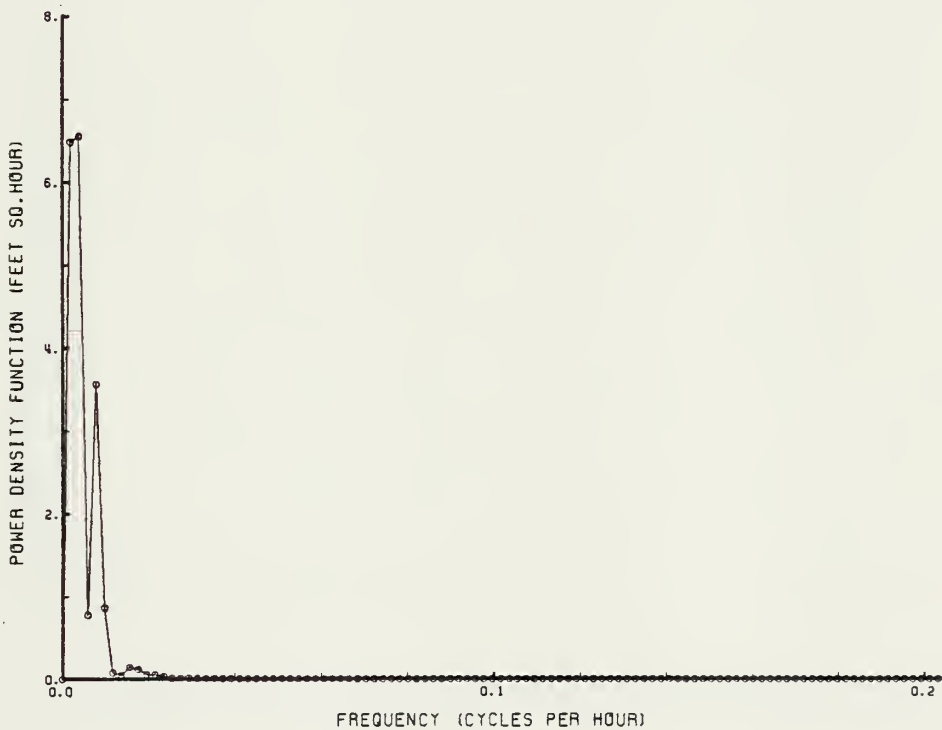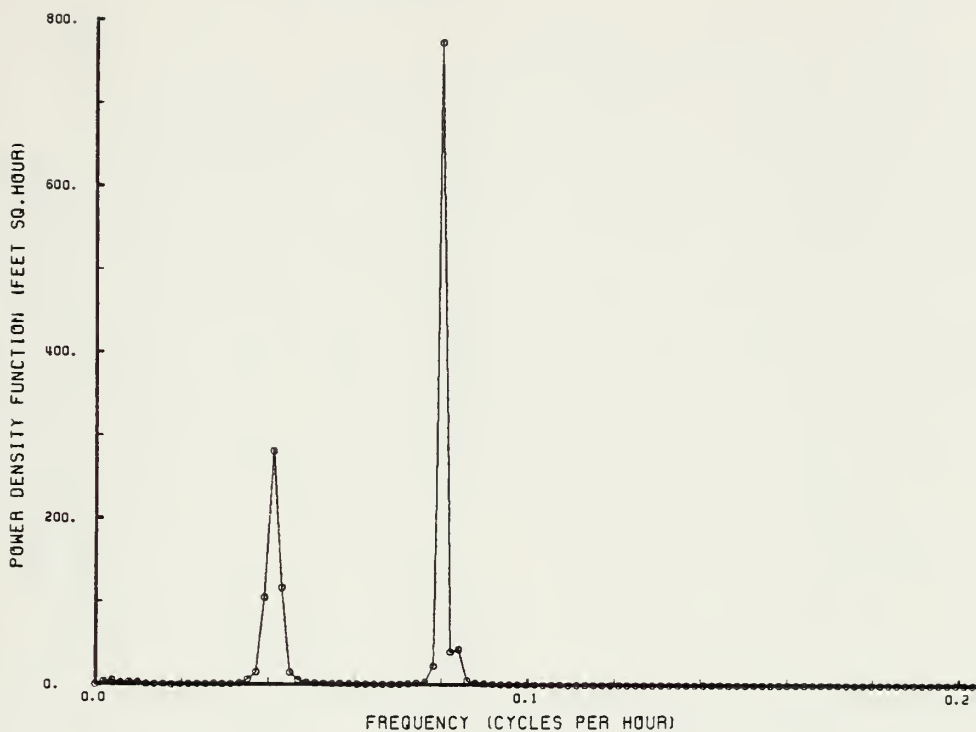
Figure 13. Monterey, January-February, 1978. (Four degrees of freedom for each spectral estimate.)
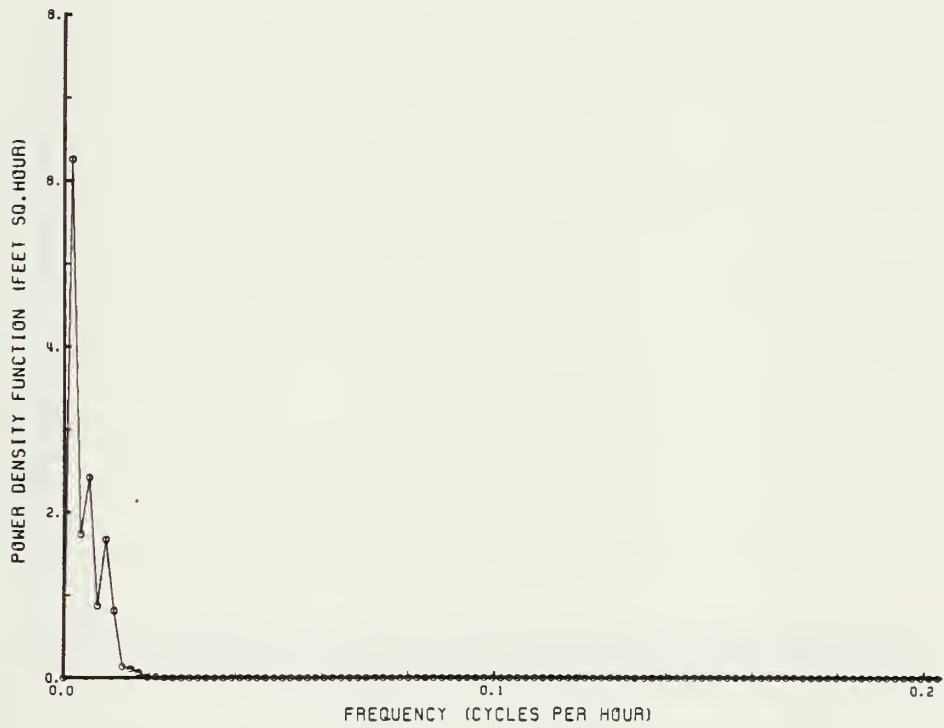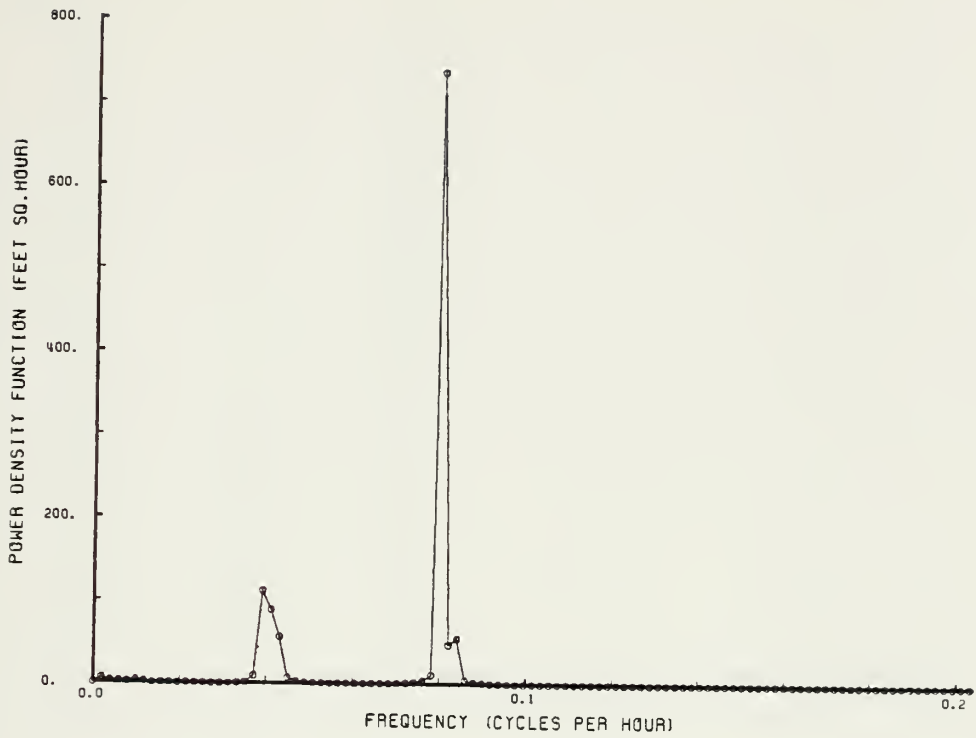
Figure 14. Monterey, March-April, 1978.
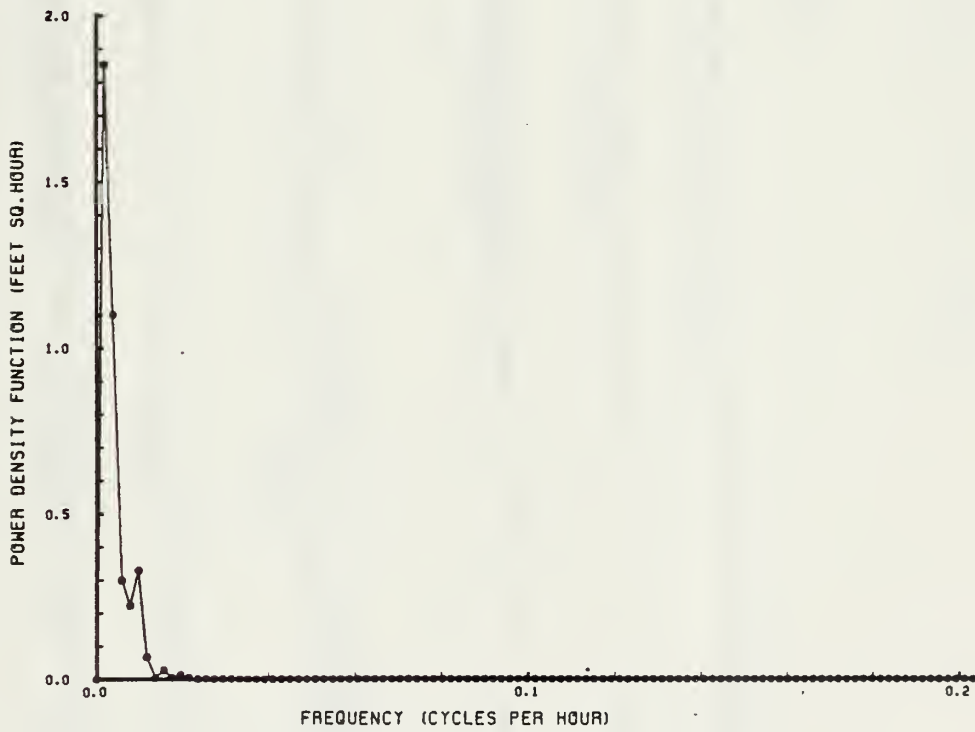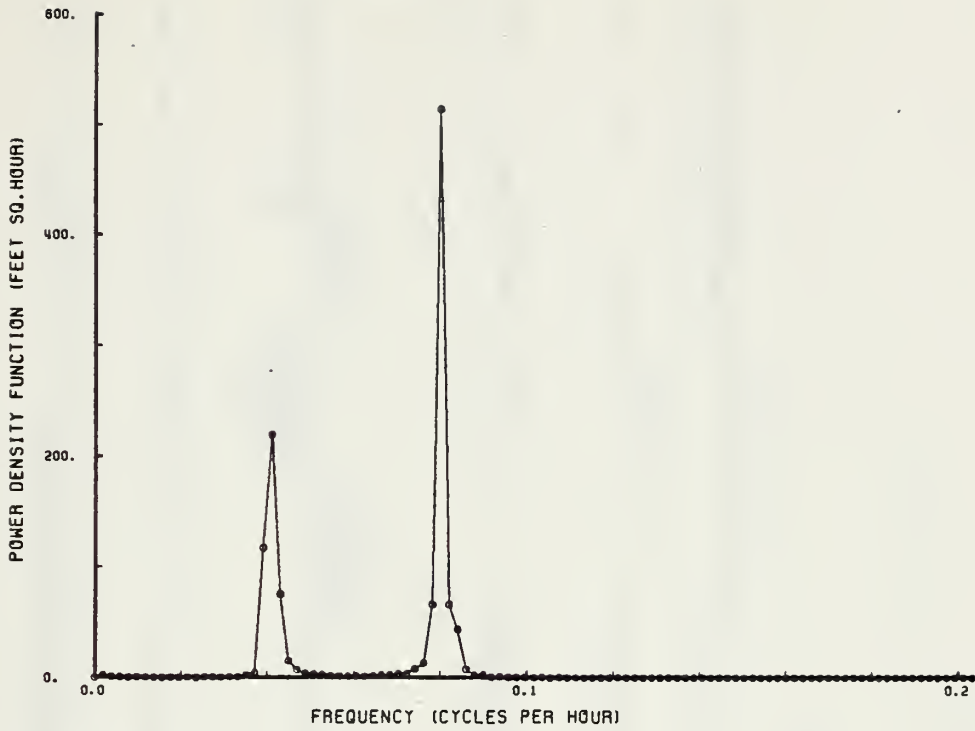(Four degrees of freedom for each
spectral estimate.)

57
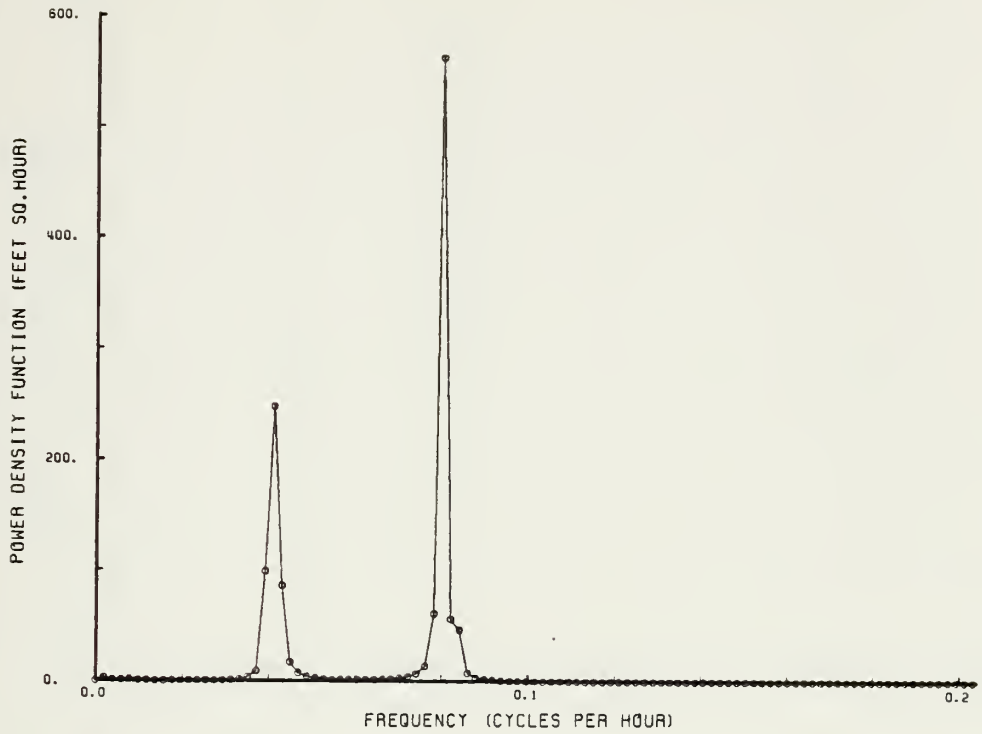
Figure 15.   Monterey, May-June, 1978.
(Four degrees of freedom for each
spectral estimate.)

58
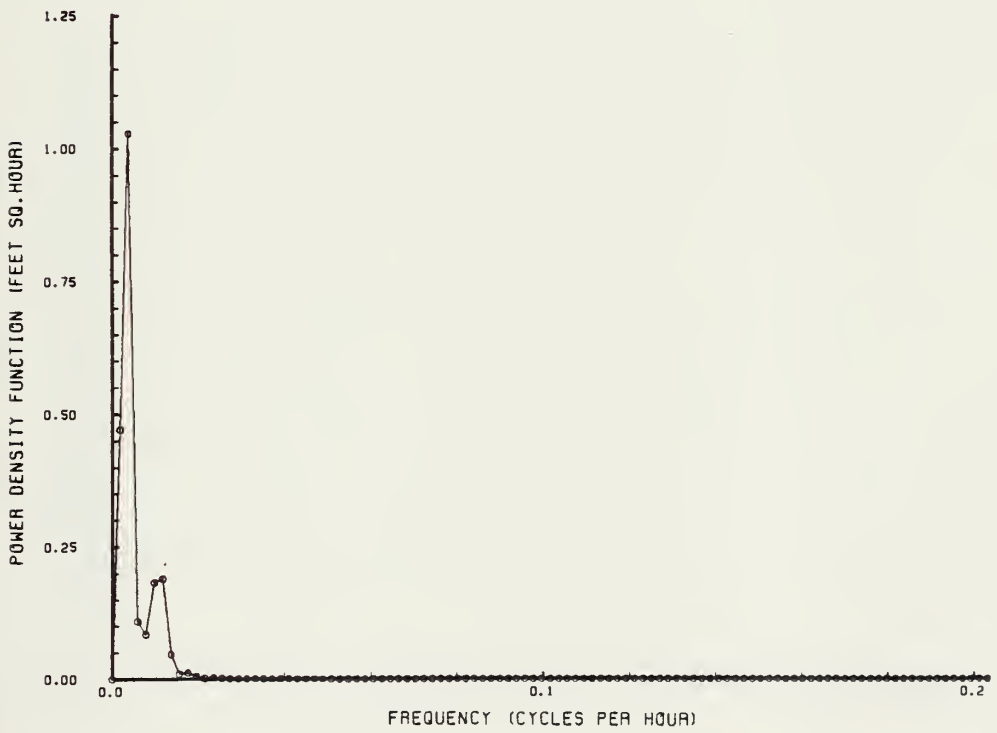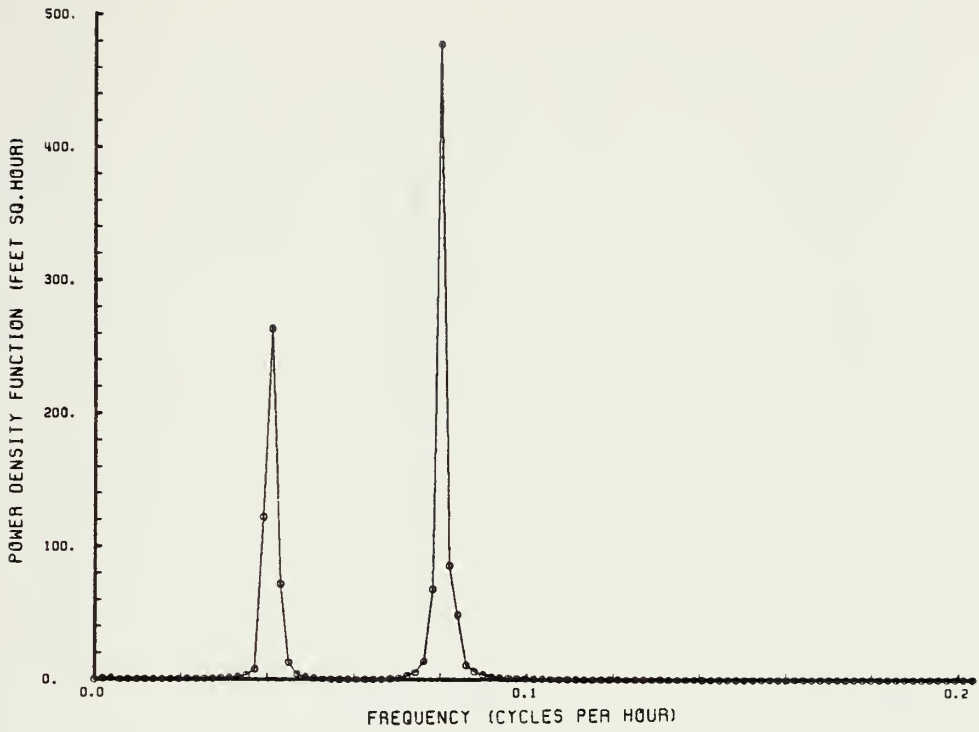
Figure 16.   Monterey, July-August, 1978.
(Four degrees of freedom for each
spectral estimate.)

59
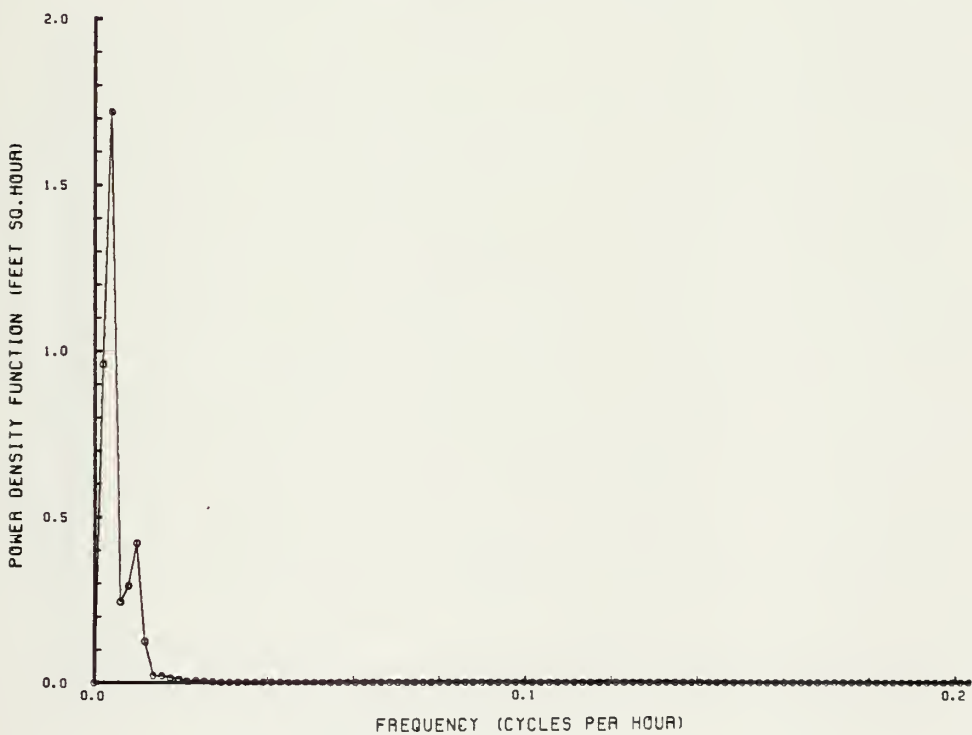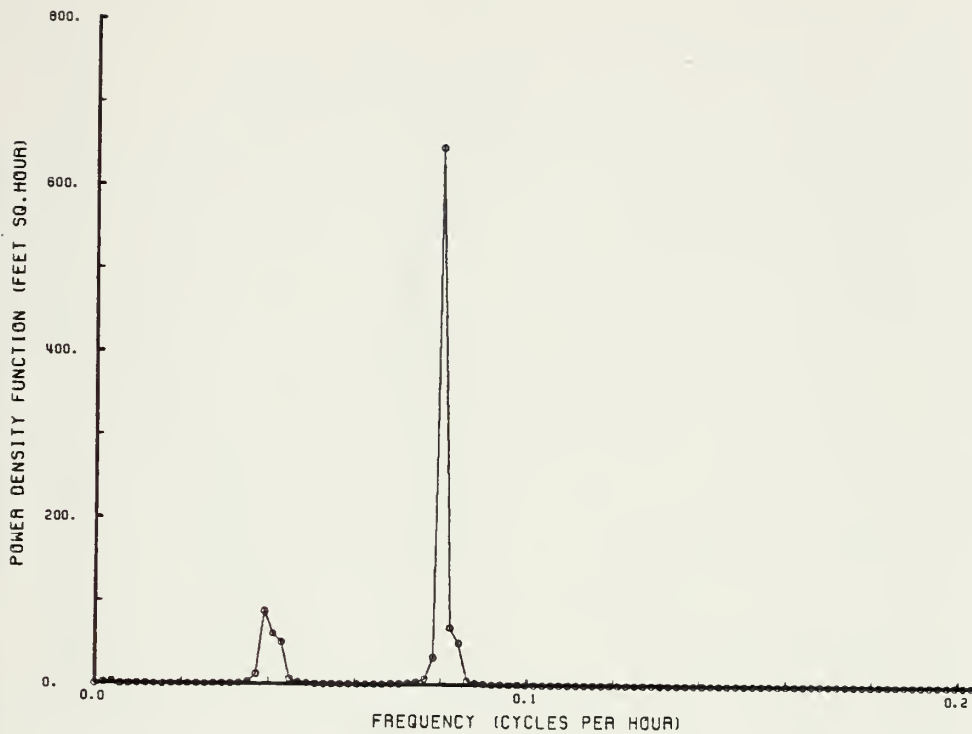
Figure 17. Monterey, September-
October, 1978. (Four degrees of
freedom for each spectral estimate.)

60
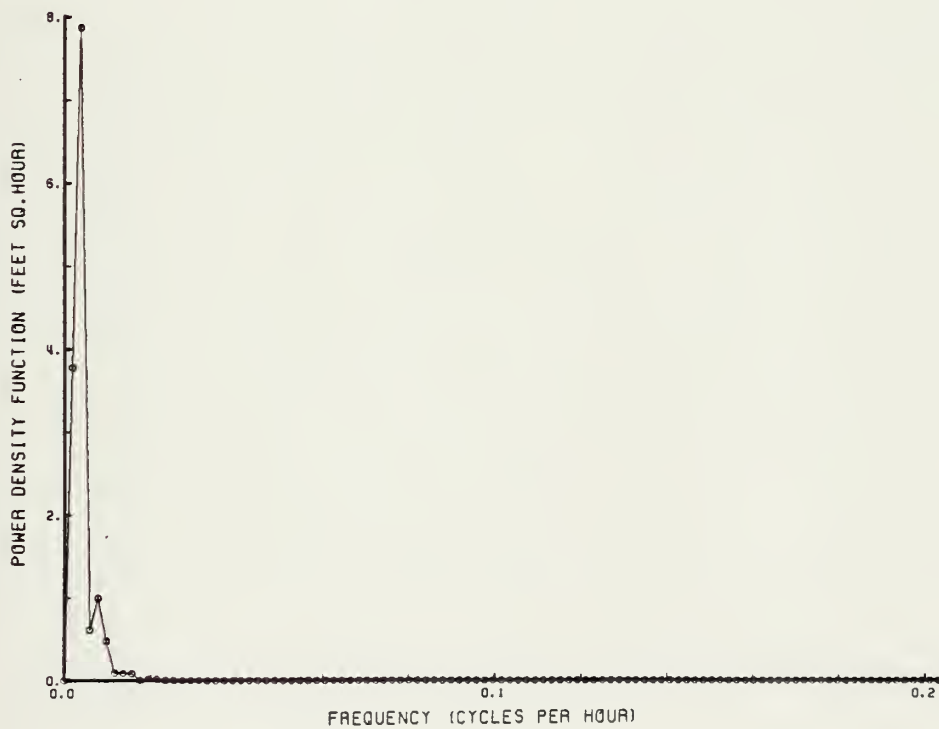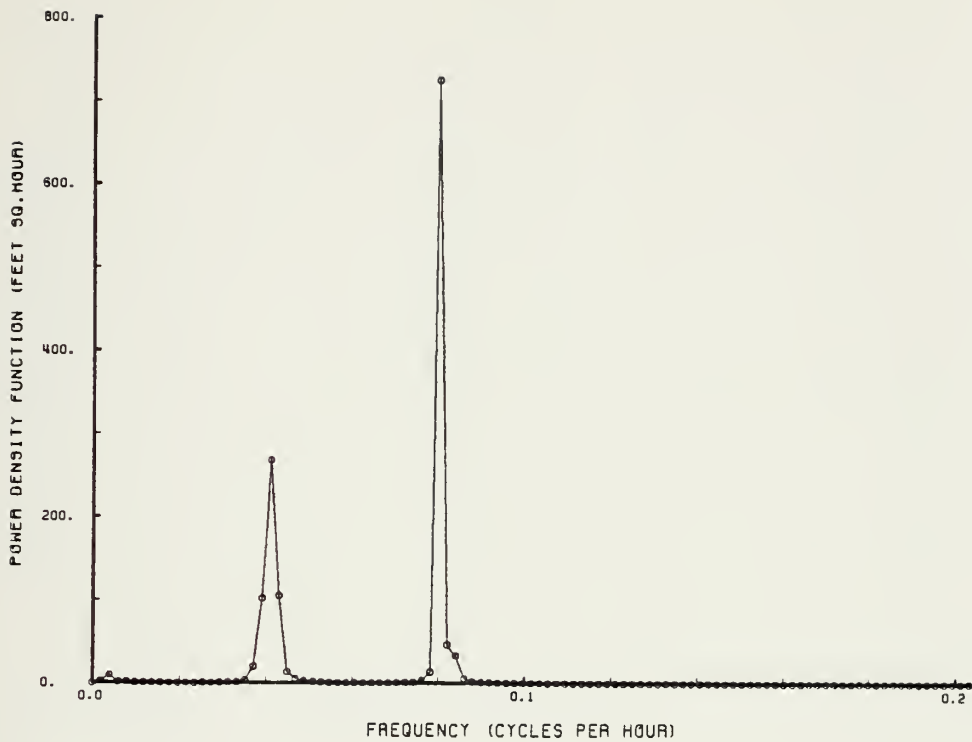
Figure 18. Monterey, November-
December, 1978. (Four degrees of
freedom for each spectral estimate.)

61
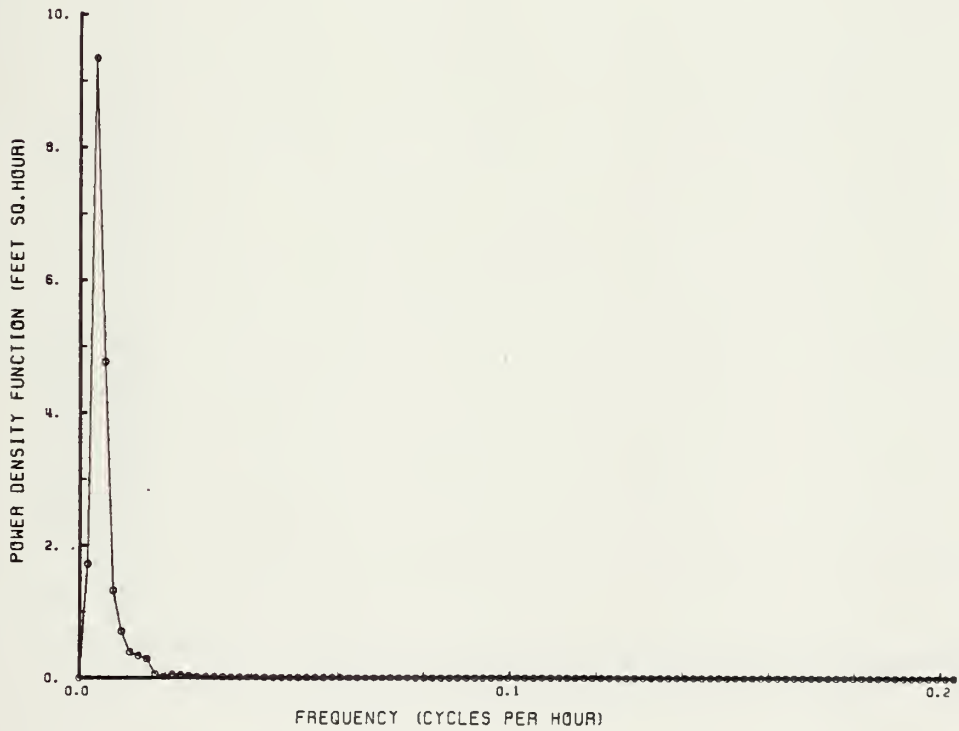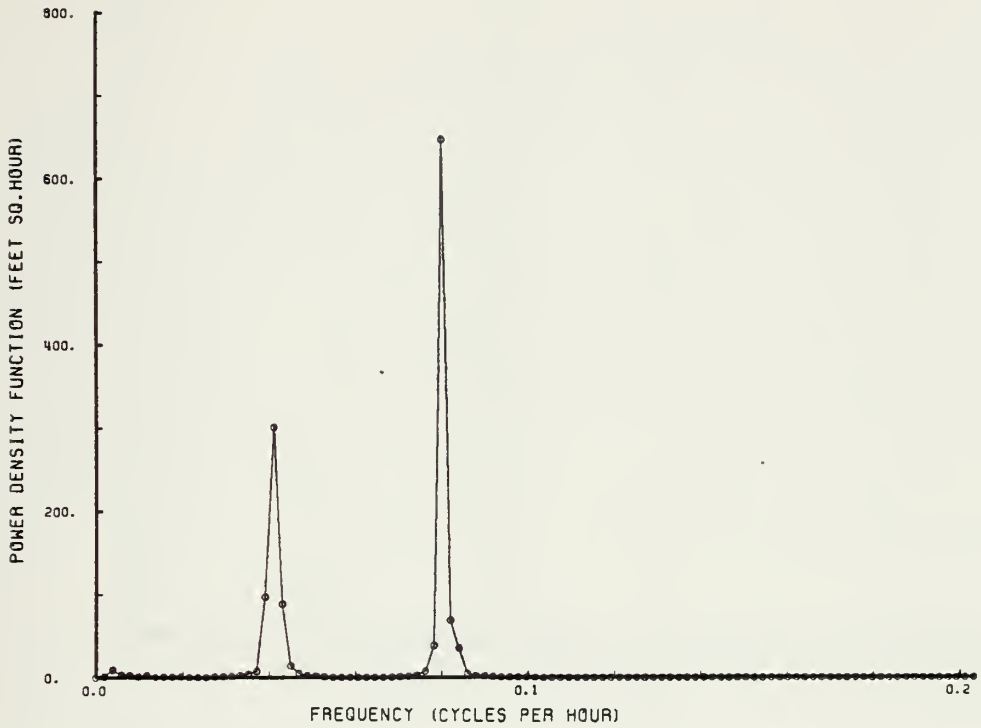
Figure 19. Monterey, January-
February, 1979. (Four degrees of
freedom for each spectral estimate.)

62
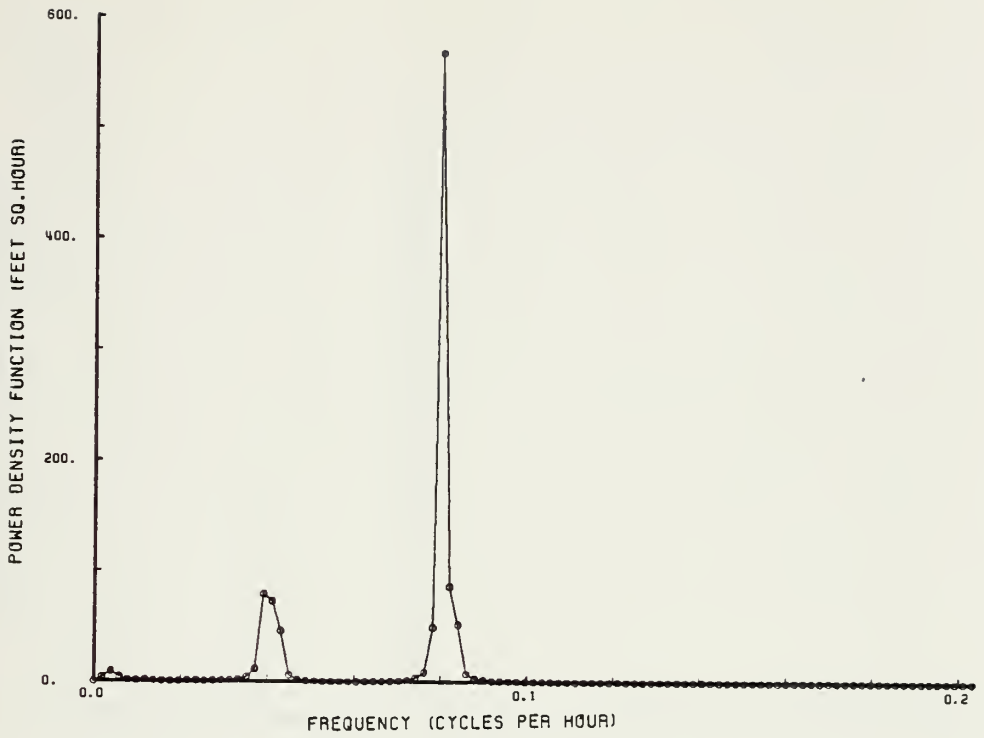
Figure 20. Monterey, March-April, 1979.
(Four degrees of freedom for each
spectral estimate.)
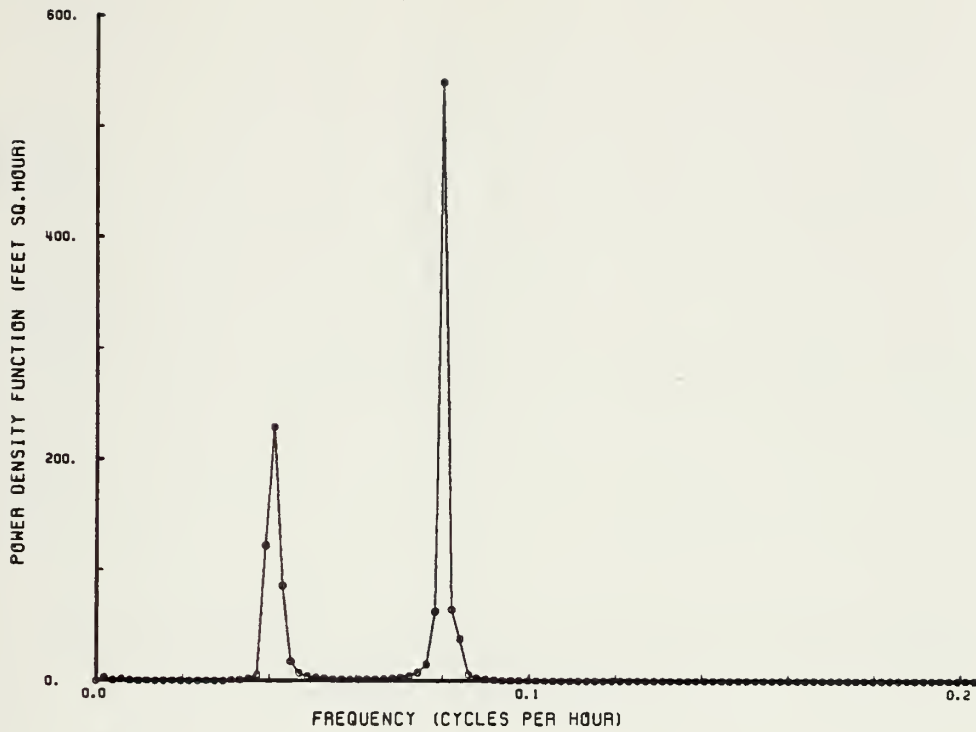
Figure 21.   Monterey, May-June, 1979
(Four degrees of freedom for each
spectral estimate.)

64
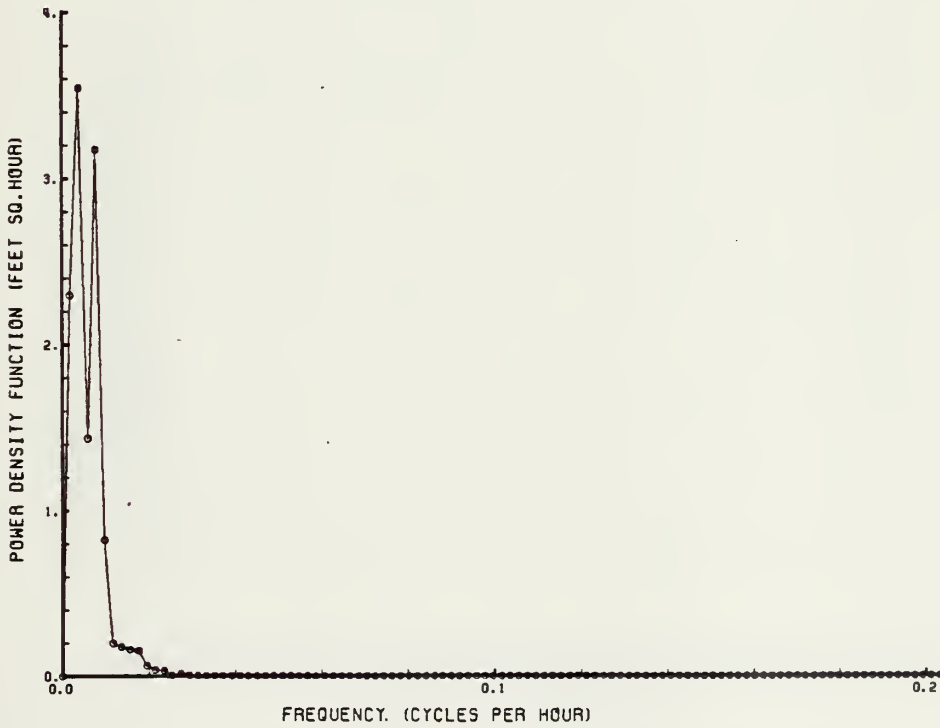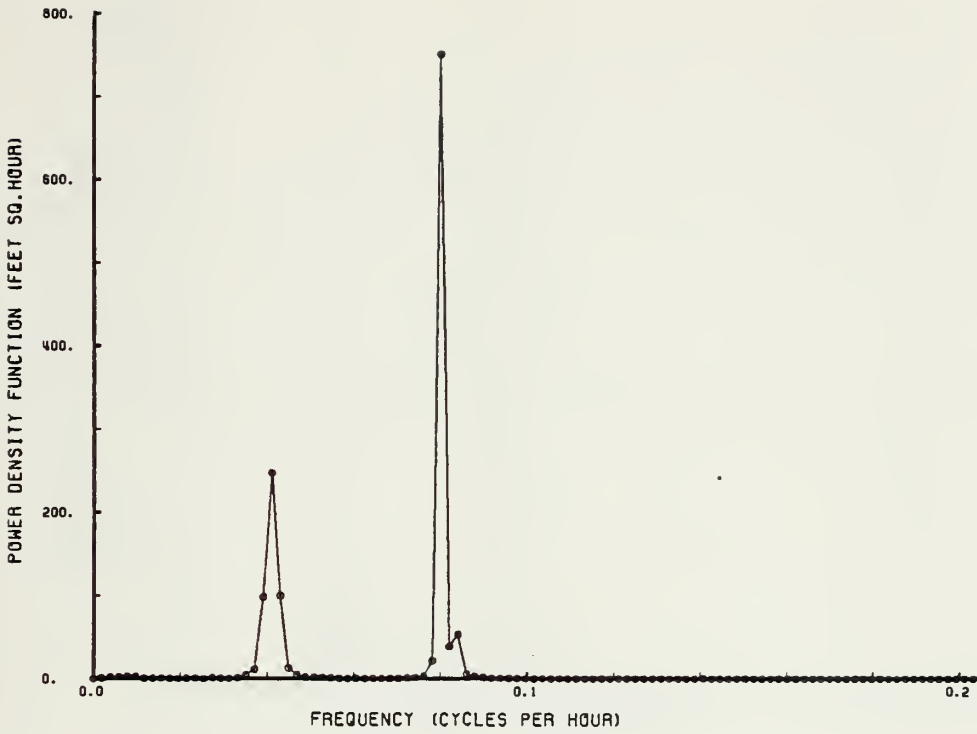
Figure 22. Port San Luis, January-
February, 1978. (Four degrees of
freedom for each spectral estimate.)

65
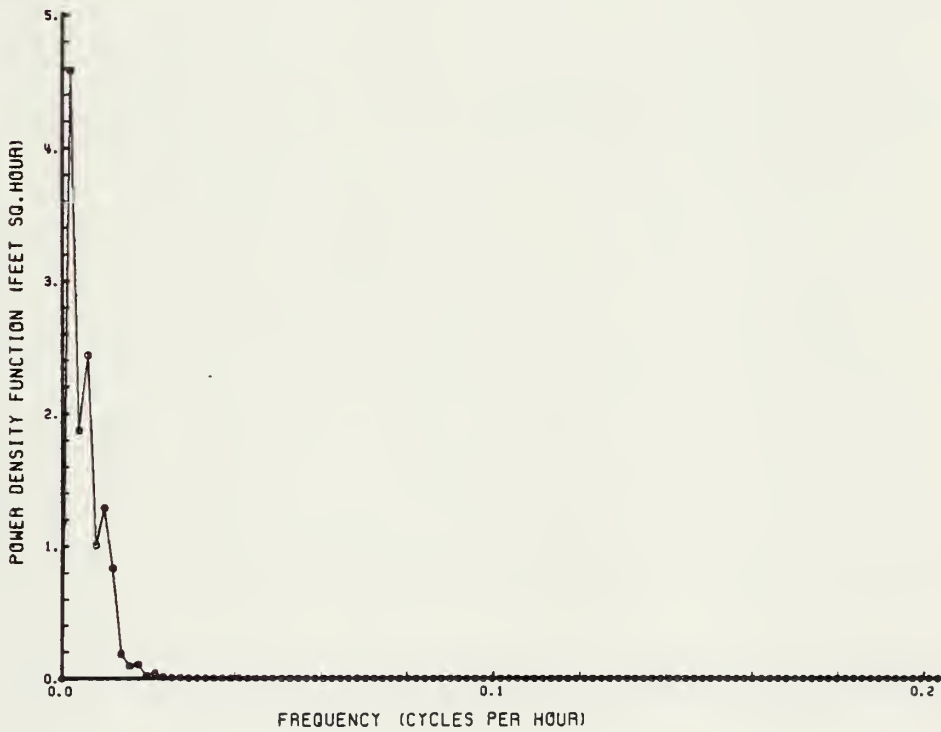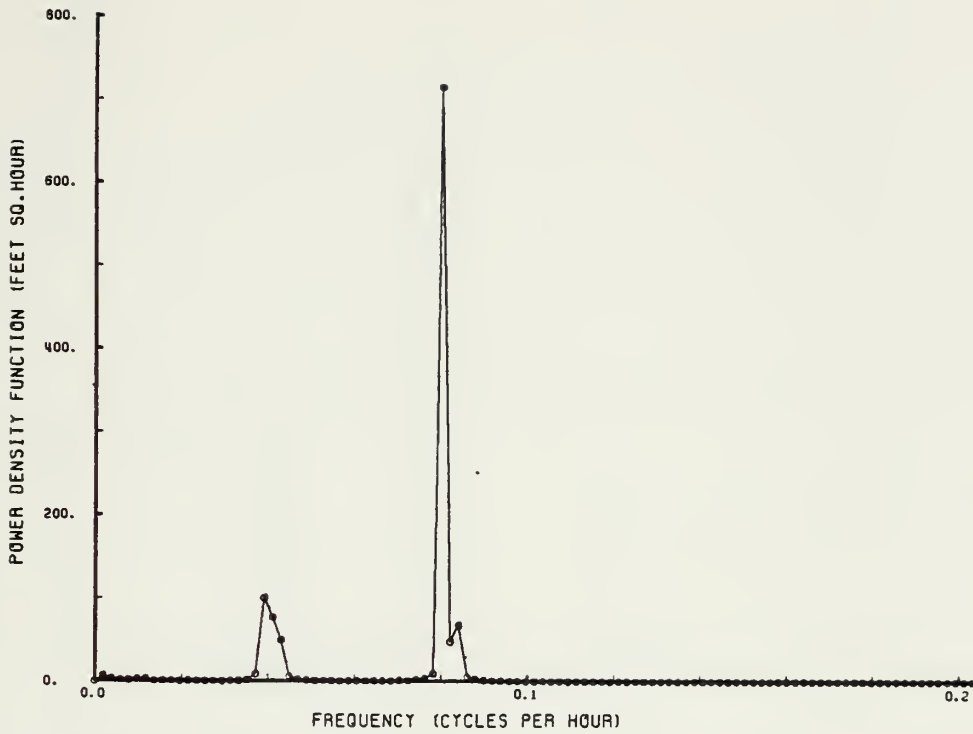
Figure 23. Port San Luis, March-April, 1978. (Four degrees of freedom for each spectral estimate.)

66
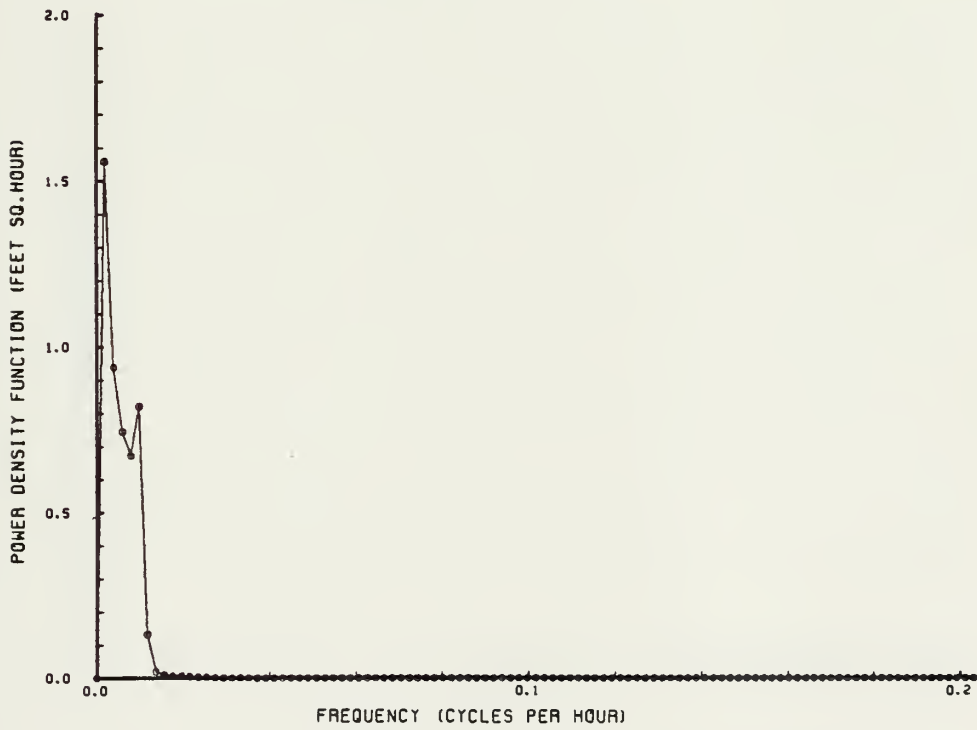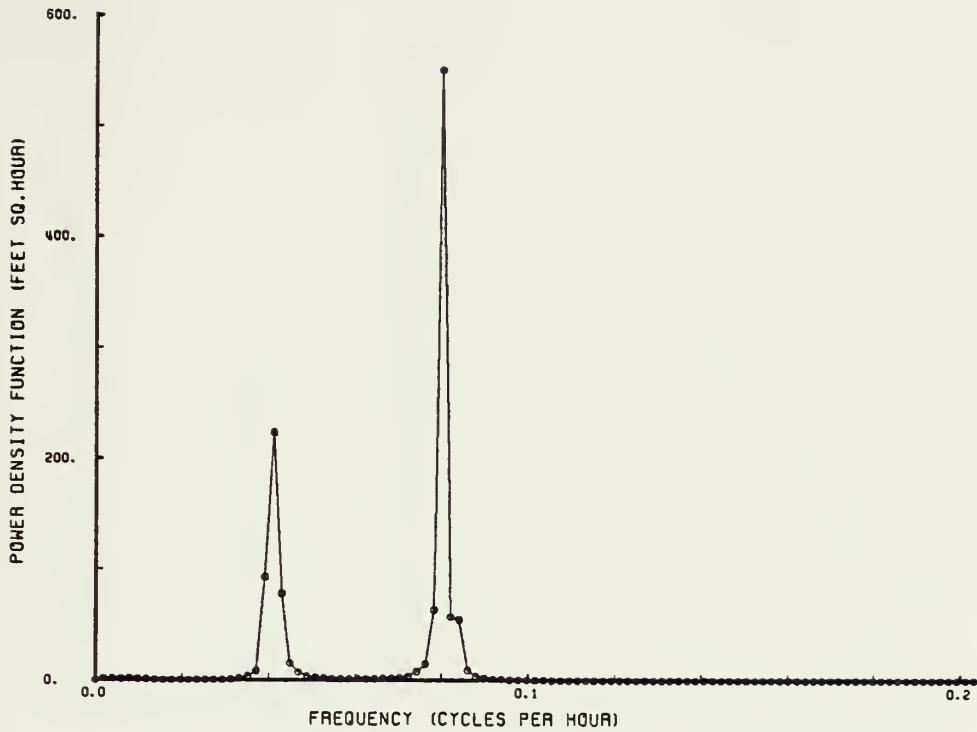
Figure 24. Port San Luis, May-June, 1978.
(Four degrees of freedom for each spectral
estimate.)

67
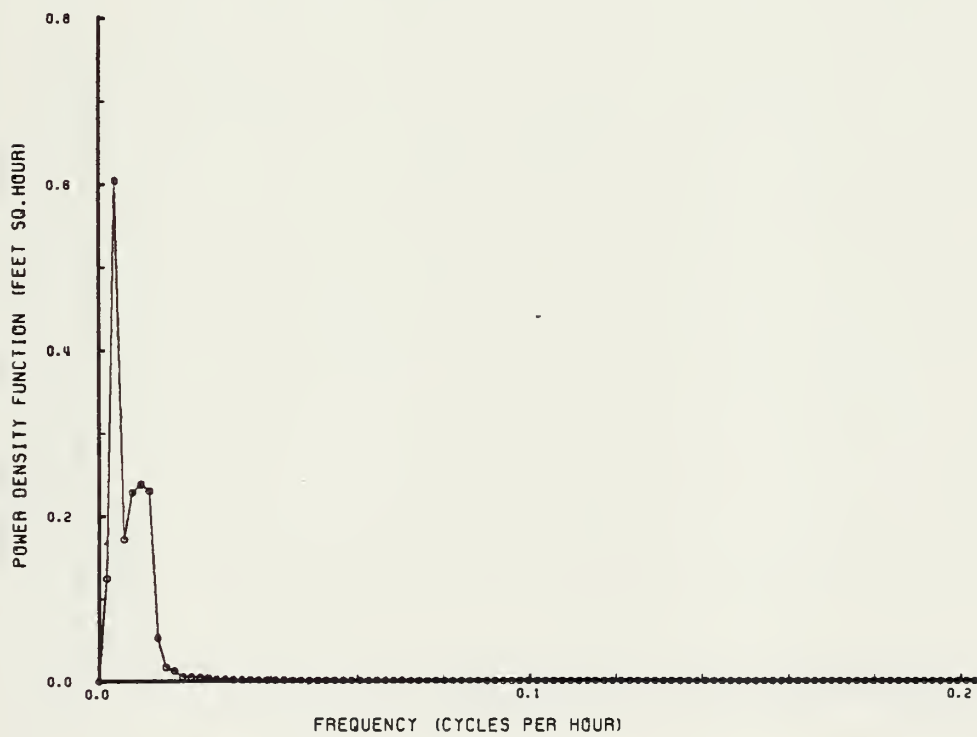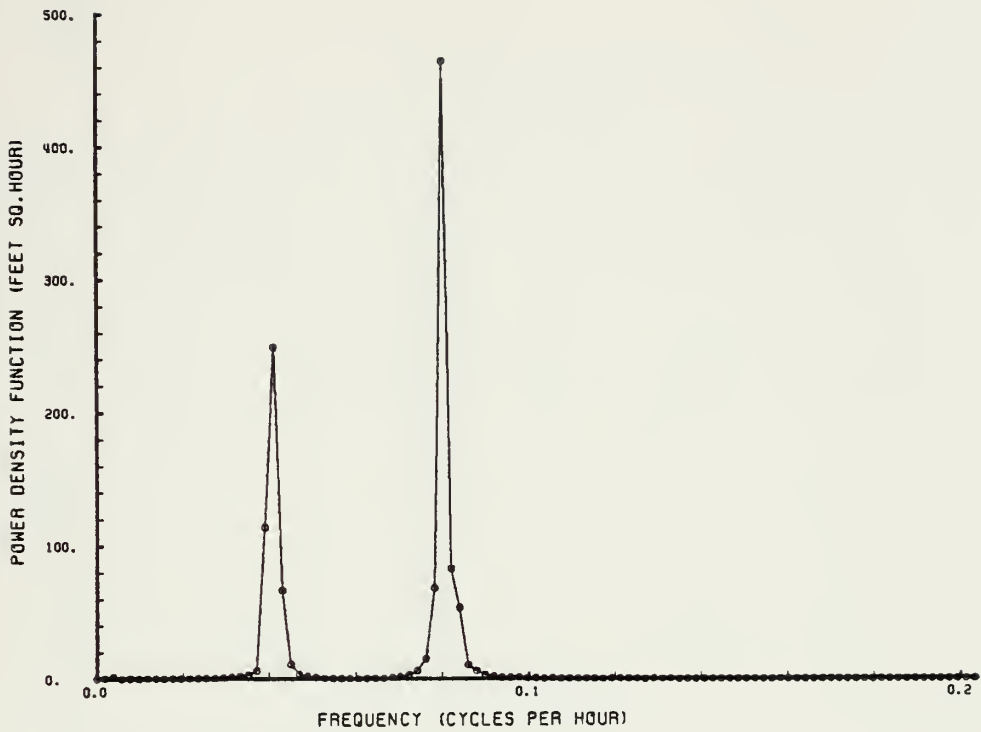
Figure 25. Port San Luis, July-August, 1978. (Four degrees of freedom for each spectral estimate.)

68
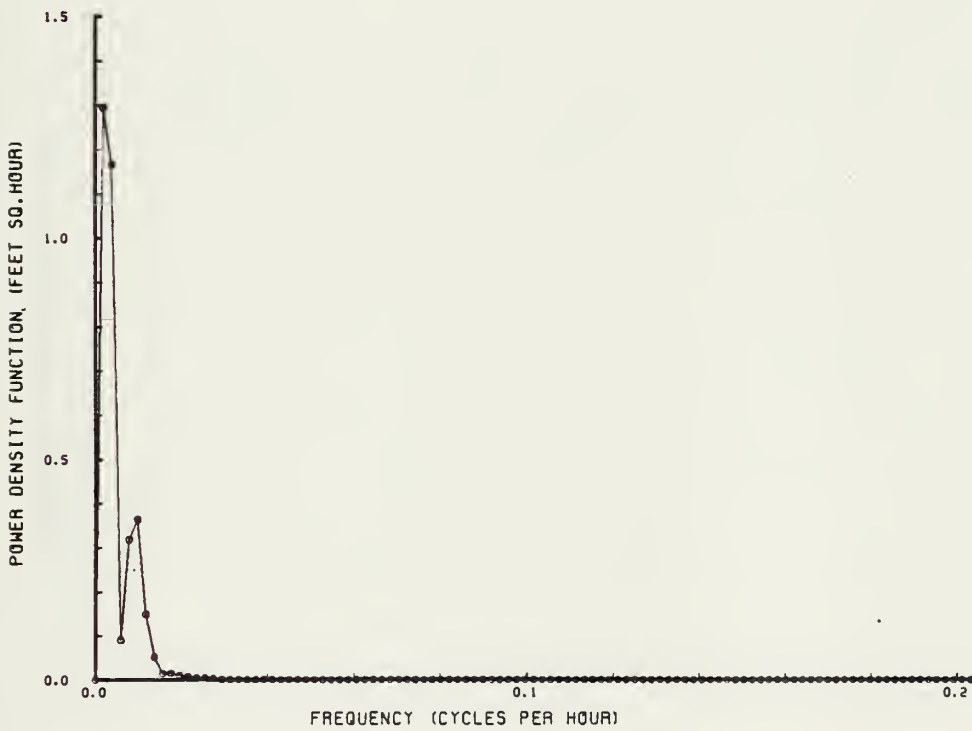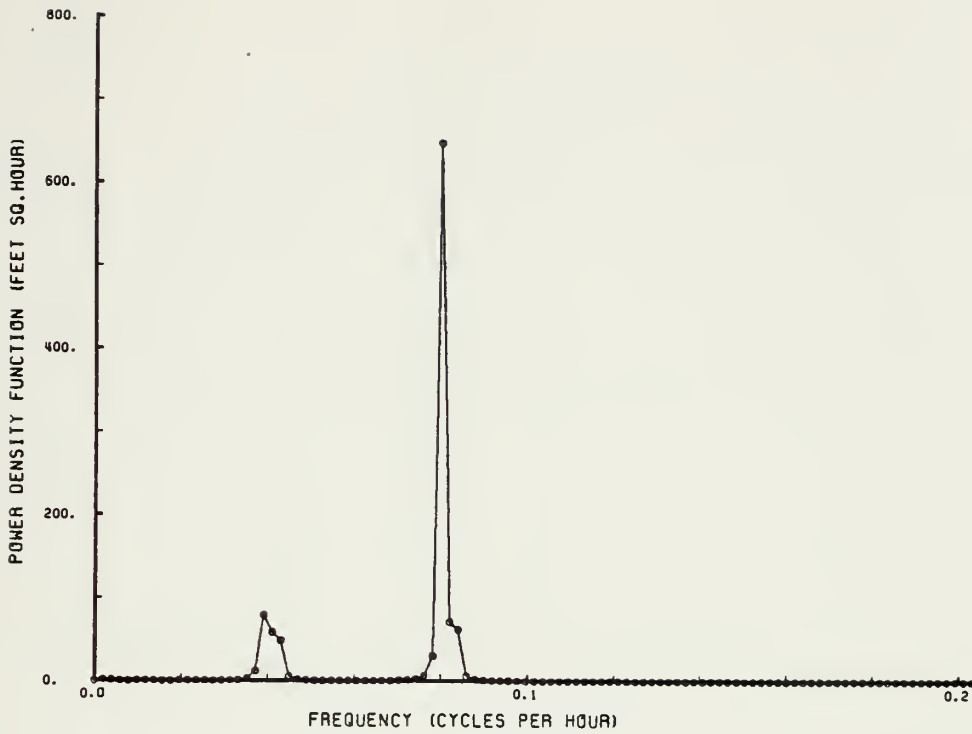
Figure 26.   Port San Luis, September-
October, 1978.   (Four degrees of
freedom for each spectral estimate.)

69
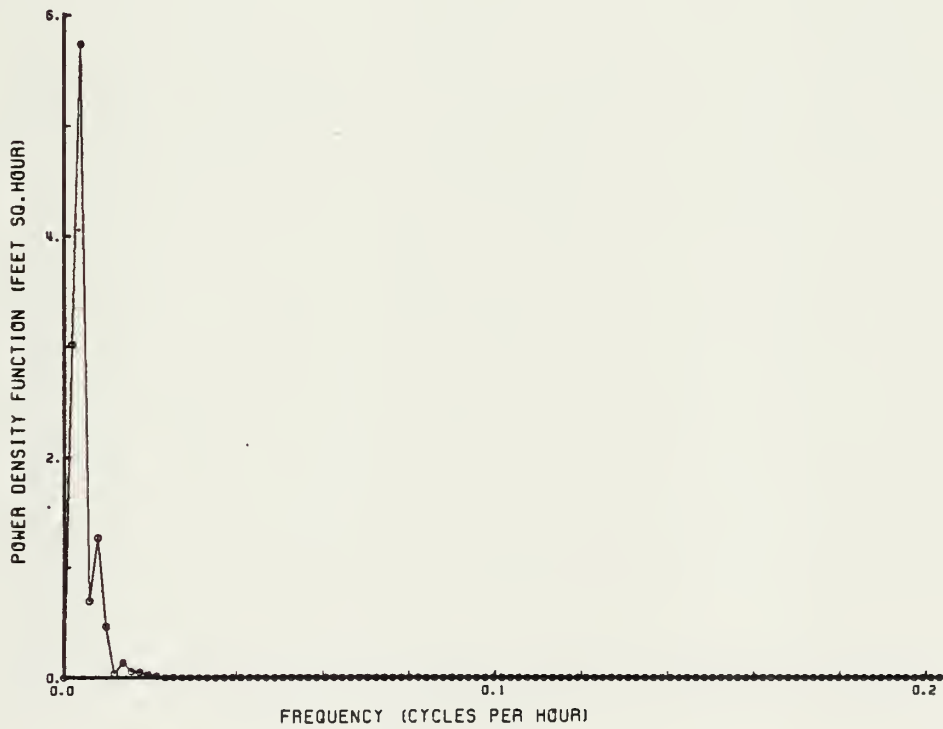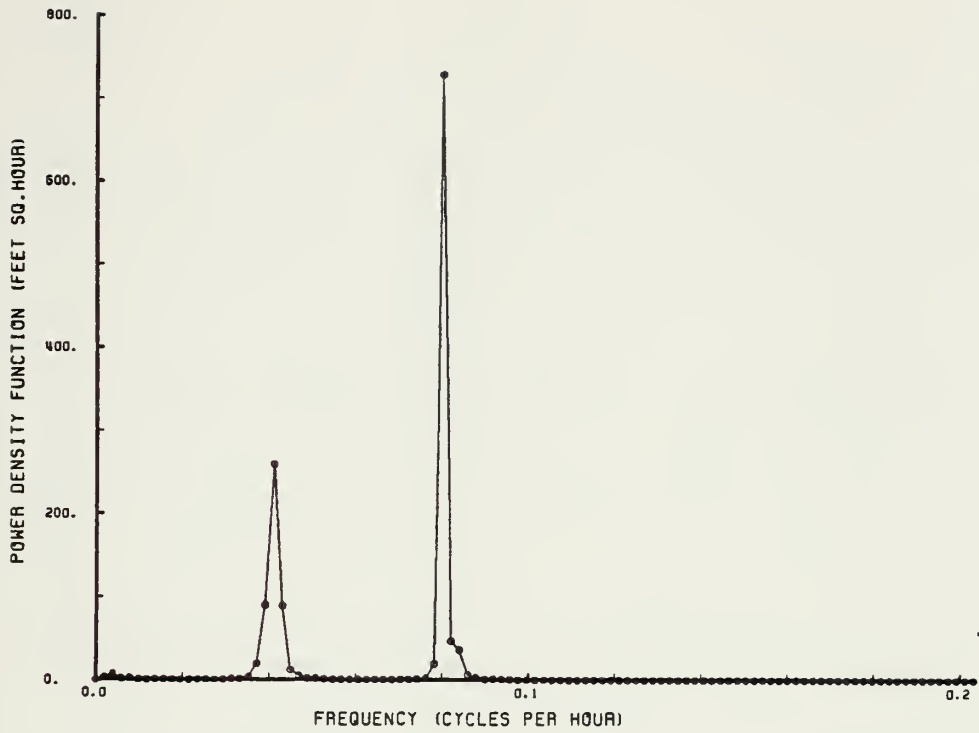
Figure 27. Port San Luis, November-December, 1978. (Four degrees of freedom for each spectral estimate.)
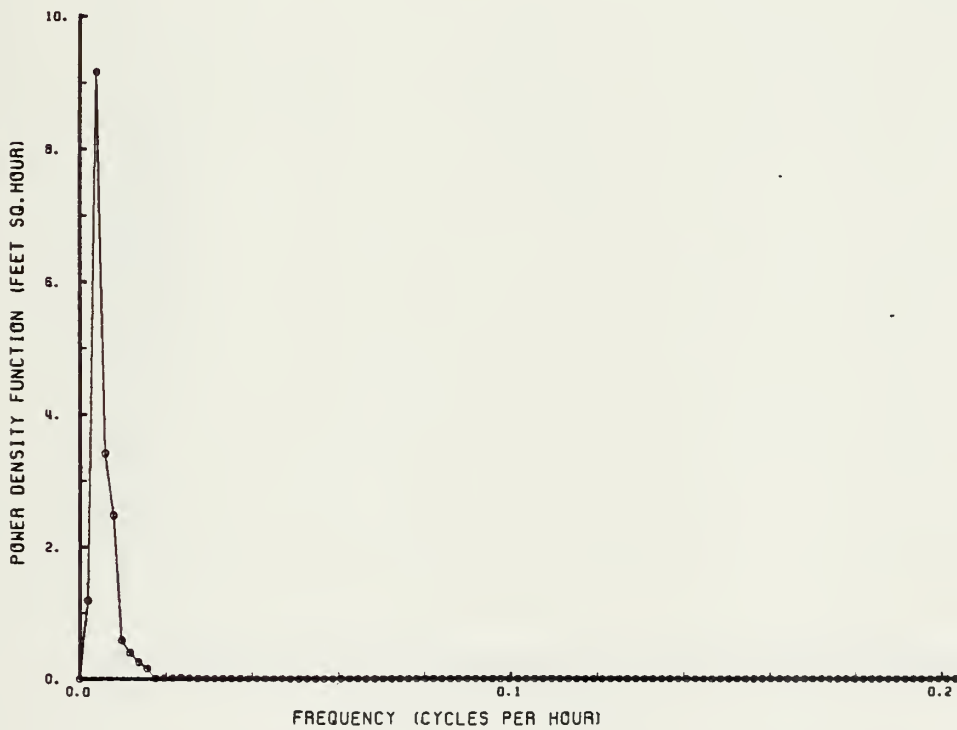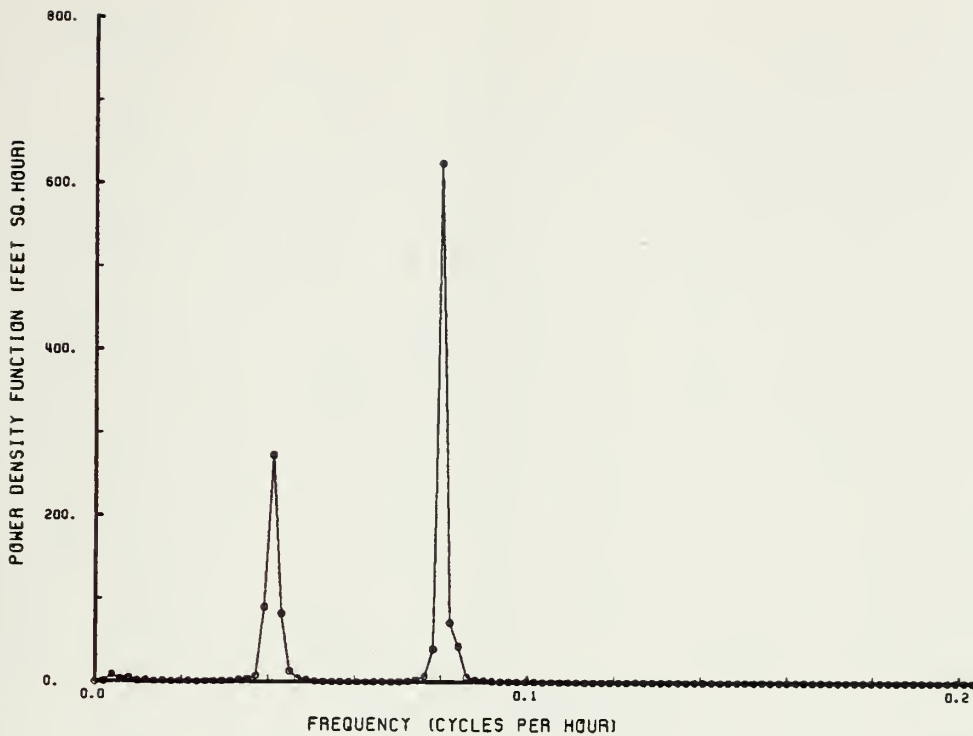
Figure 28. Port San Luis, January-
February, 1979. (Four degrees of
freedom for each spectral estimate.)
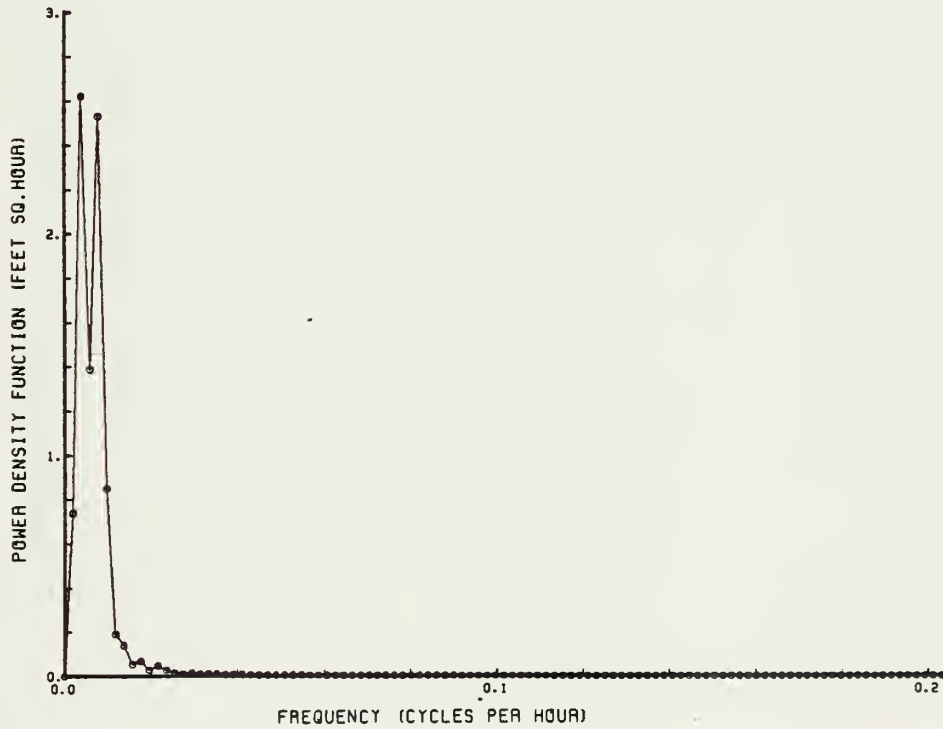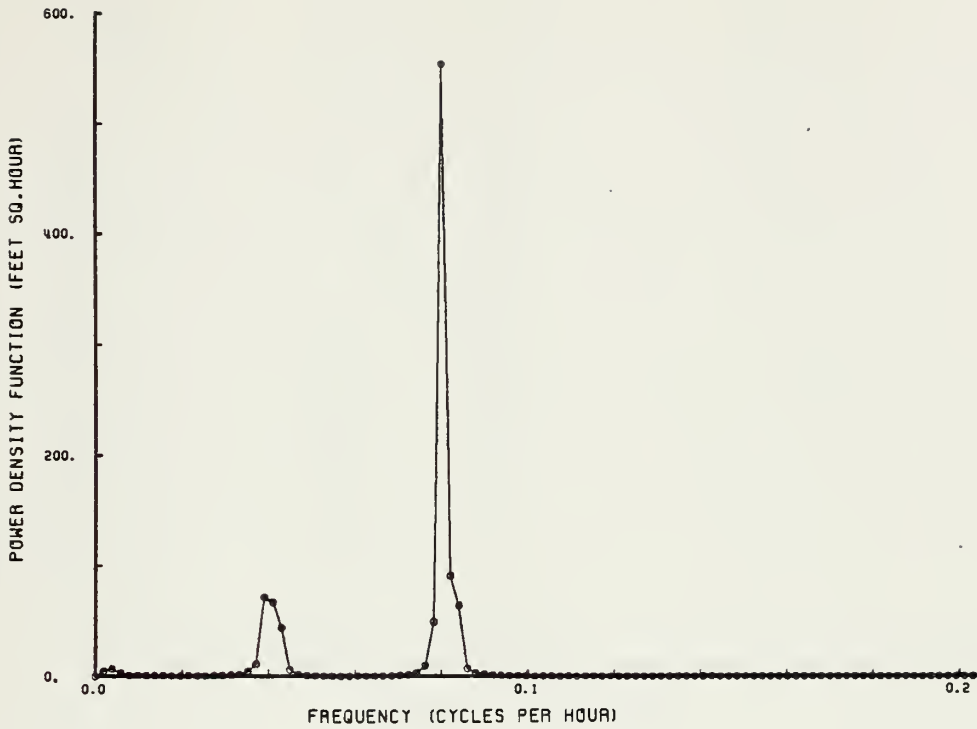
Figure 29. Port San Luis, March-April, 1979. (Four degrees of freedom for each spectral estimate.)

Figure 30. Port San Luis, May-June, 1979.
(Four degrees of freedom for each spectral
estimate.)

73
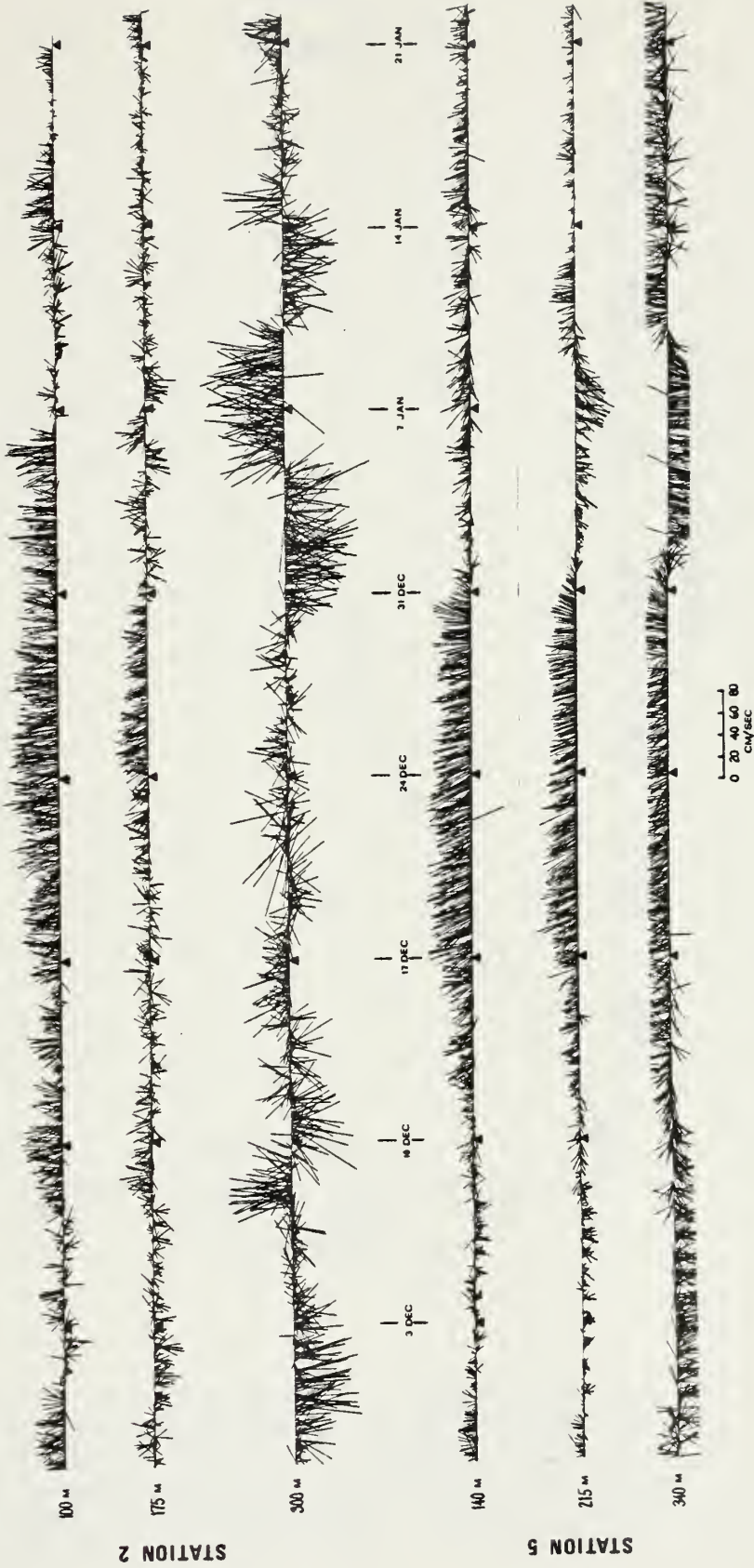
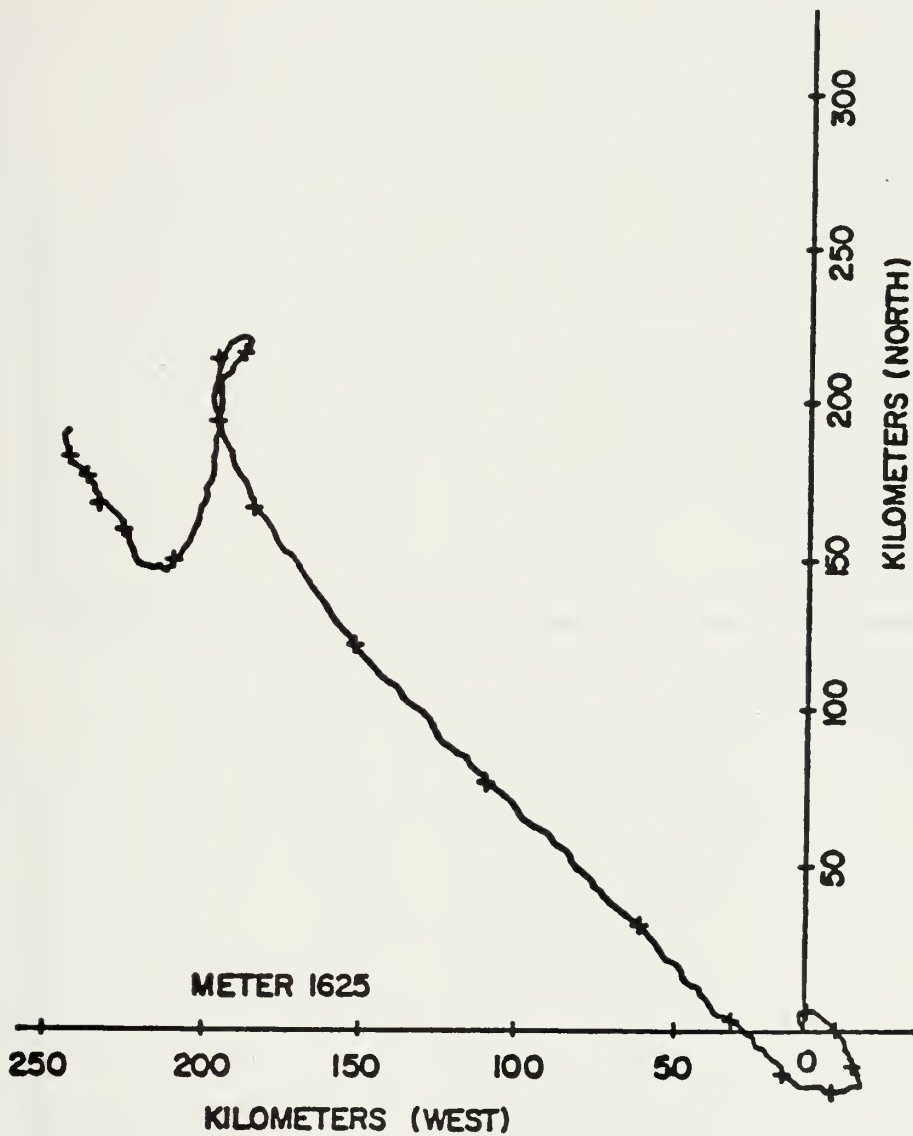Figure 31. Stickplots of calculated hourly current vectors.
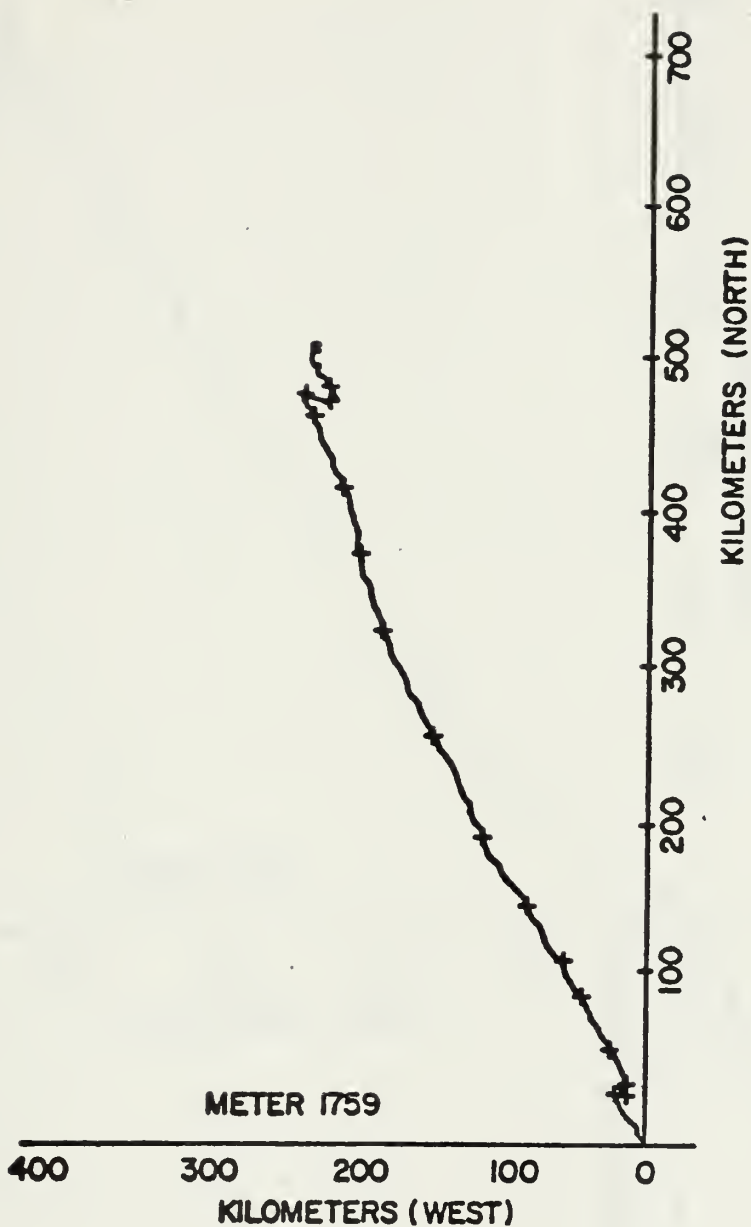
Figure 32. Progressive vector diagram
for the current meter at 100 meters depth
at station 2 from 27 November 1978 to
22 January 1979. Crosses are positioned
at three day intervals. Vertical axis
indicates Magnetic North. (Coddington, 1979)
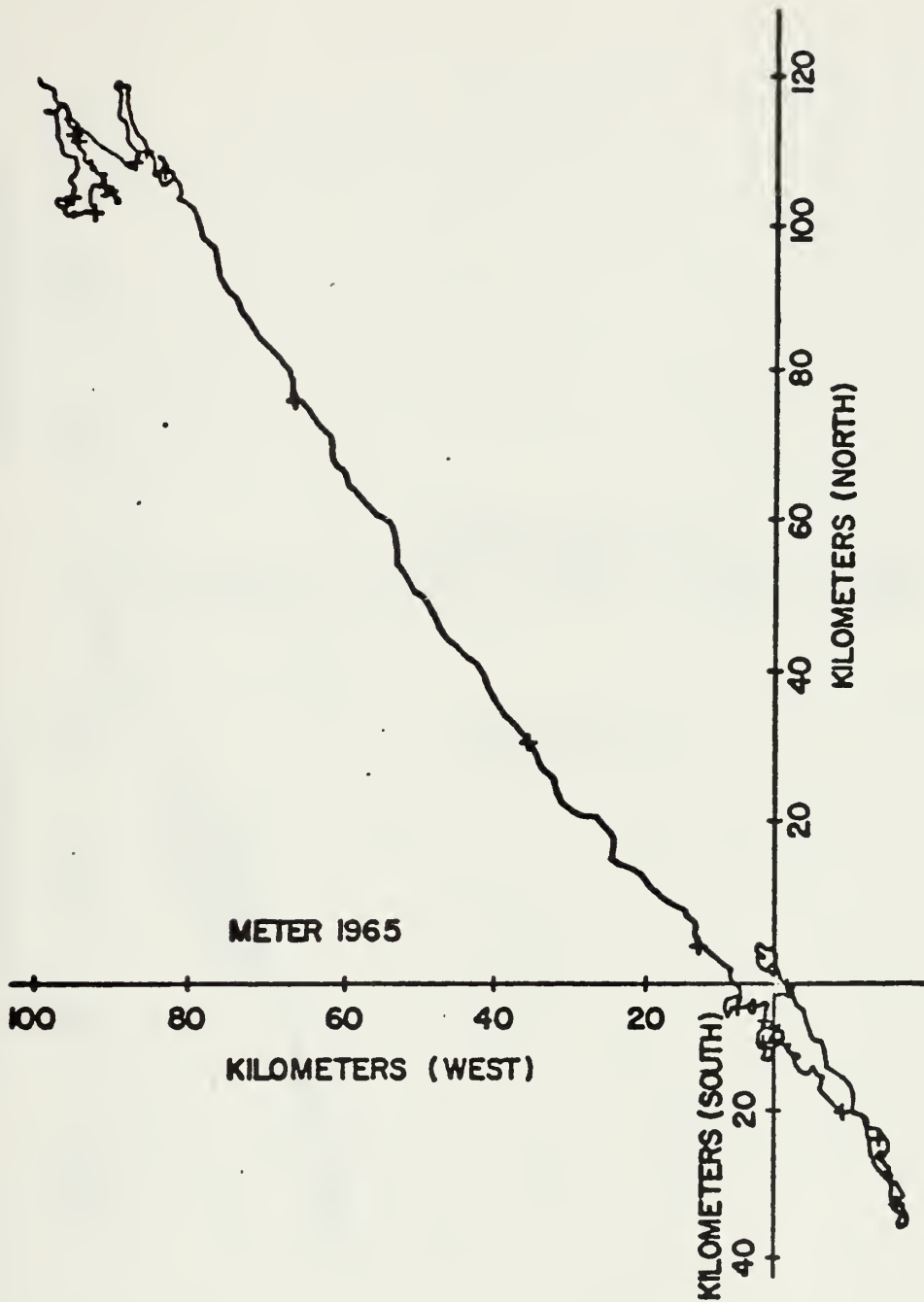
Figure 33. Progressive vector diagram for the
current meter at 175 meters depth at station 2
from 27 November 1978 to 22 January 1979. Crosses
are positioned at three day intervals. Vertical
axis indicates Magnetic North. (Coddington, 1979)
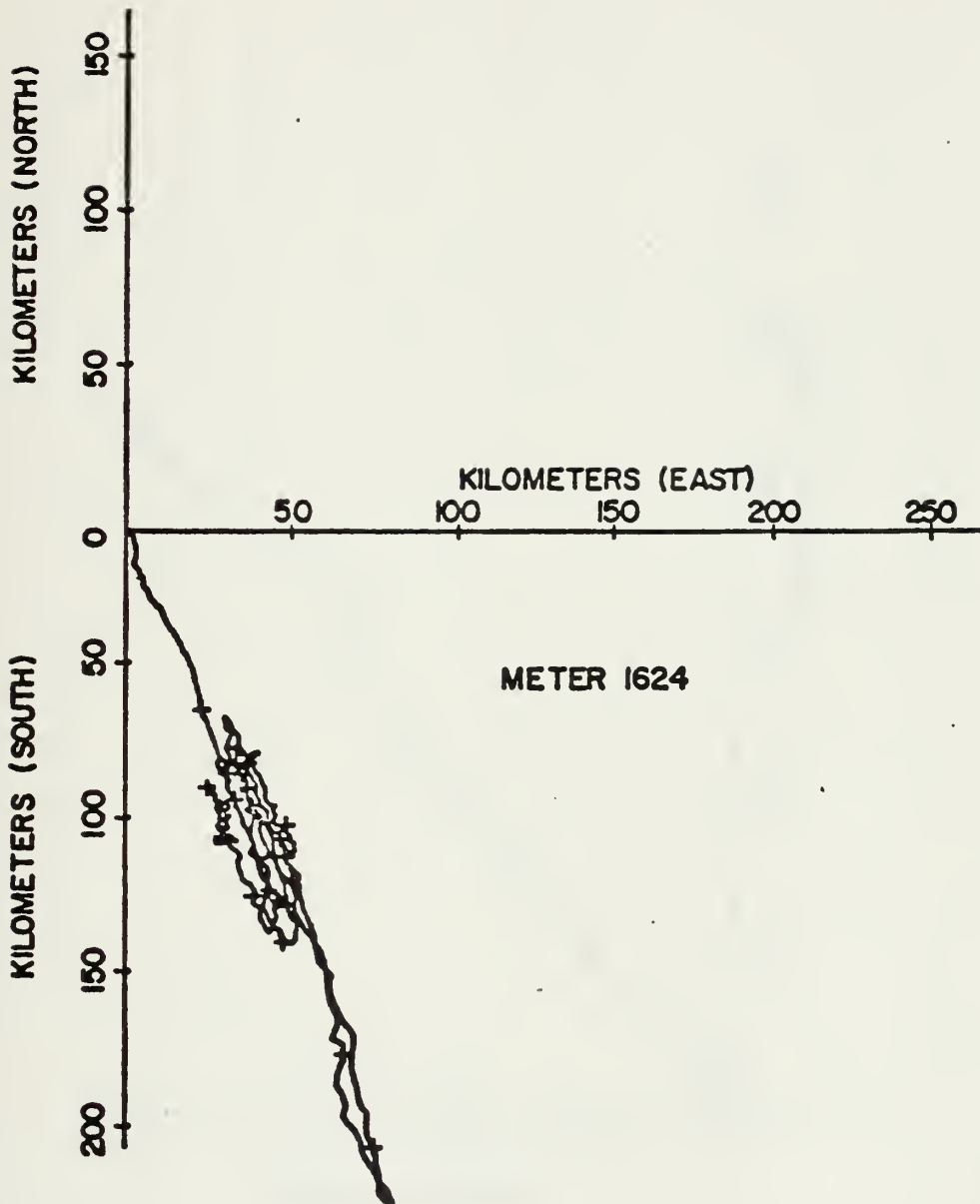
Figure 34. Progressive vector diagram for the current meter at 300 meters depth at station 2 from 27 November 1978 to 22 January 1979. Crosses are positioned at three day intervals. Vertical axis indicates Magnetic North. (Coddington, 1979)
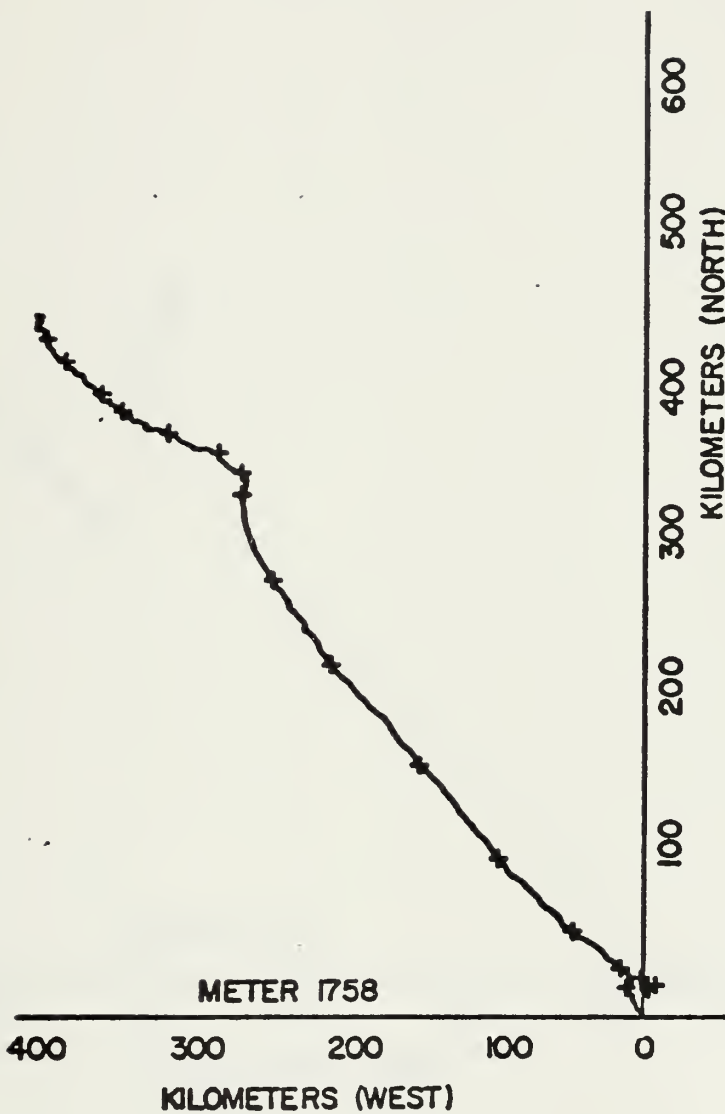
Figure 35. Progressive vector diagram for
the current meter at 140 meters depth at
station 5 from 27 November 1978 to
22 January 1979. Crosses are positioned at
three day intervals. Vertical axis indicates
Magnetic North. (Coddington, 1979)

Figure 36. Progressive vector diagram for the current meter at 215 meters depth at station 5 from 27 November 1978 to 22 January 1979. Crosses are positioned at three day intervals. Vertical axis indicates Magnetic North. (Coddington, 1979)
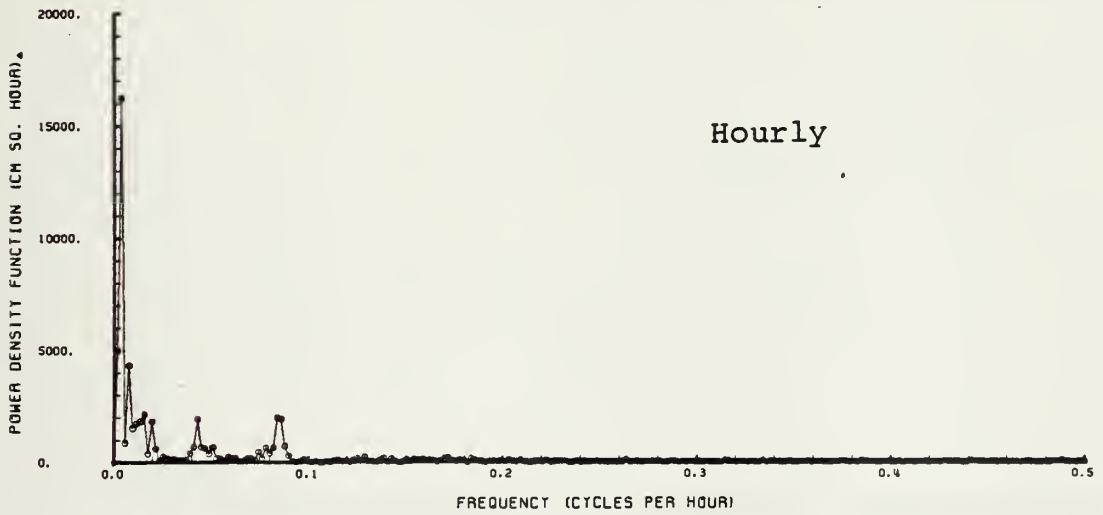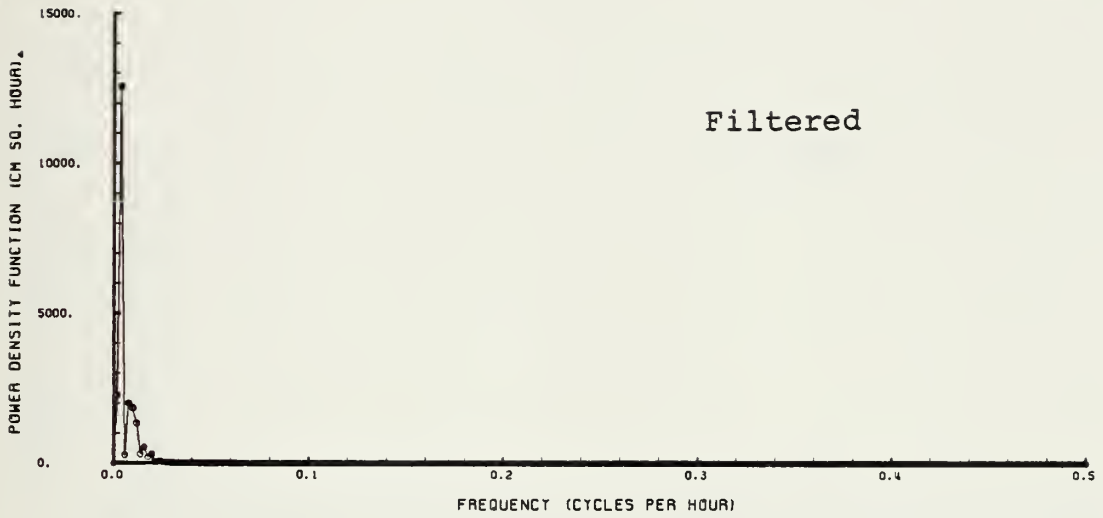
Figure 37. Station 2, 100 m depth
11/27/78-1/22/79. Low pass filtered
and hourly alongshore current.
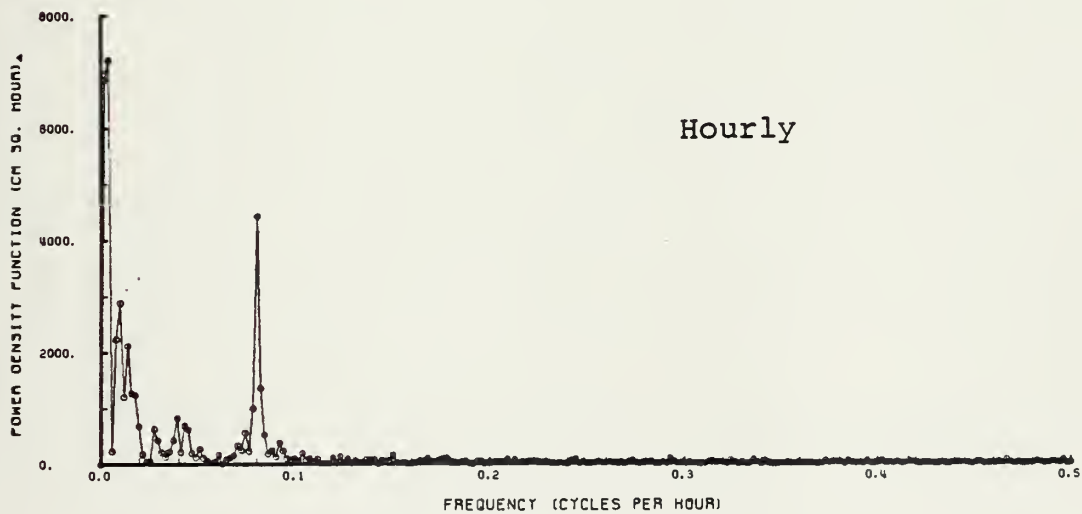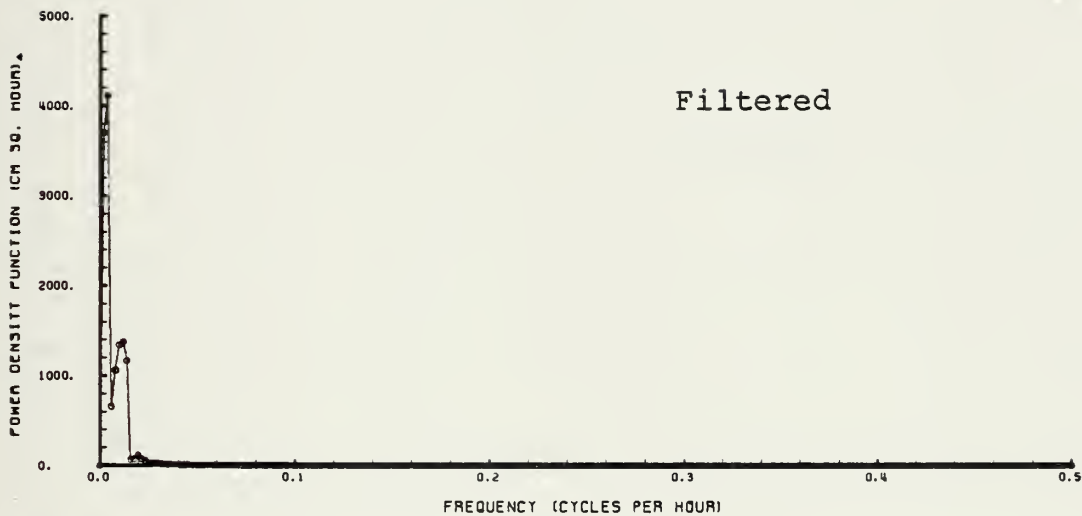
Figure 38. Station 2, 175 m depth,
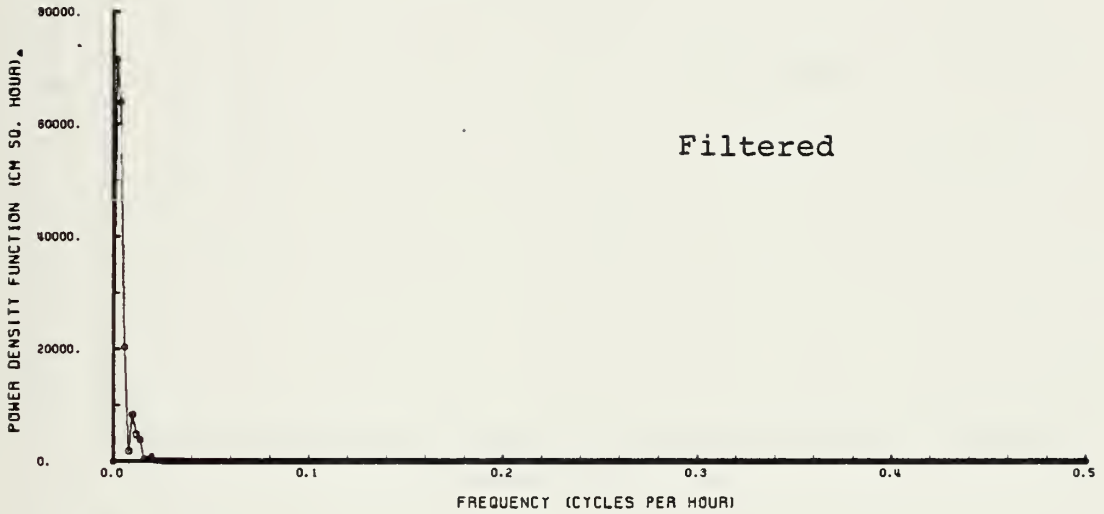11/27/78-1/22/79. Low pass filtered
and hourly alongshore current spectra.

81

Figure 39. Station 2, 300 m depth,
11/27/78-1/22/79. Low pass filtered
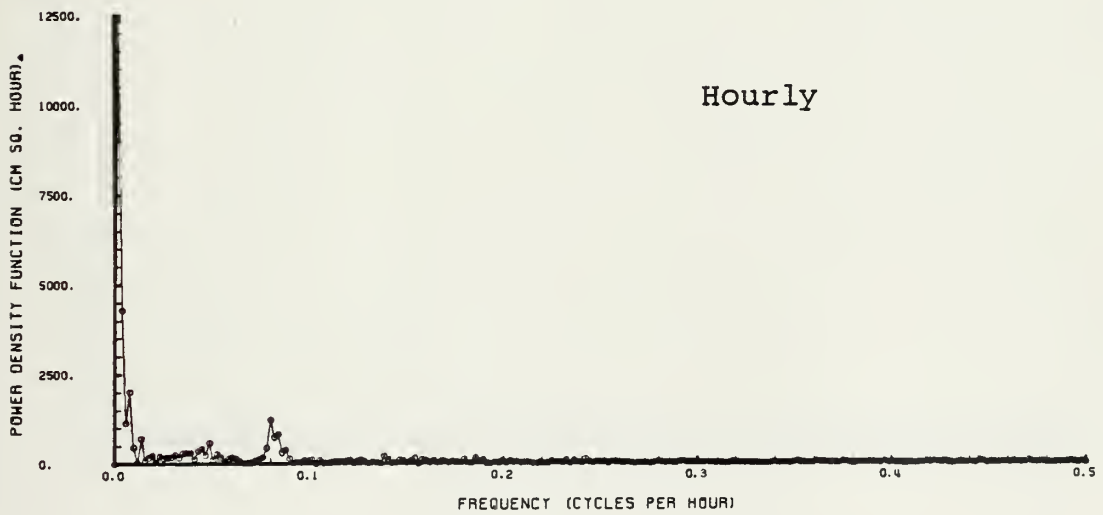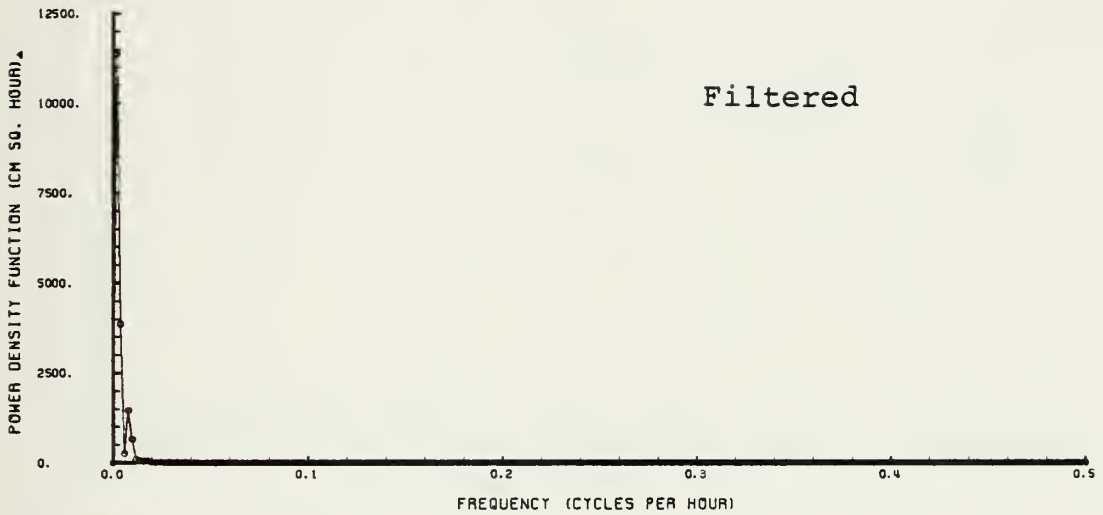and hourly alongshore current spectra.

Figure 40. Station 5, 140 m depth,
11/27/78-1/22/79. Low pass filtered
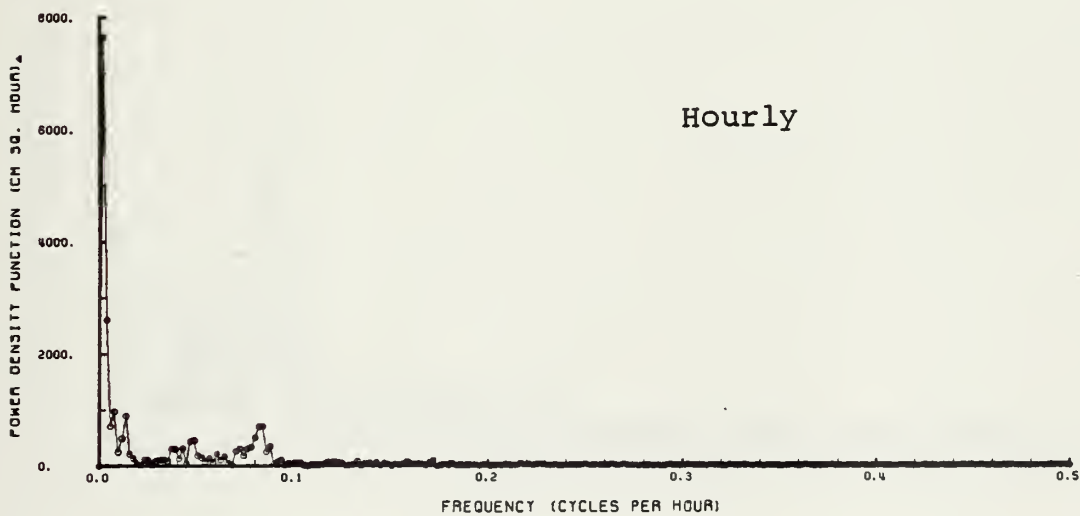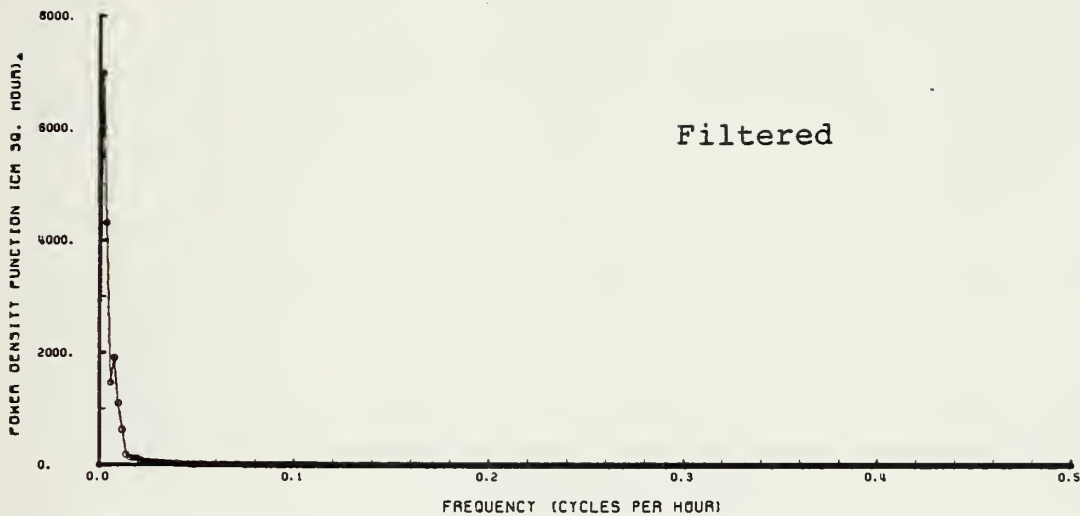and hourly alongshore current spectra.

83

Figure 41.   Station 5, 215 m depth,
11/27/78-1/22/79.   Low pass filtered
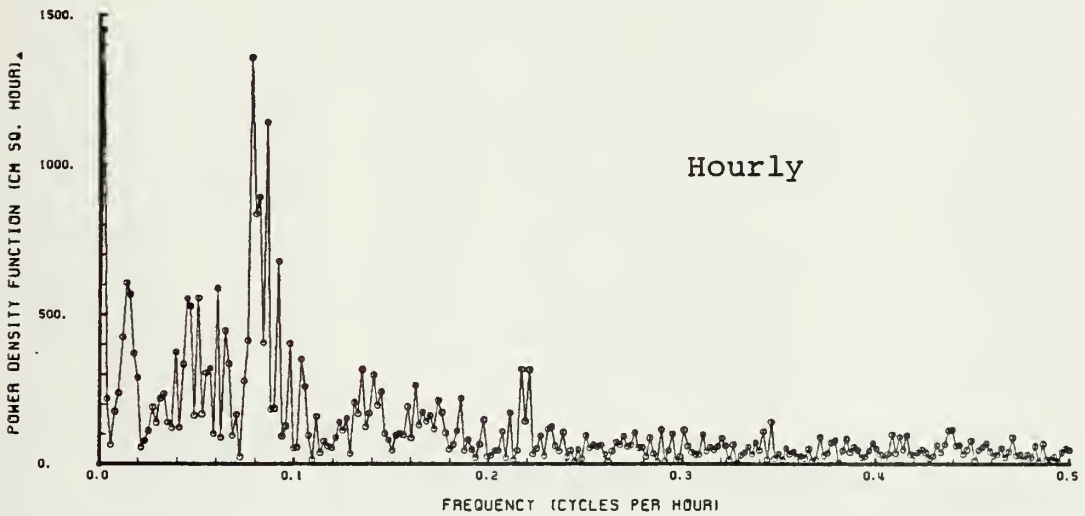and hourly alongshore current spectra.

Figure 42.   Station 2, 100 m depth,
11/27/78-1/22/79.   Low pass filtered
and hourly cross shelf current spectra.

Figure 43. Station 2, 175 m depth,
11/27/78-1/22/79. Low pass filtered
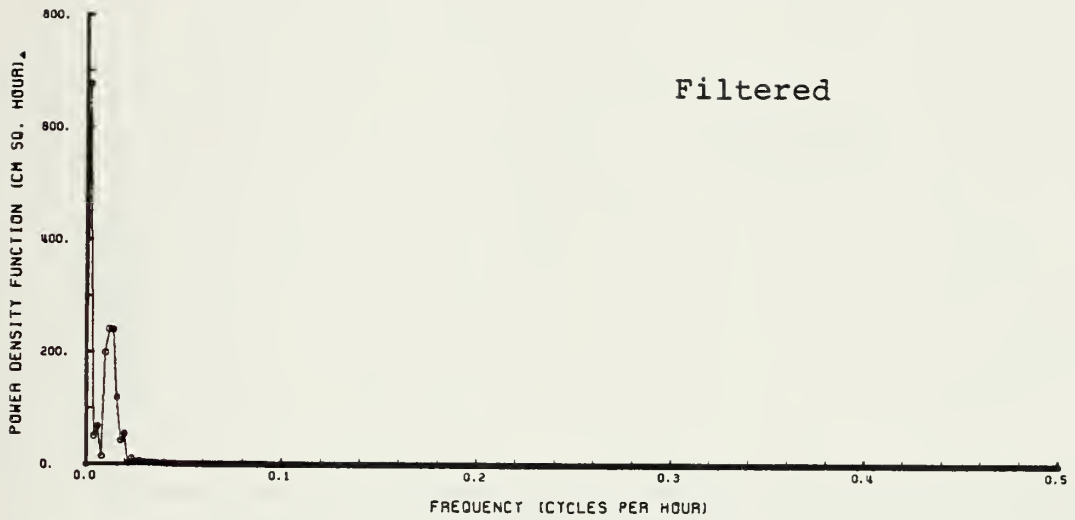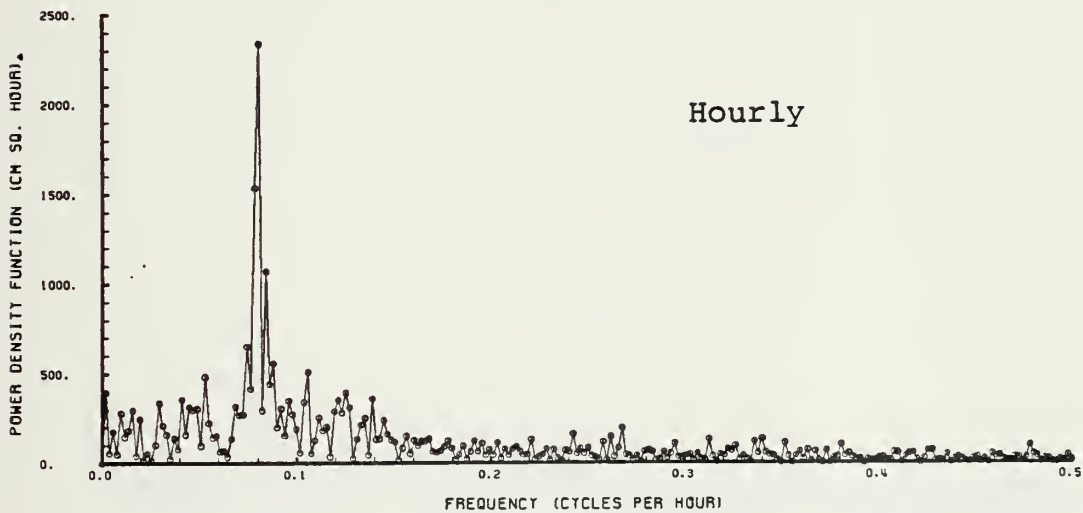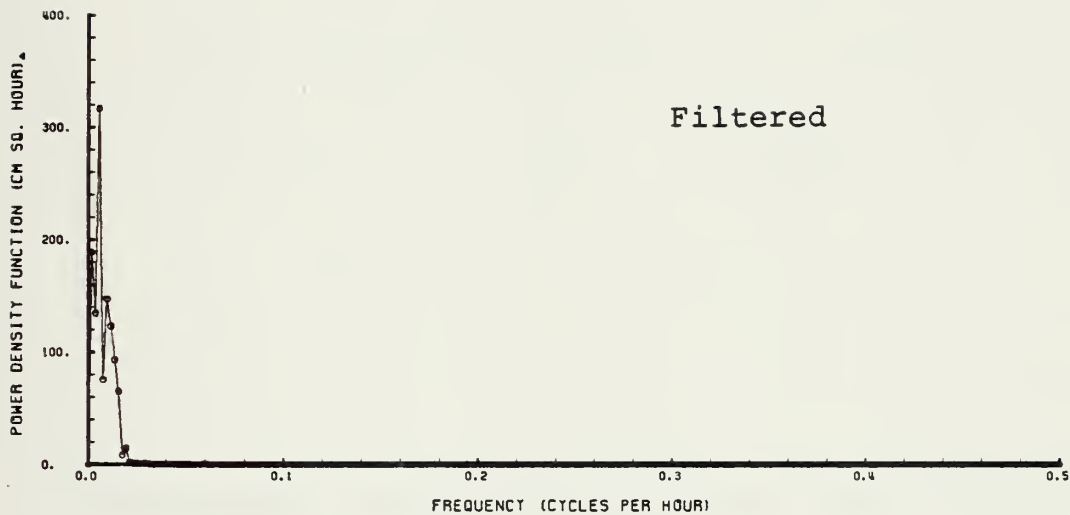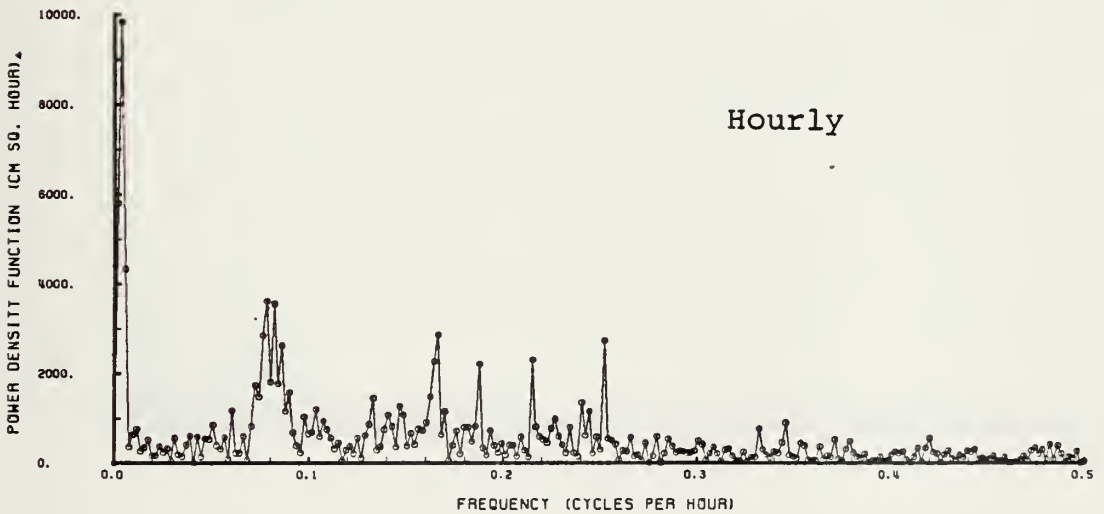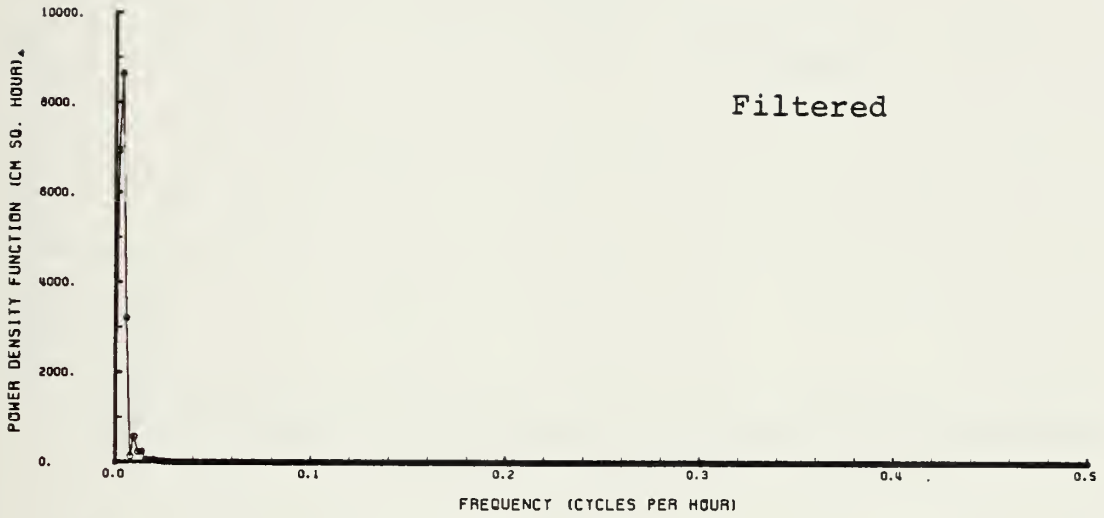and hourly cross shelf current spectra.

86

Figure 44. Station 2, 300 m depth,
11/27/78-1/22/79. Low pass filtered
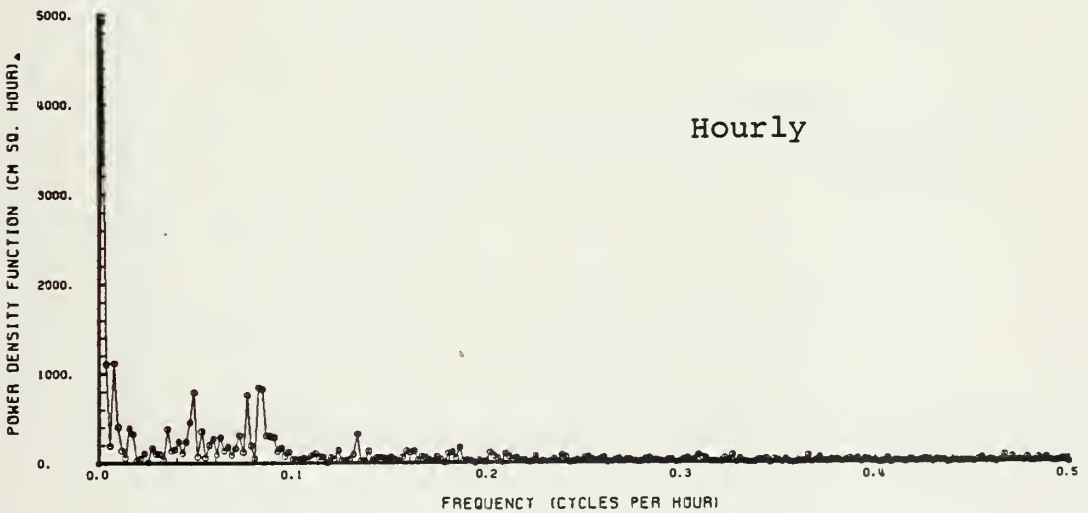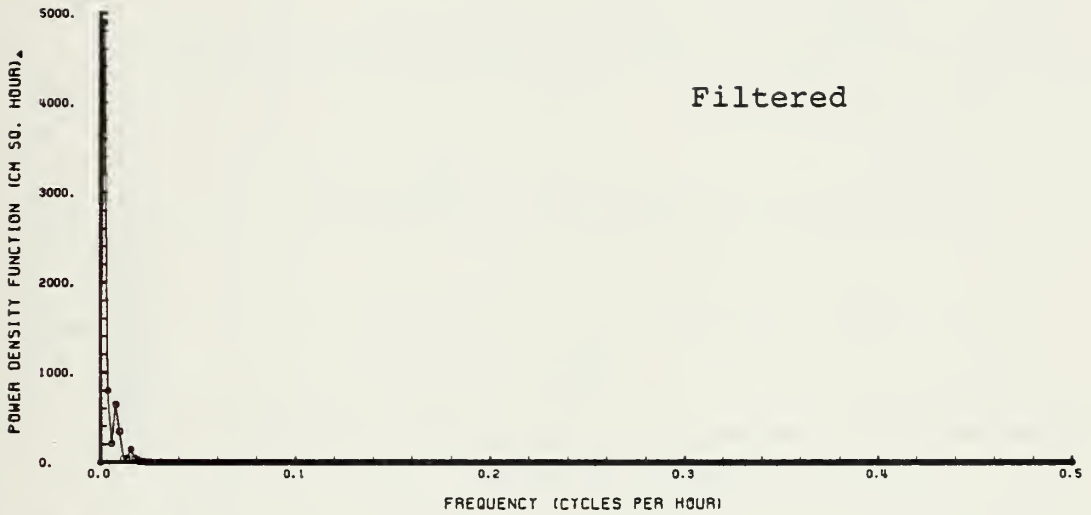and hourly cross shelf current spectra.

Figure 45. Station 5, 140 m depth,
11/27/78-1/22/79. Low pass filtered
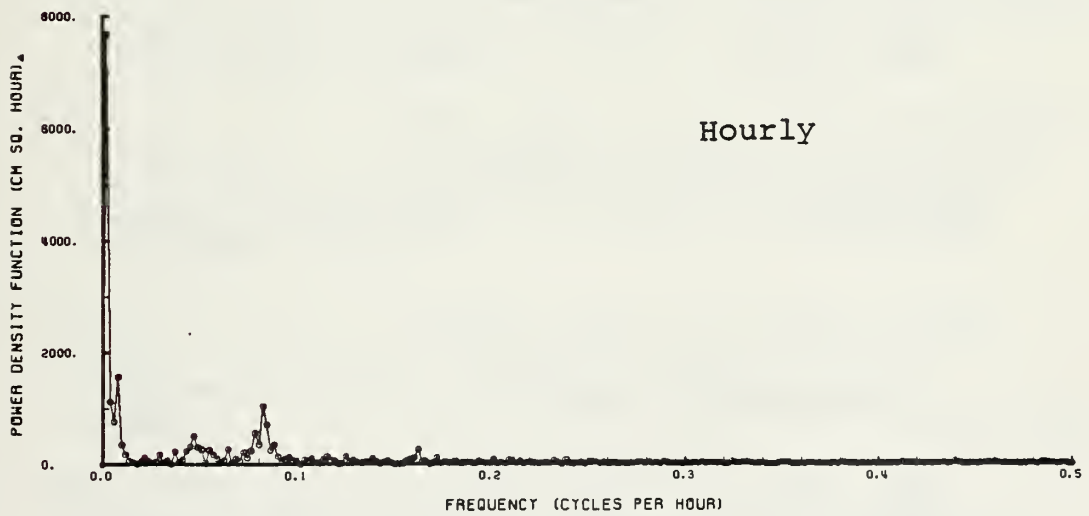and hourly cross shelf current spectra.

Figure 46. Station 5, 215 m depth,
11/27/78-1/22/79. Low pass filtered
and hourly cross shelf current spectra.

LIST OF REFERENCES

1. Coast and Geodetic Survey, US Department of Commerce, Manual of Tide Observations, Publication 30-1, 1965.

2. Coddington, K., Measurement of the California Countercurrent, Masters Thesis, Naval Postgraduate School, Monterey, California, 1979.

3. Chelton, D. B., Jr., Low Frequency Sea Level Variability Along the West Coast of North America, Ph.D. Thesis, University of California, San Diego, 1980.

4. Godin, G., "Daily Mean Sea Level and Short Period Seiches," International Hydrographic Review, v. 42(2), p. 75-89, July 1966.

5. Hickey, B. M., "The California Current System – Hypothesis and Facts," Contribution Number 1038 of the Department of Oceanography, University of Washington, 24 April 1978.

6. Hickey, B. M., and Peter Hamilton, "A Spin-Up Model as a Diagnostic Tool for Interpretation of Current and Density Measurements on the Continental Shelf of the Pacific Northwest," Journal of Physical Oceanography, v. 10, p. 12-24, 1980.

7. Huyer, A., R. L. Smith, and E. J. C. Smith, "Seasonal Differences in Low-Frequency Current Fluctuations Over the Oregon Continental Shelf," Journal of Geophysical Research, v. 83 (24), p. 5077-5089, 20 October 1978.

8. Huyer, A., E. J. C. Sobey, and R. L. Smith, "The Spring Transition in Currents Over the Oregon Continental Shelf," Journal of Geophysical Research, v. 84 (11), p. 6995-7011, 20 November 1979.

9. NOAA Technical Report NMFS SSRF-693, Daily and Weekly Upwelling Indices, West Coast of North America, 1967-73, by A. Bakun, p. 1-9, August 1975.

10. NOAA Technical Report NMFS Circ. 427, Anomalies Of Monthly Mean Sea Level Along the West Coasts of North and South America, by D. E. Bretschneider and D. R. McLain, p. 51-64, June 1979.

11. Osmer, S. R., and A. Huyer, "Variations in the Alongshore Correlation of Sea Level Along the West Coast of North America," _Journal of Geophysical Research_, v. 83, p. 1921-1927, 1978.

12. Preller, R., and J. J. O'Brien, _The Influence of Bottom Topography on Upwelling Off Peru_, unpublished manuscript, 79 pp., March 1979.

13. Skogsberg, T., "Hydrography of Monterey Bay, California. Thermal Conditions, 1929-1933," _Transactions of the American Philosophical Society_, v. 29, 152 pp., December 1936.

14. Smith, R. L., "A Description of Current, Wind, and Sea Level Variations During Coastal Upwelling Off the Oregon Coast, July-August 1972," Journal of Geophysical Research, v. 79 (3), 435-443, January 20, 1974.

15. Smith, R. L., "Poleward Propogating Perturbations in Currents and Sea Levels Along the Peru Coast," _Journal of Geophysical_ Research, v. 83 (12), p. 6083-6092, 20 December 1978.

INITIAL DISTRIBUTION LIST

No. Copies

1. Defense Technical Information Center   2
    Cameron Station
    Alexandria, VA   22314

2. Library, Code 0142   2
    Naval Postgraduate School
    Monterey, CA   93940

3. Chairman   Code 68Mr
    Department of Oceanography   1
    Naval Postgraduate School
    Monterey, CA   93940

4. Chairman   Code 63Ha   1
    Department of Meteorology
    Naval Postgraduate School
    Monterey, CA   93940

5. J. B. Wickham   Code 68Wk   2
    Department of Oceanography
    Naval Postgraduate School
    Monterey, California   93940

6. S. P. Tucker   Code 68Tx   2
    Department of Oceanography
    Naval Postgraduate School
    Monterey, California   93940

7. Donald A. Dreves   3
    5713 145th Place SW
    Edmonds, Washington   98020

8. Director   1
    Naval Oceanography Division
    Naval Observatory
    34th and Massachusetts Avenue NW
    Washington, D.C.   20390

9. Commander   1
    Naval Oceanography Command
    NSTL Station
    Bay St. Louis, MS   39529

10. Director   1
    National Ocean Survey (c)
    National Oceanic and Atmospheric
      Administration
    Rockville, MD   20852

11. Chief, Program Planning and Liasion   1
      (NC-2)
    National Oceanic and Atmospheric
      Administration
    Rockville, MD   20852

12. Chief, Marine Surveys and Maps (C3)   1
    National Oceanic and Atmospheric
      Administration
    Rockville, MD   20852

13. Director   1
    Pacific Marine Center - NOAA
    1801 Fairview Avenue East
    Seattle, WA   98102

14. Director   1
    Atlantic Marine Center - NOAA
    439 W. York Street
    Norfolk, VA   23510

15. Commanding Officer   1
    Naval Ocean Research and Development
      Activity
    NSTL Station
    Bay St. Louis, MS   39529

16. Chairman, Oceanography Department   1
    U.S. Naval Academy
    Annapolis, MD   21402

17. Francisco Abreu   1
    Instituto Hidrografico
    Rua Das Trinas, 49
    Lisboa-2
    Portugal

18. Luis Faria   1
    Instituto Hidrografico
    Rua Das Trinas, 49
    Lisboa-2
    Portugal

19. Jerry Norton , Code 68Cu   1
       Department of Oceanography
       Naval Postgraduate School
       Monterey, California   93940